Plasmacytoma Variant Translocation 1 Gene (PVT1) as a Potential Novel Target for the Treatment of Diabetic Nephropathy

A thesis submitted to Auckland University of Technology

in fulfilment of the requirements for the degree of

Doctor of Philosophy

Sao Keng Mok

School of Science

Auckland University of Technology

Auckland, New Zealand

20 October 2020

ABSTRACT

Diabetic nephropathy (DN) is clinically characterized by the development of proteinuria with a subsequent decline in glomerular filtration rate which progresses over time. It is a common complication in patients with diabetes, predominantly type 2 diabetes. It is the leading cause of end-stage renal disease (ESRD) and accounts for most of the reduced life expectancy in diabetic patients. Despite the prevalence of DN is increasing worldwide, the molecular mechanism underlying the pathogenesis of DN remains poorly understood. Recent genome-wide association studies suggested plasmacytoma variant translocation 1 (PVT1) is a key determinant of ESRD. Some *in vitro* studies suggested PVT1 plays an important role in mediating the development of DN through the extracellular matrix (ECM) accumulation.

In this study, we hypothesized that PVT1 promotes the development of DN *in vivo*, whereas inhibition of PVT1 prevents such development through reducing ECM accumulation. To begin with, a murine model of DN was successfully established using a combination treatment of high fat diet and low dose streptozotocin in male C57BL/6 mice. This diabetic model exhibited hallmarks of DN (including hyperglycemia, kidney hypertrophy, albuminuria, reduced creatinine clearance, and increased glomerular and mesangial areas) which were not observed in the normal controls. These manifestations were significantly different from that in the age-matched normal controls (9-wk-old as young, 16-wk-old as middle-aged and 24-wk-old as old) and were intensified as the diabetic mice aged. This set of diabetic and control models were considered suitable for testing the treatment of DN. To study the role of PVT1 on progression of DN, the gene expression of PVT1 and ECM components (FN1 and COL4A1) and regulators (TGF-β1, PAI-1 and BMP7) were determined. Our results showed that the glomerular PVT1

expression was significantly increased in diabetic mice when compared with the age-matched controls (without disease). The upregulation of PVT1 was paralleled with upregulation of TGF-β1, PAI-1, FN1, COL4A1, while downregulation of BMP7 in diabetic model. This suggested PVT1 might play a role in ECM accumulation. We then conducted a PVT1 inhibition experiment using RNA interference. Diabetic mice were treated with either PVT1-siRNA or scramble-siRNA, and normal controls without siRNA treatment were used and compared. PVT1 expression was inhibited in diabetic mice treated with PVT1-siRNA but not in those with scramble-siRNA at all ages (young, middle-aged and old). Significant differences in blood glucose, proteinuria (UAE, UACR, UPE, UPCR), serum creatinine, creatinine clearance and glomerular mesangial areas were observed between diabetic mice with scramble-siRNA and the age-matched controls. While hyperglycemia persisted, PVT1-siRNA treatment reduced kidney hypertrophy, proteinuria (UAE, UACR, UPE, UPCR), serum creatinine, glomerular and mesangial areas, and increased creatinine clearance in diabetic mice to levels closer to the age-matched controls. The PVT1-siRNA treatment markedly supressed the upregulation of TGF-β1, PAI-1, FN1, COL4A1, and downregulation of BMP7 in the diabetic mice.

In conclusion, PVT1 inhibition ameliorates DN in terms of kidney function and histology in a diabetic mouse model without altering hyperglycemia. The renal protection might be resulted from the reduction of ECM accumulation through suppression of TGF-β1 and PAI-1 expression as well as the preservation of BMP7 expression. It is therefore suggested that PVT1 plays an important role in ECM accumulation and its inhibition might be a potential approach for the management of DN.

TABLE OF CONTENTS

LIST OF FIGURES

LIST OF TABLES

ATTESTATION OF AUTHORSHIP

I hereby declare that this submission is my own work and that, to the best of my knowledge and belief, it contains no material previously published or written by another person (except where explicitly defined in the acknowledgements), nor material which to a substantial extent has been submitted for the award of any other degree or diploma of a university or other institution of higher learning.

Signature:

Name: Sao Keng MOK

Date: 20 Oct 2020

ACKNOWLEDGEMENTS

Pursuing a PhD is one of my dreams. It is a long journey, which is full of challenges, excitement and stress. I am very grateful to AUT for offering me the Vice-Chancellor Doctoral Scholarship, which made my journey possible. I am glad to receive the biannual AUT and Cyclone Scholarship as well.

I would like to express my deepest gratitude to my primary supervisor, Professor Jun Lu, for his invaluable guidance, patience and critiques of this research project. The project has been delayed for some time owing to some technical issues and my personal reasons. I am very grateful that Prof Lu is always positive and supportive, and guided me on the right track. I don't know how many "Thank You" I should say to truly show my appreciation towards his guidance and thoughtfulness. Prof Lu, Thank you!

I would like to give my sincere thanks to Professor Ahmed Al-Jumaily, my secondary supervisor, for his generous support on this project. He has provided a specific laboratory unit for my animal studies and offered me a good opportunity to work for the IBTec where I gained precious experience. Prof Al-Jumaily, Thank you!

My special thanks are extended to the Animal Ethics Committee for approval of this project; Professor Fabrice Merien, Dr Sharita Meharry, Dr Yan Li, Associate Professor Dong Xu Liu, the laboratory manager and technicians in the School of Science for their kind support.

I am thankful to my fellow schoolmates who are always warm-hearted and cheerful.

Finally, I wish to thank my family for the unconditional love, support and encouragement throughout my life.

CHAPTER 1: INTRODUCTION

1.1 Diabetic nephropathy (DN) and end-stage renal disease (ESRD)

1.1.1 Prevalence of DN and ESRD

DN or diabetic kidney disease refers to a characteristic set of structural and functional kidney abnormalities that occur in patients with diabetes (Reeves & Andreoli, 2000). It is a common complication in patients with either type 1 or type 2 diabetes, which has long been recognized to cause severe morbidity and mortality (Sharma et al., 1997; Ziyadeh et al., 2000). It is the leading cause of end-stage renal disease (ESRD) or renal failure, and is epidemic worldwide (Jefferson, Shankland, & Pichler, 2008; Mohanram et al., 2004). Between 20-40% of patients with diabetes ultimately develop nephropathy, although the reason why this complication does not occur in all diabetic patients is unknown (Dronavalli, Duka, & Bakris, 2008; F. Li et al., 2010; Susztak et al., 2004). The incidence of DN continues to rise far more rapidly than rates due to any other primary diagnosis of ESRD as a result of the ageing population and the increasing prevalence of diabetes, predominantly those with type 2 diabetes (Locatelli, Pozzoni, & Del Vecchio, 2004; van Dijk & Berl, 2004).

ESRD due to diabetes has been estimated to be 30-47% of all incident cases worldwide (Satirapoj & Adler, 2014). It accounts for up to 50% of patients receiving renal replacement therapy (RRT, dialysis or renal transplantation) (Beulens, Grobbee, & Nealb, 2010). Patients with DN and ESRD are associated with high mortality rates (van Dijk & Berl, 2004). The cost of renal replacement therapy in New Zealand is estimated at NZD 90 million annually, and DN is responsible for at least NZD 36 million in direct annual healthcare costs. Therefore, prevention of DN and its progression to ESRD is important

to improve health outcomes of persons with diabetes and to reduce the socioeconomic health burden of chronic kidney disease.

1.1.2 Pathogenesis of DN

The development and progression of DN is highly complex given the diversity of cell populations present within the kidney and the various physiological roles of this organ. Hyperglycemia induces hemodynamic and metabolic changes and inflammation, which lead to kidney injury contributing to DN. The hemodynamic changes including hyperperfusion and hyperfiltration occur early in DN, which involve increased systemic and intraglomerular pressure and activation of various vasoactive hormones. They facilitate the albumin leakage from the glomerular capillary compartment into Bowman's space, mesangial matrix expansion, podocyte injury and nephron loss (Wolf & Ziyadeh, 2007). The metabolic changes involve increased intracellular glucose availability leading to the activation of signalling cascades favouring glomerulosclerosis, including pathways mediated by transforming growth factor-β (TGF-β), advanced glycosylation end products (AGEs), protein kinase C, and various cytokines and growth factors (Wolf & Ziyadeh, 2007). Inflammation promotes renal fibrosis through overproduction and activation of various inflammatory cells, cytokines (e.g. interleukins) and growth factors. These changes activate inflammatory, pro-oxidant, ischemic, and fibrotic pathways leading to mesangial matrix accumulation; glomerular basement membrane (GBM) thickening; podocyte effacement and loss; endothelial dysfunction; tubular atrophy, fibrosis and dropout; tubulointerstitial inflammation, and renal arteriolar hyalinosis (Satirapoj & Adler, 2014; Brownlee 2001).

1.1.3 Determination of DN

DN is clinically characterized by the development of proteinuria with a subsequent decline in glomerular filtration rate (GFR), which progresses over a long period of time, often over 10-20 years (Forbes & Cooper, 2013). It usually progresses through the stages of hyperfiltration and hypertrophy (initial stage), normoalbuminuria (silent stage), microalbuminuria (incipient nephropathy), macroalbuminuria (overt nephropathy) and eventually ESRD (Mogensen, 1987). Microalbuminuria is an early sign of DN which denotes low-grade albuminuria (Gansevoort et al., 2005; Jefferson et al., 2008). Once macroalbuminuria (> 300 mg per day) occurs, there is concomitant loss of GFR in both type 1 and type 2 diabetes (Satirapoj & Adler, 2014). Albuminuria can be determined using 24-hr urine or spot urine and the stages are shown in

Table 1.1. Urinary albumin excretion (UAE) in a 24-hr collection is considered as the gold standard method, while urinary albumin to creatinine ratio (UACR) in spot collection is widely adopted with strong association with 24-hr UAE (Dyer et al., 2004; Witte et al., 2009). Proteinuria results from defects in the glomerular filtration barrier as well as abnormalities in tubular albumin reabsorption. The glomerular filtration barrier comprises of a series of layers separating the glomerular capillary from the Bowman's space, which are the innermost fenestrated endothelium, the middle glomerular basement membrane, and the outermost podocyte. Each layer likely contributes uniquely to the impermeability to albumin (Jefferson et al., 2008). All three major glomerular cell types, namely epithelial cells, mesangial cells and podocytes, participate in the ECM accumulation and renal fibrosis process (Lopez-Hernandez & Lopez-Novoa, 2012). In addition to functional changes, the renal histological changes (e.g. glomerular basement membrane thickening, mesangial expansion, and glomerulosclerosis) are found in DN (Couchman, Beavan, & McCarthy, 1994). Characteristics of normal and diabetic glomerulus and glomerular filtration barrier is summarized in Figure 1.1. The glomerular classification of DN, which based on glomerular lesions, with a separate evaluation for interstitial and vascular lesions, is shown in Table 1.2 (Satirapoj & Adler, 2014; Tervaert et al., 2010).

Table 1.1: Stages in DN (adapted from Gross et al., 2005)

Stages	Albuminuria cutoff values (ref. 14)	Clinical characteristics (ref. no.)
Microalbuminuria	20–199 μg/min	Abnormal nocturnal decrease of blood pressure and increased blood pressure levels (163)
	30–299 mg/24 h	Increased triglycerides, total and LDL cholesterol, and saturated fatty acids (164, 165)
	30–299 mg/g*	Increased frequency of metabolic syndrome components (166)
		Endothelial dysfunction (167)
		Association with diabetic retinopathy, amputation, and cardiovascular disease (168)
		Increased cardiovascular mortality (2, 169)
		Stable GFR (82)
Macroalbuminuria†	≥200 μg/min	Hypertension (99)
	≥300 mg/24 h	Increased triglycerides and total and LDL cholesterol (170)
	>300 mg/g*	Asymptomatic myocardial ischemia (171, 172)
		Progressive GFR decline (83, 84)

*Spot urine sample. †Measurement of total proteinuria (≥500 mg/24 h or ≥430 mg/l in a spot urine sample) can also be used to define this stage.

Figure 1.1: Characteristics of (a) normal and (b) diabetic glomerulus, and (c) glomerular filtration barrier (adapted from Jefferson et al., 2008)

(a) Normal glomerulus (b) diabetic glomerulus is characterized with increased mesangial extracellular matrix, mesangial cell hypertrophy, glomerular basement membrane thickening, reduced podocyte number and density. Glomerular capillaries are narrowed by mesangial matrix expansion which reduces glomerular filtration rate. (c) Glomerular filtration barrier consists of the innermost glomerular endothelial cells, the middle GBM, and outermost podocytes; and serves to serially limit albumin escaping from the capillary loops. Fenestrae within specialized endothelial cells are covered by a negatively charged glycocalyx. Podocytes attach to the outermost aspect of the GBM by foot processes, between which are proteins comprising the size barrier slit diaphragm. In normal glomerulus, albumin normally remains within the capillaries of the glomerular tuft and does not escape into the urinary Bowman's space.

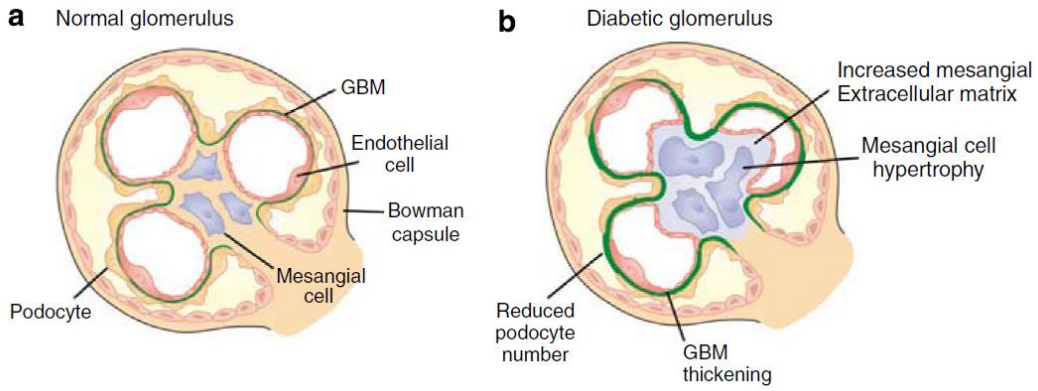

c Glomerular filtration barrier

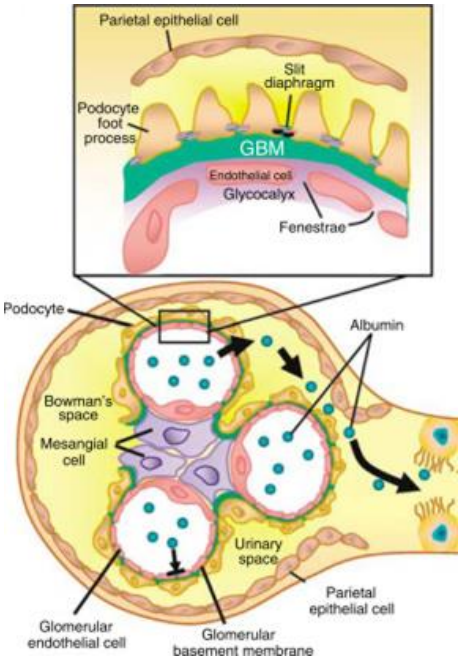

Table 1.2: Glomerular classification of DN (adapted from Tervaert et al., 2010)

Class	Description	Inclusion Criteria
I	Mild or nonspecific LM changes and EM-proven GBM thickening	Biopsy does not meet any of the criteria mentioned below for class II, III, or IV GBM > 395 nm in female and >430 nm in male individuals 9 years of age and older[a]
IIa	Mild mesangial expansion	Biopsy does not meet criteria for class III or IV Mild mesangial expansion in >25% of the observed mesangium
IIb	Severe mesangial expansion	Biopsy does not meet criteria for class III or IV Severe mesangial expansion in >25% of the observed mesangium
III	Nodular sclerosis (Kimmelstiel–Wilson lesion)	Biopsy does not meet criteria for class IV At least one convincing Kimmelstiel–Wilson lesion
IV	Advanced diabetic glomerulosclerosis	Global glomerular sclerosis in >50% of glomeruli Lesions from classes I through III

LM, light microscopy.
[a]On the basis of direct measurement of GBM width by EM, these individual cutoff levels may be considered indicative when other GBM measurements are used.

1.1.4 Structural-functional relationships in DN

The severity of functional deterioration in DN correlates with the glomerular structural lesions (Ruth Østerby, Parving, Hommel, Jørgensen, & Løkkegaard, 1990; R Østerby et al., 2001). The structural-functional relationships are similar in both types of diabetes (White & Bilous, 2000). The GBM forms an essential part of the selectively permeable glomerular filtration barrier (GFB) that separates the vasculature from the urinary space, which plays a crucial role in glomerular filtration (Miner, 2012). The clinical manifestations, albuminuria and decreased glomerular filtration rate, correlated strongly to mesangial expansion while related poorly or not at all to GBM thickening (Mauer et al., 1984). Mesangial expansion appears to be the main cause of declining renal function in DN (Steffes, Østerby, Chavers, & Mauer, 1989). Previous studies showed mesangial expansion had strong inverse correlations with capillary filtering surface area density, glomerular filtration rate and microalbuminuria (Caramori et al., 2002; Lehmann & Schleicher, 2000; Mauer, 1994; Mauer et al., 1984; White & Bilous, 2000). As matrix accumulation in the mesangial area increases, the mesangial area expands to impinge on glomerular capillaries, reducing the capillary surface area available for filtration and narrowing or occluding the lumen, which subsequently lead to progressive loss of renal function (Adler, 1994; Mason & Wahab, 2003; Wolf, Chen, & Ziyadeh, 2005). Even though GBM thickening and mesangial expansion are the hallmarks of DN, they do not completely explain the decline in renal function as some patients with persistent proteinuria did not have diabetic glomerulopathy (Dalla Vestra et al., 2003) or *vice versa* (Caramori, Fioretto, & Mauer, 2003; MacIsaac et al., 2004). Other structural changes, such as podocyte foot process effacement, decrease in podocyte number and density, have gained increasing attentions where a significant inverse correlation between the latter two changes and proteinuria was observed as well as podocyte injury leads directly to

proteinuria (Dronavalli et al., 2008; Jefferson et al., 2008; Wolf et al., 2005). Further study is necessary to delineate the mechanism of proteinuria in DN.

1.1.5 Accumulation of extracellular matrix in the glomeruli

Accumulation of extracellular matrix contributes to the GBM thickening and mesangial expansion in DN. Compositions of the GBM and mesangium are similar but not identical. The GBM mainly consists of a highly crosslinked network of type IV collagen, laminin, nidogen (also known as entactin), and heparan sulfate proteoglycan (HSPG) (Couchman et al., 1994; Miner, 2012; Nerlich & Schleicher, 1991). The highly negatively charged heparan sulfate (HS) side chain of HSPG is a major determinant of the charge-dependent permeability of the glomerular capillary wall (Tamsma et al., 1994). The importance of heparan sulfate remains inconclusive since some studies demonstrated loss of HS from the GBM increased the GBM permeability and enhanced proteinuria (Van Den Born et al., 1993; Vernier, Steffes, Sisson-Ross, & Mauer, 1992), whereas some showed normal renal function in animals with HS removal by heparanase infusion or overexpression (Van Den Hoven et al., 2008; Wijnhoven et al., 2007). The mesangial matrix consists predominantly of type IV and V collagen, laminin, fibronectin and several proteoglycans (Floege et al., 1991). Biochemical and immunohistochemical studies have indicated marked increase in type IV collagen and fibronectin (FN) in DN (Makino et al., 1995). Type IV collagen is the predominant ECM protein found in healthy and diabetic glomeruli. Fibronectin is one of the first ECM protein increases in the early stages of DN. High glucose-induced type IV collagen deposition is shown to be dependent on the FN matrix assembly (binding of FN dimers to α5β1 integrins to promote FN matrix formation), which suggested a role for FN as a mediator of ECM accumulation (Miller, Pozzi, Zent, & Schwarzbauer, 2014; Singh, Carraher, & Schwarzbauer, 2010). Some compositional changes in glomerular matrix proteins in DN is shown in Table 1.3 (Mason & Wahab,

2003). ECM accumulation is modulated by several different cytokines, growth factors and matrix-degrading proteases, which includes transforming growth factor-β1 (TGF-β1), plasminogen activator inhibitor-1 (PAI-1), angiotensin II (Ang II), connective tissue growth factor (CTGF) and tissue inhibitors of metalloproteinases (TIMPs) (Mason & Wahab, 2003). The mediators, TGF-β1, PAI-1 and BMP7, are discussed in detailed below.

Table 1.3: Glomerular matrix proteins in DN (adapted from Mason & Wahab, 2003)

Protein	Comment
Mesangium	
collagen I	Only detected in late glomerulosclerosis.
	May bind decorin and TGF-β.
collagen III	Only detected in late glomerulosclerosis.
collagen IV	α1(IV), α2(IV) chains expressed in normal mesangium, increased in DN.
collagen V	Minor component in normal mesangium.
	Increased in DN.
collagen VI	Present in normal mesangium. Same distribution as α1(IV) in normal mesangium.
	Reports of increase in DN not substantiated in type I "fast track" DN, using quantitative immunogold EM.
fibronectin	Present in normal mesangium.
	Increased in DN.
	Oncofetal, ED-A, and ED-B isoforms expressed in glomerulosclerosis.
laminin	Minor component in normal mesangium.
	Report of increase in diffuse mesangial expansion not confirmed.
SLR proteoglycans	Includes decorin, biglycan, lumican, fibromodulin; mRNAs for all overexpressed in DN, but proteins barely detected, except in advanced glomerulosclerosis.
GBM	
collagen IV	α3(IV), α4(IV) chains present normally, increased in DN.
	α1(IV), α2(IV), minor components normally decreased in DN.
entactin	Present normally.
	Increased in DN.
laminin	Present normally, may be increased in early DN, but generally reported to decrease.
heparan sulfate proteoglycan	Present normally.
	Decreased in DN.

1.2 Mediators of ECM accumulation

1.2.1 Transforming growth factor-β (TGF-β)

It is evident that TGF-β plays an integral role in the pathogenesis of DN (S. V. Mclennan et al., 2000). TGF-β is a prototype member of cytokines (Border, Yamamoto, & Noble, 1996). Virtually every cell in the body produces TGF-β, including several renal cell types, and has receptors for it (Border et al., 1996; Epstein, Blobe, Schiemann, & Lodish, 2000; Ziyadeh, Sharma, Ericksen, & Wolf, 1994). It consists a family of three isoforms TGF-β1, -β2 and -β3 which are structurally and functionally closely related to each other (Border & Ruoslahti, 1992). Among all isoforms, TGF-β1 is the most important in fibrosis (Reeves & Andreoli, 2000). TGF-β plays an essential role in tissue repair, in which its excessive action can result in tissue damage caused by scarring in many serious diseases including DN (Border & Ruoslahti, 1992). It is upregulated in diabetes and has been proven to mediate virtually all of the pathological changes of DN (S. Chen et al., 2001). Almost all of the molecular mediators and intracellular signalling pathways that have been identified in diabetic kidney injury have also been found to stimulate the renal TGF-β activity as an intermediate step (Ziyadeh, 2004). TGF-β system mediates the renal hypertrophy, glomerulosclerosis, and tubulointerstitial fibrosis of DN (S. Chen, Jim, & Ziyadeh, 2003). Pathologic accumulation of extracellular matrix is a pivot event of DN (Nicholas et al., 2005). TGF-β promotes accumulation of extracellular matrix in four ways. First, TGF-β directly upregulates the genes of most matrix proteins leading to their increased synthesis. The key matrix proteins include type I collagen, type IV collagen, fibronectin, laminin, proteoglycans, and tenascin (Border & Ruoslahti, 1992; Ziyadeh, 2004). Second, TGF-β decreases matrix degradation by inhibiting the synthesis of proteases (e.g. plasminogen activator, collagenases, elastase, and stromelysin) and activating the protease inhibitors (e.g. plasminogen activator inhibitor-1 (PAI-1) and tissue inhibitors of metalloproteinases (TIMPs)) (S. Chen et al., 2001; Ziyadeh, 2004).

Third, TGF-β modulates the expression of integrins on the cell‘s surface in a manner that facilitates attachment to the newly synthesized matrix (Border et al., 1996). Finally TGF-β autoinduces its own production, which greatly amplifies its actions (Border et al., 1996).

1.2.2 Plasminogen activator inhibitor-1 (PAI-1)

Plasminogen activator inhibitor-1 (PAI-1), a 50 kDa single chain glycoprotein, is a serine protease inhibitor (SERPIN). It is the primary physiological inhibitor of tissue-type and urokinase-type plasminogen activators (tPA and uPA, respectively). It irreversibly forms complexes with active plasminogen activators (PA), which are subsequently endocytozed and degraded (Rerolle, Hertig, Nguyen, Sraer, & Rondeau, 2000). Within blood vessels, PAI-1 blocks tPA-dependent plasmin generation and degradation of fibrin clots. In extravascular areas, PAI-1 impairs matrix turnover by inhibiting uPA-dependent activation of plasminogen. Plasmin, the active form of plasminogen, is a broad-spectrum protease that degrades fibrin clots and various extracellular matrix proteins (type IV collagen, fibronectin, laminin, and proteoglycan) (H. B. Lee & Ha, 2005). It also activates matrix metalloproteinases (MMPs) from their latent forms. These components are part of the two main enzyme systems, PA/plasmin/PAI system and MMP/TIMP system, involved in ECM degradation. PAI-1 interferes with the generation of plasmin and activation of MMP by blocking PA (E. A. Lee et al., 2005). PAI-1 is overexpressed in pathologic conditions associated with renal fibrosis including DN, while it is undetectable in normal human kidneys (Nicholas et al., 2005).

1.2.3 Bone morphogenetic protein 7 (BMP7)

Bone morphogenetic protein 7, formerly called osteogenic protein 1 (OP 1), is one of over twenty currently known BMPs which are within the TGF-β superfamily of secreted

growth factors (Katagiri & Watabe, 2016; G. Mitu & Hirschberg, 2008; Zeisberg, Müller, & Kalluri, 2004). BMPs are highly conserved across animal species and mature human and mouse BMP7 share 98% amino acid sequence identity (Ozkaynak et al., 1990; Zeisberg, 2006). BMP7 has vital functions during kidney and eye development (Godin, Takaesu, Robertson, & Dudley, 1998). Mice deficient for BMP7 gene have very small kidneys and die shortly after birth from renal failure (Dudley, Lyons, & Robertson, 1995; Hogan, 1996; Luo et al., 1995). BMP7 is the most abundant BMP in fetal and adult mammalian kidney, and conversely, kidney is the most abundant site of BMP7 production (Kopp, 2000). It is specifically expressed in podocytes, distal tubules and collecting ducts (G. Mitu & Hirschberg, 2008). BMP7 expression was down regulated in patients with DN at advanced stage (Ivanac-Janković et al., 2015). The reduction in renal BMP7 is observed early at the onset of DN in rodents and is paralleled by the appearance and subsequent increase in TGF-β (G. Mitu & Hirschberg, 2008). *In vitro* and *in vivo* studies have demonstrated BMP7 plays a role in protecting the kidney from injury which counteract TGF-β1 mediated fibrosis (Patel & Dressler, 2005; Zeisberg et al., 2004).

1.3 Current treatment of DN and ESRD and their drawbacks

The current approaches to treating DN or reduce renal insufficiency primarily rely on reducing hyperglycemia or blood pressure in an indirect manner. Hyperglycemia is a major determinant of development of DN (Cooper, 1998). The two landmark studies, the Diabetes Control and Complications Trial (DCCT) and the United Kingdom Prospective Diabetes Study (UKPDS), showed that intensive control of hyperglycemia can reduce the occurrence or progression of DN, retinopathy and neuropathy in patients with type 1 and type 2 diabetes, respectively (Sheetz & King, 2002). Antihypertensive treatment reduces the risk of cardiovascular events and provides renoprotection in patients with DN. Many patients may need two or three different antihypertensive drugs (e.g. β blockers, diuretics,

angiotensin-converting enzyme (ACE) inhibitors, calcium channel antagonists, and angiotensin receptor blockers (ARBs)) (Gross et al., 2005; Stumvoll, Goldstein, & van Haeften, 2005). Although ACE inhibitors and ARBs provide blood pressure-independent renoprotection, their intensive use are limited by severe hyperkalemia, further reduction in the systemic blood pressure and renal blood flow. Even when maximized, they may decrease rate of progression but do not arrest or reverse DN (Sharma et al., 2011). Furthermore, combined therapy of ACE inhibitors and ARBs has shown to increase the risk of acute kidney injury and hyperkalemia, which fails to render overall clinical benefits (Fried et al., 2013). Management of dyslipidemia with a statin, dietary restriction, smoking cessation, physical activity and weight reduction provide additive renal benefits (Declèves & Sharma, 2010; Satirapoj & Adler, 2014).

If DN is left untreated or uncontrolled, the renal function will further deteriorate to reach ESRD. Patient with ESRD will require dialysis (hemodialysis or peritoneal dialysis) or kidney transplant for survival eventually (Locatelli et al., 2004). However, these treatment options have drawbacks. Hemodialysis, the most common modality, gives rise to several clinical problems such as difficulties in the management of vascular access and high frequency of intradialytic hypotension. Patients receiving peritoneal dialysis have to face a progressive increase in peritoneal membrane permeability, loss of ultrafiltration, and peritoneal fibrosis, ultimately leading to an increased technique failure (Locatelli et al., 2004). Although renal transplantation is regarded as the first-choice option, only a limited proportion of patients with ESRD receives kidney transplants due to limited availability of donated kidneys and transplantation selection criteria.

Recent trial results for DN have been disappointing owing to increase in adverse events, no beneficial effects or economic reasons (Satirapoj & Adler, 2014). Novel treatment approaches for prevention and treatment of DN is needed as the number of patients with DN and ESRD continues to increase. Recently, the role of non-coding RNAs (such as plasmacytoma variant translocation, PVT1) in regulating genes involved in progression of DN is recognized, which may represent the novel potential therapeutic target for DN and further study is necessary.

1.4 Plasmacytoma variant translocation 1 (*PVT1*) gene

1.4.1 Background of PVT1

PVT1 is a long noncoding RNA (lncRNA) (1.9 kb) that encodes a number of alternative transcripts but no protein product has been identified so far (Sonoki, 2014; Wu et al., 2015). Long noncoding RNAs (more than 200 nucleotides in length) is a functionally diverse set of noncoding RNAs that act as modular molecules regulating many processes including transcription and RNA expression (Leung & Natarajan, 2014). The human PVT1 gene is homologous to the mouse plasmacytoma variant translocation gene (Colombo, Farina, Macino, & Paci, 2015). PVT1 is strongly conserved between human and mouse (Guan et al., 2007). In mouse, PVT1 locus is a site of recurrent translocation in plasmacytomas and is a common site of tumorigenic retroviral insertion in lymphomas. In human, the region homologous to PVT1 is a site of recurrent translocation between chromosomes 2 and 8 (Guan et al., 2007). Most studies of PVT1 are related to cancers, particularly lymphomas, ovarian and breast cancers. PVT1 is known to contribute to ovarian and breast cancers when overexpressed and amplified. Silencing of PVT1 expression by RNA interference decreases cell proliferation and increases apoptosis in breast and ovarian cancer cell lines in which it was amplified and overexpressed but not in cell lines where it is not amplified and overexpressed (Guan et al., 2007). PVT1 is

expressed at high levels in the kidneys, although its role is not yet well defined (Hanson et al., 2007).

1.4.2 Genome-wide association study for DN

Genetic susceptibility plays an important role in the pathogenesis of DN (Craig, Millis, & DiStefano, 2009; Maeda, 2008). Different research approaches, such as linkage analysis, candidate gene approach, mapping by admixture linkage disequilibrium (MALD) and genome-wide association study (GWAS), are used to identify the susceptibility genes for common diseases including DN (Divers & Freedman, 2010; Freedman, Bostrom, Daeihagh, & Bowden, 2007; Palmer & Freedman, 2012). GWAS scans hundreds of thousands of single nucleotide polymorphism (SNP) for association with a disease or quantitative trait, is a powerful and promising approach for identification of the susceptibility genes (Böger & Heid, 2011; Maeda, 2008; O'Seaghdha & Fox, 2012). To date, more than 100 loci for diseases including diabetes and chronic kidney disease have been identified using this approach (Garrett, Pezzolesi, & Korstanje, 2010). Three GWAS for DN in Japanese, Pima Indians (native Americans), and Caucasians have been conducted (McDonough et al., 2011). A landmark GWAS, an analysis of 115,352 SNPs in pools of 105 unrelated case subjects with ESRD and 102 unrelated control subjects who have had type 2 diabetes for 10 years or more without macroalbuminuria, was performed in Pima Indians. It indicated that SNPs showing the strongest evidence for association with ESRD were located within the PVT1 gene, which provided the first evidence supporting PVT1 as a potential gene for ESRD (Hanson et al., 2007). Another SNP genotyping study demonstrated PVT1 was associated with ESRD in Caucasians with type 1 diabetes, which was an independent and ethnically distinct population (Millis, Bowen, Kingsley, Watanabe, & Wolford, 2007). Taken together, PVT1 is suggested to be a key determinant of ESRD across populations.

1.4.3 *In vitro* studies

Expression of PVT1 was found in human renal cells such as epithelial cells, mesangial cells, cortical epithelial cells and proximal tubule epithelial cells (Millis et al., 2007). In response to high glucose conditions, expression of PVT1, secreted collagen type IV alpha 1 (COL4A1), TGF-β1, fibronectin 1 (FN1) and PAI-1 were significantly upregulated in human mesangial cells when compared to those under normal glucose conditions. Inhibition of PVT1 expression using RNA interference showed significant decreases in both mRNA and protein levels of fibronectin, collagen type IV alpha 1, TGF-β1 and PAI-1. Of note, PVT1 knockdown in mesangial cells led to a significantly higher and more rapid reduction in levels of secreted FN1, COL4A1, and PAI-1 compared with TGF-β1. This finding suggested that PVT1 may regulate expression of ECM proteins at least in part independent of TGF-β1 (Alvarez & DiStefano, 2011).

1.4.4 *In vivo* study

At present, PVT1 is the only lncRNA that have been reported to be associated with DN. However, its mechanism of action is not yet clearly elucidated. In order to further characterize the role of PVT1 in the development of DN, *in vivo* study should be conducted. There is limited *in vivo* data elaborating the relationship between PVT1 and DN so far. Therefore, this study was conducted to investigate the role of PVT1 on development of DN in murine models, the feasibility of *in vivo* knockdown of PVT1 using target siRNA, the potential mechanism of action, and if PVT1 would be a novel therapeutic target for DN. It was hypothesized that inhibition of PVT1 would prevent the development of DN, in which the important role of PVT1 could be concluded in agreement with the GWAS and *in vitro* studies.

Figure 1.2: Potential mechanism for PVT1 involvement in ECM accumulation (adapted from Alvarez & DiStefano, 2011)

Hyperglycemia causes an excessive ECM accumulation in the glomerular mesangium which constitutes the major pathological feature of the glomerulosclerosis or glomerular fibrosis. Hyperglycemic conditions induce an increase in PVT1 expression in mesangial cells which contributes to the increase of the two main ECM components, FN1 and COL4A1, as well as the two main regulators of ECM accumulation in the glomeruli, PAI-1 and TGF-β1. PAI-1 is the main inhibitor of glomerular ECM degradation and TGF-β1 promotes glomerular fibrosis by upregulating genes encoding ECM proteins and PAI-1. PAI-1 and TGF-β1 transcriptionally regulate each other creating a vicious cycle of reciprocal stimulation that perpetuates the fibrotic response. PVT1 may contribute to ECM accumulation mainly through a TGF-β1-independent mechanism. FN1: fibronectin 1; COL4A1: alpha 1 type IV collagen; PAI-1: plasminogen activator inhibitor; TGF-β1: transforming growth factor-β1.

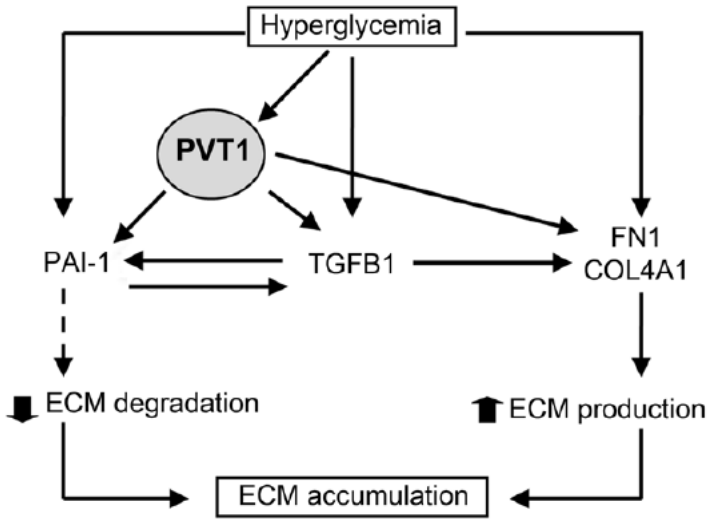

1.5 Animal models of DN

1.5.1 Ideal animal model of DN

There is no single animal model develops the full range of renal changes that are identical to those seen in human DN (Inada et al., 2005; Soler, Riera, & Batlle, 2012). Although some mouse strains are more susceptible to DN, progressive development of renal insufficiency leading to ESRD is not seen in murine models (Schlöndorff, 2010). The NIH-supported Animal Models of Diabetic Complications Consortium (AMDCC) was established in part to develop and characterize models of DN and other complications (Brosius et al., 2009). The AMDCC proposed three criteria for a desirable murine model of DN: (1) more than 50% decline in glomerular filtration rate (GFR) over the lifetime of the animal; (2) greater than 10-fold increase in albuminuria compared with controls for that strain at the same age and gender; (3) histopathology findings which include mesangial sclerosis (a 50% increase in mesangial volume), any degree of arteriolar hyalinosis, glomerular basement membrane thickening (a >25% increase compared with baseline by electron microscopy morphometry), and tubulointerstitial fibrosis (Alpers & Hudkins, 2011; Brosius et al., 2009; Inada et al., 2005; Kong et al., 2013; Schlöndorff, 2010; Greg H Tesch & Allen, 2007). Although there are no murine models that meet all of the three criteria (Kong et al., 2013), a number of rodent of models of DN have been characterized and used.

1.5.2 Chemical induction of diabetes and DN

Rodent models of DN can be generated by artificial induction, spontaneously developed and genetical engineering (knockout and transgenic). Although the spontaneous and genetically engineered diabetic models are valuable tools, they could not be used for this study due to regulatory concern. Chemical substances, such as streptozotocin (STZ) and

alloxan, are most widely used to induce experimental diabetes in animals (Szkudelski, 2001). Both STZ and alloxan are glucose analogues that preferentially accumulate in pancreatic β-cells via the GLUT2 glucose transporter. STZ and alloxan exert their cytotoxicity via DNA alkylation and generation of reactive oxygen species (ROS) respectively (Lenzen, 2008). They selectively damage the insulin-producing β-cells resulting in hyperglycemia, which subsequently causes kidney damage with similarities to DN in human (Kong et al., 2013). STZ is the preferred diabetogenic agent for reproducible induction of diabetes (Lenzen, 2008; Sugano et al., 2006). STZ-induced diabetes has proved to be a good model with which to study the pathophysiology of DN (Kraynak et al., 1995). These models are typically regarded as models of type 1 diabetes and are usually performed in mice, Sprague-Dawley and Wistar-Kyoto rats. A range of early functional and structural manifestations of DN is exhibited depending on the genetic background.

Higher dosage of STZ causes greater cytotoxicity and more rapid destruction of pancreatic β-cells, resulting in a higher incidence and severity of diabetes. Injection of moderate to high-dose STZ (such as a single-dose of ≥200 mg/kg STZ or a two-dose of 100-125 mg/kg STZ for two consecutive days) has shown to cause acute kidney damage in mice and rats (Kraynak et al., 1995; Greg H Tesch & Allen, 2007). Although models treated with higher dosage of STZ displayed higher albuminuria than those with low dosage, the nephropathy resulted from hyperglycemia-induced injury superimposed on acute renal STZ cytotoxicity which confound the interpretation of results (Kong et al., 2013; Tay et al., 2005).

In order to reduce nonspecific nephrotoxicity of STZ, the regimen of multiple low-dose injections of STZ (e.g. daily intraperitoneal injections of 40-60 mg/kg STZ for five consecutive days) which induces repetitive low-grade β-cell damage accompanied by pancreatic insulitis is suggested (Kolb-Bachofen, Epstein, Kiesel, & Kolb, 1988; A. Like, Appel, Williams, & Rossini, 1978; A. A. Like & Rossini, 1976). Moreover the low-dose STZ regimen did not result in loss of podocyte markers such as WT-1 or apparent decrement in podocyte number 3 days after the regimen completion in C57BL/6J mice, which suggested that such regimen has no toxic effects on podocytes (Breyer, 2005; Siu, Saha, Smoyer, Sullivan, & Brosius, 2006). According to the AMDCC, mouse models of DN should be induced by daily intraperitoneally injections of 50 mg/kg STZ for five consecutive days after fasting. Previous studies demonstrated that low-dose STZ-treated mice developed marked hyperglycemia, glomerular hypertrophy, modest levels of albuminuria and mild mesangial matrix expansion (Gurley et al., 2006; Kong et al., 2013). However, these models do not progress to more advanced DN seen in human. Advanced structural lesions such as arteriolar hyalinosis and nodular glomerulosclerosis that are characteristics of advanced DN in human are generally absent in mice (Alpers & Hudkins, 2011; Breyer, 2005).

1.5.3 High fat diet-induced DN

High fat diet is widely used to induce insulin resistance and obesity, as well as accelerated atherosclerosis in mice and rats. Diabetic animals developed by this approach is referred to models of type 2 diabetes. The effect of high fat diet depends on the strain of mouse (R. Surwit et al., 1995). Previous studies demonstrated that C57BL/6J mice respond strongly to high-fat diet and are a robust model for type 2 diabetes (Kunjathoor, Wilson, & LeBoeuf, 1996; R. S. Surwit, Kuhn, Cochrane, McCubbin, & Feinglos, 1988; Winzell & Ahrén, 2004). C57BL/6J mice fed on high fat diet (e.g. 45% total calories from fat for

9-13 weeks) exhibit obesity, hyperglycaemia, hyperinsulinemia, increased type IV collagen deposition, mesangial cell dedifferentiation, enlarged glomerular tufts and hyperfiltration (Wei, Lane, Lane, Padanilam, & Sansom, 2004). Similarly, mice receiving a higher fat diet (e.g. 60% total calories from fat for 12 weeks) showed other early signs of DN, which include kidney hypertrophy, increased UAE, GBM thickening, glomerular lesions with accumulation of extracellular matrix proteins. In addition, lipid accumulation, macrophage infiltration, increased oxidative stress and impaired sodium handling were also noted (Deji et al., 2009; Jiang et al., 2005).

1.5.4 New models of type 2 diabetes and DN

Recently some researchers developed a new rodent model by treating the animal with high-fat diet and low-dose STZ which would closely mimic the natural history of the disease events (from insulin resistance to pancreatic β-cell dysfunction) as well as metabolic characteristics of human type 2 diabetes in a shorter timescale (Skovsø, 2014; Srinivasan & Ramarao, 2007; M. Zhang, Lv, Li, Xu, & Chen, 2009). The combined treatment of high fat diet (40% calories from fat) and low-dose STZ (50 mg/kg) has shown to induce significant increase in serum glucose, insulin, free fatty acid and triglycerides in SD rats when compared with controls with normal diet (Reed et al., 2000). A similar study demonstrated the combined treatment (using 35 mg/kg STZ and 58% calories from fat) induced stable hyperglycemia for a period over 10 weeks, which suggested this model could be useful for the long-term studies on diabetic complications such as nephropathy and hypertension (Srinivasan, Viswanad, Asrat, Kaul, & Ramarao, 2005). These models responded to the antihyperglycemic compounds such as metformin, troglitazone, pioglitazone, or glipizide. In C57BL/6J mice, treatment of STZ and high fat diet synergistically exacerbated DN, as indicated by marked increase in albuminuria, mesangial expansion, podocyte damage, glomerular macrophage infiltration, and gene

expression of proinflammatory and ECM-associated components (such as PAI-1, fibronectin) (Kuwabara et al., 2012). Collectively, combination of high fat diet and low-dose STZ provides a novel animal model for type 2 diabetes and DN (D. Chen & Wang, 2005).

1.5.5 Uninephrectomized models of STZ-induced DN

Models of DN induced by STZ alone required a long period (9-12 months) for clear renal structural alterations to be observed. Therefore some researchers performed uninephrectomy in parallel to STZ and/or high fat diet regimen which caused enlargement of the remaining kidney and accelerated the progression of DN in rats (W. Qi et al., 2011). Uninephrectomy accelerated mesangial expansion, increased glomerular blood flow and glomerular capillary pressures, which is an important determinant of the diabetic glomerulopathy (Mauer, Steffes, & Brown, 1981). It is reported that rats with three-fourths nephrectomy and single STZ injection developed significant proteinuria, creatinine clearance decline, histological changes (e.g. extensive diffusion in glomerular capillary loops, mesangial areas, Bowman's capsule and glomerular capillary coagulation) within a fairly short period (Yokozawa, Nakagawa, Wakaki, & Koizumi, 2001). In SHR rats with STZ treatment, uninephrectomy led to an increase in glomerular capillary pressure which promoted diabetic glomerular injury (Kang, Ingram, Ly, Thai, & Scholey, 2000). Significant increase in glomerular size and mesangial matrix was observed in uninephrectomized STZ-treated CD-1 mice (Wada et al., 2001). However, interpretation of this kind of model is complex because it is difficult to dissect the relative contributions of STZ-induced hyperglycemia and uninephrectomy-induced glomerular hemodynamics in the development of DN (Greg H Tesch & Allen, 2007). Furthermore, uninephrectomy is an invasive procedure that require surgical intervention and longer time for the animals

to recover, which is less convenient to perform than the simple intravenous or intraperitoneal injection of STZ.

1.5.6 Genetic, gender and age susceptibility to induced DN

Genetic background, gender and age affect the susceptibility of rodents to STZ-induced and diet-induced diabetes and development of nephropathy as well (R. Surwit et al., 1995; Greg H Tesch & Allen, 2007). Male rodents are generally more susceptible to the effects of STZ and tend to develop greater hyperglycemia (Leiter, 1982; Greg H Tesch & Allen, 2007). A large amount of literature has used male mice and rats as STZ-induced models of diabetes.

It is noted young rodents like young people have the capacity of increasing β-cell mass, while old rodents (> 1 yr of age) have no such capacity (Skovsø, 2014). Therefore some study adopted two rounds of low-dose STZ injections to avoid recovery of some degree of β-cell function and to ensure durable hyperglycemia (Gurley et al., 2006). A study using 4-6 month-old STZ-diabetic C57BL/6J mice failed to demonstrate effects of high fat diet on kidney functions (e.g. urinary albumin excretion and creatinine clearance) and renal morphology (e.g. mesangial expansion, GMB thickening, glomerulosclerosis and tubulointerstitial fibrosis) when compared to those fed with normal diet (F. Li et al., 2010). It appeared that induction of diabetes by STZ and/or diet at a relatively old age in mice result in a less responsive model. Although there is no absolute agreement of age for induction of diabetes, numerous literatures generally adopted to use mice at a relatively young age (e.g. 4-8 weeks of age).

In response to multiple low-dose of STZ, a hierarchical response of blood glucose level follows in the order of mouse strain DBA/2J > C57BL/6J > MRL/MP > 129SvEv > BALB/c (Gurley et al., 2006). Although albuminuria, GBM thickness, mesangial expansion and HbA1c were increased in response to STZ treatment, C57BL/6J mice are relatively resistant to DN when compared to DBA/2J and KK/HIJ mice (Z. Qi et al., 2005). However C57BL/6J mice are highly susceptible to obesity-induced insulin resistance resulting high fat diet (Gregory H Tesch & Nikolic-Paterson, 2006). As mentioned above, the fat-fed and STZ-treated mice have displayed characteristics of type 2 DN. Importantly, the PVT1 gene to be investigated in this study is firstly discovered in mice and is homologous to human, which implying that mouse is the preferred and genetically relevant animal model for the study (Colombo et al., 2015). Taken together, male C57BL/6J mice of relatively young age are used in this study.

1.6 Gene silencing by RNA interference (RNAi)

1.6.1 Mechanism and significance of RNAi

The phenomenon of RNA interference (RNAi) or post-transcriptional gene silencing (PTGS) was first discovered in the nematode worm *Caenorhabditis elegans* as a response to double-stranded RNA (dsRNA), which resulted in sequence-specific gene silencing (Hannon, 2002). RNAi is mediated by small interfering RNAs (siRNAs) which are intracellularly generated from long endogenous or exogenous double-stranded RNA molecules through the cleavage activity of a ribonuclease III-type protein. More specifically, the protein Dicer which typically contains an N-terminal RNA helicase domain, an RNA-binding so-called Piwi/Argonaute/Zwille (PAZ) domain, two RNase III domains and a double-stranded RNA binding domain (dsRBD), leads to the formation of short 21–23 nt duplexes with a symmetric 2 nt overhang at the 3’-end and a 5’-phosphate and 3’-hydroxy group referred to as siRNAs. This siRNA molecule is incorporated into a

nuclease-containing multi-protein complex called RNA-induced silencing complex (RISC) which becomes activated (RISC*) upon the loss of one strand of the siRNA duplex by an RNA helicase activity. By binding of the now single-stranded siRNA to a complementary target RNA molecule, it sequence-specifically guides the RISC complex to the target RNA and induces endonucleolytic cleavage of the mRNA strand within the target (Aigner, 2006; Akhtar & Benter, 2007). The schematic representations of siRNA and mechanism of RNAi are shown in Figure 1.3 and Figure 1.4, respectively.

The discovery of the mechanism behind RNAi was acknowledged by the award of Nobel Prize in Physiology and Medicine in 2006 to Andrew Fire and Craig Mello (Edelstein, Abedi, & Wixon, 2007). RNAi has become a powerful tool for exploring gene function and developing potential RNAi-based therapies through targeted gene silencing (Hannon, 2002). Clinical trials using RNAi-based therapies for diseases including age-related macular degeneration (AMD), respiratory syncytial virus (RSV) infection, hepatitis C, asthma and Huntington's disease have been conducted (de Fougerolles, Vornlocher, Maraganore, & Lieberman, 2007; Edelstein et al., 2007; D. H. Kim & Rossi, 2007). The first clinical trial was performed in patients with AMD using a single intravitreal dose of sirna-027 targeting vascular endothelial growth factor receptor I, which showed that the sirna-027 was safe and stabilization or improvement in visual acuity and foveal thickness was observed (Kaiser et al., 2010; Whelan, 2005). In 2007, clinical trial with the first systemic delivery of siRNA, AKIi-5, for treatment of acute kidney injury was performed (Burnett, Rossi, & Tiemann, 2011; Nguyen, Menocal, Harborth, & Fruehauf, 2008). The principal advantages of RNAi over traditional pharmaceutical drugs (small molecules, proteins and antibodies) are that all targets, including 'non-druggable' targets, can be inhibited with RNAi and that lead compounds can be rapidly identified and optimized. However only antagonism of the specific molecular target is possible in RNAi-based

therapy, whereas traditional pharmaceutical drugs provide an opportunity for agonism of a molecular target (Bumcrot, Manoharan, Koteliansky, & Sah, 2006). Even so, RNAi remains to be a promising approach for development of novel therapeutics for a range of human diseases.

Figure 1.3: A schematic presentation of siRNA. A siRNA typically consists of two 21-nucleotide (nt) single-stranded RNAs that form a 19-bp duplex with 2-nt 3' overhangs (referenced to (McManus & Sharp, 2002)).

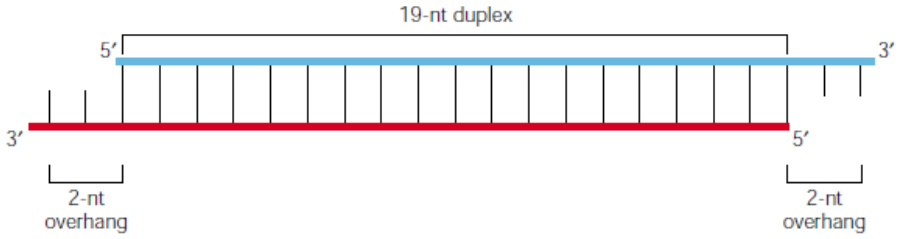

Figure 1.4: Mechanism of RNA interference (RNAi) in mammalian system (referenced to (Aigner, 2006))

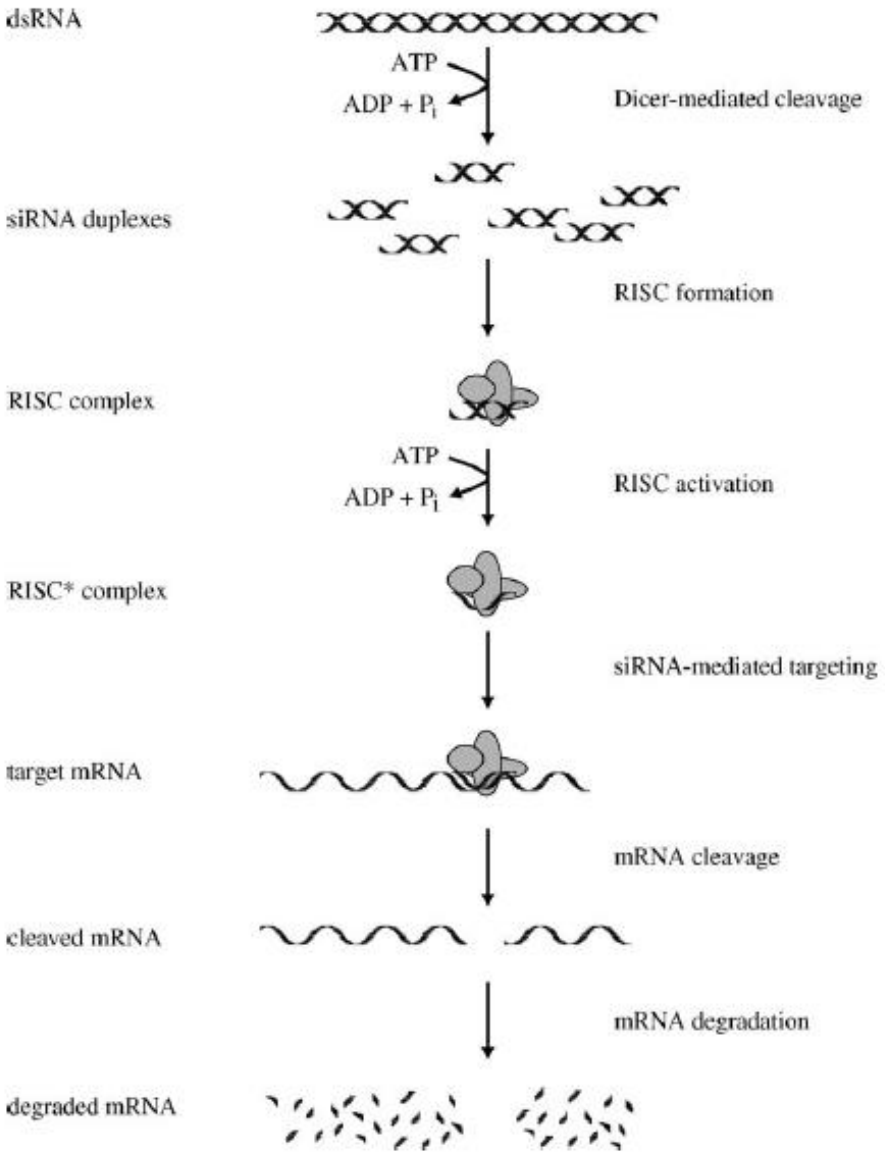

1.6.2 Challenges of siRNA delivery *in vivo*

Effective delivery of siRNA is the most challenging hurdle in RNAi *in vivo* (de Fougerolles et al., 2007). Despite quite efficient and reliable gene silencing *in vitro*, only limited RNAi has been achieved *in vivo* because of rapid enzymatic degradation by endogenous nucleases, uptake by phagocytes, aggregation with serum proteins, poor cellular uptake of siRNA, and kidney filtration (Shim & Kwon, 2010). In order to enhance RNAi efficacy, delivery strategy (local or systemic), delivery system (chemical modification or transfection agents/ siRNA carriers) and siRNA design, must be carefully considered. The route of administration depends on the types of target tissues and cells. Systemic delivery via intravenous (i.v.) or intraperitoneal (i.p.) is widely applicable when the target sites are not locally confined or not readily accessible, such as kidneys. Of note, systemic siRNA delivery imposes additional barriers that the siRNA should remain in its active form during circulation and reach target tissues after passing through multiple barrier organs (e.g. liver, kidney and lymphoid organs) (Shim & Kwon, 2010).

Since the naked siRNA has large molecular weight (about 13 kDa) and polyanionic nature (about 40 negative phosphate charges), it does not freely cross the cell membrane (Akhtar & Benter, 2007). As the siRNA has relatively short half-life *in vivo* due to rapid degradation by endogenous enzymes, delivery systems or chemical modification of siRNA are required to facilitate its access to the target cells. Judicious use of chemical modifications can improve the stability of a siRNA duplex, decrease the likelihood of triggering an innate immune response, lower the incidence of off-target effects (OTEs), and improve pharmacodynamics. However chemical modifications can alter the potency of the siRNA and frequently a chemically modified siRNA will show lower potency than the unmodified one of the same sequence, especially when extensively modified (Behlke, 2008). To date, several types of delivery systems have been developed to facilitate siRNA

delivery *in vivo*, which includes liposomes, cationic polymers, cationic liposomes (Whitehead, Langer, & Anderson, 2009). Complex formation with cationic polymers or incorporation into liposomes are a promising approach for delivery of siRNAs because they are prevented from being excreted from the kidney due to their size. In addition, the positive charge of the complex of siRNAs and carriers could enhance cellular uptake through electrostatic interaction with the negative charge on the cell membrane. Moreover, surface modification of cationic compounds with polyethyleneimine (PEG) and/or ligands enables the cell-selective targeting of siRNAs *in vivo* (Kawakami & Hashida, 2007). The effectiveness of RNAi also relies on the design of siRNA. Effective gene silencing comes with perfect or near-perfect Watson-Crick base pairing between the mRNA transcript and the antisense or guide strand of the siRNA, which results in cleavage of the mRNA by the RISC (D. H. Kim & Rossi, 2007). It is reported at least eight specific determinants of siRNA functionality have been identified through analysing thermodynamic characteristics of the siRNA test panel. Three criteria are particularly important for siRNA functionality, which includes moderate to low G/C content, low internal stability of the sense 3'-end (5' antisense) and a lack of internal repeats or palindromes that may form internal fold-back structures to reducing the effective concentration and silencing potential of the siRNA. The remaining five criteria describe base preferences at specific positions (positions 3, 10, 13 and 19) of the sense strand. (Reynolds et al., 2004).

1.7 Hypothesis, aims and significance of this study

Recent genome-wide association studies suggested PVT1 is a key determinant of ESRD, which is largely accounted from DN. Some *in vitro* studies suggested PVT1 plays an important role in mediating the development of DN through the ECM accumulation. It is

hypothesized that PVT1 promotes the development of DN *in vivo*, whereas inhibition of PVT1 prevents such development through reducing ECM accumulation.

This study aims to study the role of PVT1 in murine models of DN. Evaluations at functional level (e.g. UAE, UACR, UPE, UPCR, creatinine clearance and serum creatinine), histological level (e.g. kidney hypertrophy, glomerular area and mesangial area) and molecular level (e.g. gene expressions of PVT1, TGF-β1, PAI-1, FN1, COL4A1 and BMP7) were covered.

The specific aims are:

(1) to establish early, intermediate and relatively advanced stages of DN in C57BL/6 mice using a combination treatment of high fat diet and low dose STZ; and

(2) to study expression levels of PVT1 and extracellular matrix (ECM) components at early, intermediate and relatively advanced stages of DN in C57BL/6 mice; (Chapter 3)

(3) to study the effectiveness of PVT1 inhibition in C57BL/6 mice using RNAi; and

(4) to study the effect of PVT1 inhibition on progression of DN in diabetic C57BL/6 mice at early, intermediate and relatively advanced ages. (Chapter 4)

Findings for the former aims (1) and (2) were covered in Chapter 3 while for the later aims (3) and (4) were covered in Chapter 4. Discussions and conclusions are covered in Chapter 5.

Since there is only limited study on PVT1 in relation to development of DN, this study helps to provide some scientific evidence on their relationship, the potential mechanism of action and therapeutic target for DN. Furthermore, the establishment of DN in

C57BL/6 mice using the combination treatment of high fat diet and low dose STZ provides a useful tool for *in vivo* study of DN.

CHAPTER 2: MATERIALS AND METHODS

2.1 Animals and treatments

2.1.1 Animals

All animal experiments were approved by the Animal Ethics Committee at University of Auckland. Male C57BL/6J mice were obtained from Vernon Jansen Unit (VJU) of University of Auckland. They were housed in the animal facility maintained on constant temperature (22-25 °C), relative humidity (55-65%) and 12 hr light/12 hr dark cycles.

After weaning, the mice were fed with either high fat diet (HFD, 60% kcal from fat; TD06414, Enivgo, Madison, WI) or low fat control diet (LFD, 10% kcal from fat; TD08806, Enivgo, Madison, WI), and were supplied with tap water *ad libitum*. At 5 weeks of age, the HFD-fed mice were intraperitoneally administered with low-dose STZ (40 mg/kg of body weight per day) for three consecutive days after 4 hr fasting, while the LFD-fed mice were administered with vehicle (sodium citrate buffer). Type 2 diabetes was induced by the combination treatment of HFD and STZ. The diabetic group and normal control group were represented by the HFD-STZ-treated mice (diabetic) and the LFD-vehicle-treated mice (control), respectively. The effect of PVT1 inhibition on diabetic mice and control mice were investigated using *in vivo* RNA interference. Body weights and blood glucose were measured weekly on the commence of the study. The mice were culled at the age of 9 (young), 16 (middle-aged) or 24 (old) weeks old which represented early, intermediate and relatively advanced stages of diabetes. Samples (e.g. blood, urine, and kidneys) were collected on or before culling.

2.1.2 **Animal study design**

The study was divided into 4 parts, namely Part I, Pilot study, Baseline study, and Part II. Part I experiment was aimed to study the effect of combination treatment of HFD and STZ on development of DN (Figure 2.11). Pilot study was aimed to study the efficacy of RNA interference of PVT1 in diabetic mice through siRNA administration (Figure 2.2). Baseline study was conducted to study the effect of PVT1 inhibition on control mice (Figure 2.3). Part II was aimed to study the effect of PVT1 inhibition on diabetic mice of different ages (Figure 2.4). Details on *in vivo* RNA interference, sample collection and analyses were mentioned in the sections below.

Figure 2.1: Part I experiment to study the effect of combination treatment of high fat diet and STZ to development of DN.

After weaning, the mice were divided into two groups. The diabetic and control group were fed with high fat diet and low fat control diet, respectively. At 5 weeks of age, the HFD-fed mice were intraperitoneally administered with low-dose STZ for three consecutive days, while the LFD-fed mice were administered with vehicle (sodium nitrate buffer). The mice were culled at the age of 9 (young), 16 (middle-aged) or 24 (old) weeks old.

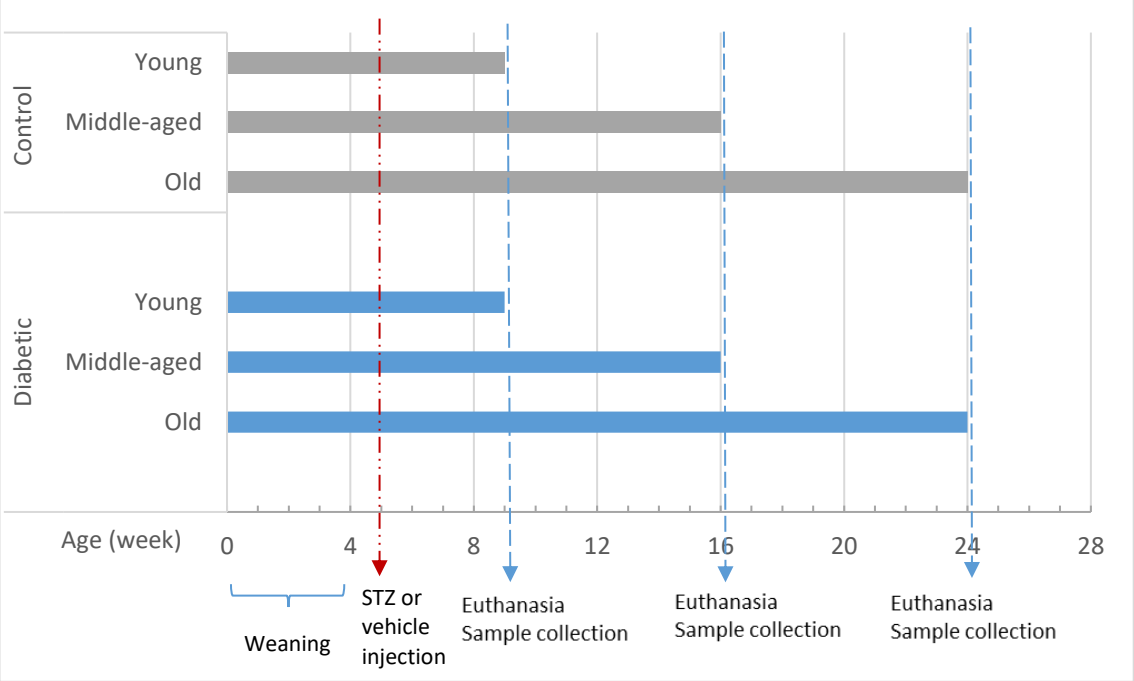

Figure 2.2: Pilot study to study the efficacy of RNA interference in diabetic mice. After weaning, the mice were fed with high fat diet. At 5 weeks of age, the HFD-fed mice were intraperitoneally administered with low dose STZ for three consecutive days. At 6 weeks of age, the mice were administered with either scramble-siRNA or PVT1-siRNA. The diabetic mice were culled at 2 days post siRNA injection.

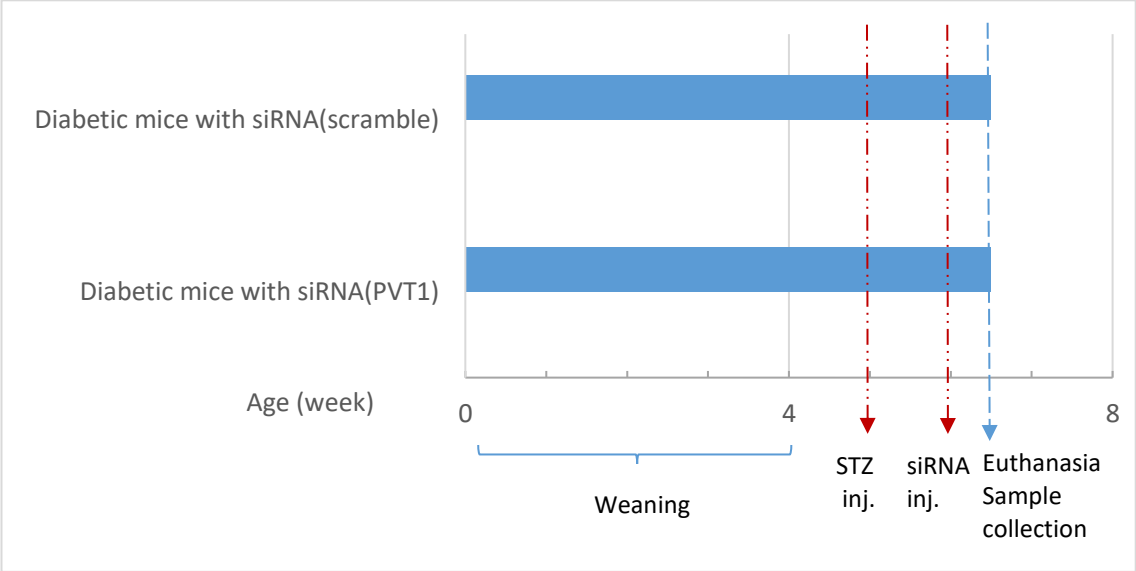

Figure 2.3: Baseline study to study the effect of PVT1 inhibition in control mice.

After weaning, the mice were fed with low fat control diet. At 5 weeks of age, the LFD-fed mice were intraperitoneally administered with vehicle (sodium nitrate buffer) for three consecutive days. At 6 weeks of age, the mice were administered with either scramble-siRNA or PVT1-siRNA. The control mice were culled at 2 days post siRNA injection.

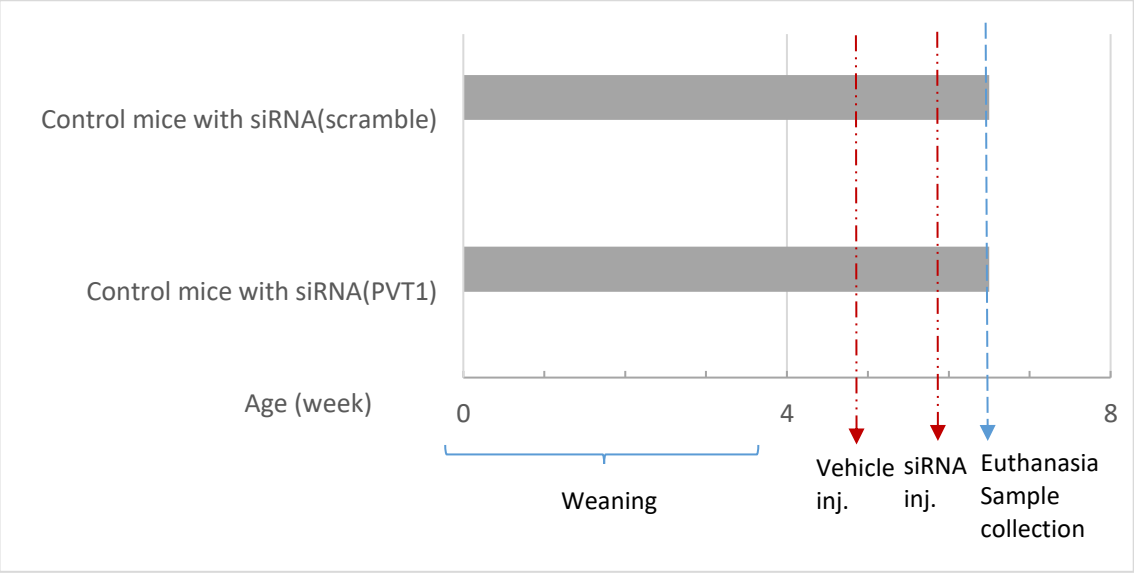

Figure 2.4: Part II experiment to study the effect of PVT1 inhibition in diabetic mice. After weaning, the mice were divided into two groups. The diabetic and control group were fed with high fat diet and low fat control diet, respectively. At 5 weeks of age, the HFD-fed mice were intraperitoneally administered with low-dose STZ for three consecutive days, while the LFD-fed mice were administered with vehicle (sodium nitrate buffer). From 6 weeks of age, the diabetic mice were monthly administered with either scramble-siRNA or PVT1-siRNA. The mice were culled at the age of 9 (young), 16 (middle-aged) or 24 (old) weeks old.

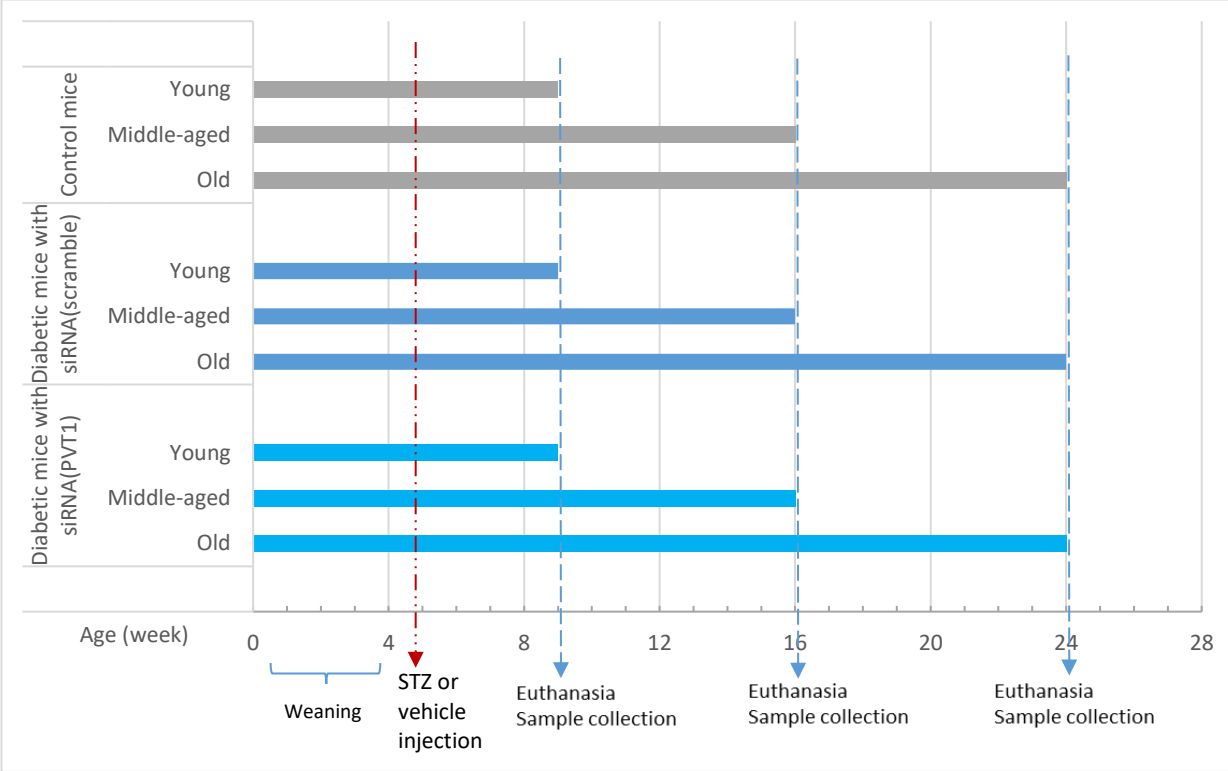

2.1.3 **Intraperitoneal injection of low dose STZ or vehicle**

The vehicle (sodium citrate buffer) was prepared by dissolving 1.47g of sodium citrate dihydrate (W302600, Sigma, Germany) in 50ml distilled water and followed by pH adjustment to pH 4.5. The solution was then filtered through a sterile 0.22μm filter (SLGP05010 Millipore, Merck, Germany) to remove bacteria. The filtered vehicle was ready for injection or for preparation of the STZ-vehicle solution.

The STZ-vehicle solution of 7.5mg/ml was prepared immediately prior to each injection. After mixing the STZ (S-0130, Sigma, Germany) into the filtered vehicle, the solution was covered with aluminium foil and used within 15mins to avoid degradation of STZ.

The mice were manually restrained. The injection sites (lower abdominal quadrant) were cleaned with 70% alcohol swabs. The sterile insulin syringes (29 G 1/2 in. 1.0 ml) were used to deliver the solution into the intraperitoneal cavity. The mice in diabetic group were injected with the STZ solution at a dose of 40mg/kg, while the mice in control group were injected with the filtered vehicle only.

2.1.4 ***In vivo*** **RNA interference of PVT1**

For PVT1 inhibition experiments, the mice were intravenously injected with PVT1-siRNA and those injected with scramble-siRNA were used as negative controls. The proprietary pre-designed PVT1-siRNA, scramble-siRNA, Invivofectamine 3.0 reagent (IVF3001), DNase/RNase-free distilled water (10977) and PBS (10010-23) were purchased from ThermoFisher Scientific, Carlsbad, CA.

The mice were injected at a dose of 2.5 mg/kg, which corresponded to 200 µl of 0.25 mg/ml injection solution for a 20 g mouse. The injection solution was prepared by mixing the 5 mg/ml siRNA solution ((PVT1-siRNA for treatment group or scramble-siRNA for control group) with the complexion buffer in a 1:1 ratio. The siRNA complex was immediately mixed with an equal volume of Invivofectamine reagent, which was then incubated for 30 min at 50°C. After a 6-fold dilution with PBS, the siRNA complex was ready for injection.

The mice were placed in the rodent retainer. The tails were covered with a warm water towel transiently to facilitate visualization of the lateral veins. Excess water on the tail was blotted dry. The injection sites were disinfected with the alcohol swabs. The sterile insulin syringes (29 G 1/2 in. 1.0 ml) were used to slowly inject (20-40 µl/second) the siRNA complex into the lateral tail veins. Transverse section view and sagittal view of the mouse tail were shown in Figure 2.5. A photo of intravenous injection into the lateral tail vein was shown in Figure 2.6. A successful injection was marked by a clearing of the blood (the siRNA complex solution was colourless). After completing the injection, the needle was removed and the injection site was gently pressured for several seconds to avoid backflow or bleeding.

Figure 2.5: (a) Transverse section view of the mouse tail; (b) sagittal view of the mouse tail (the tail is turned 90 degree).

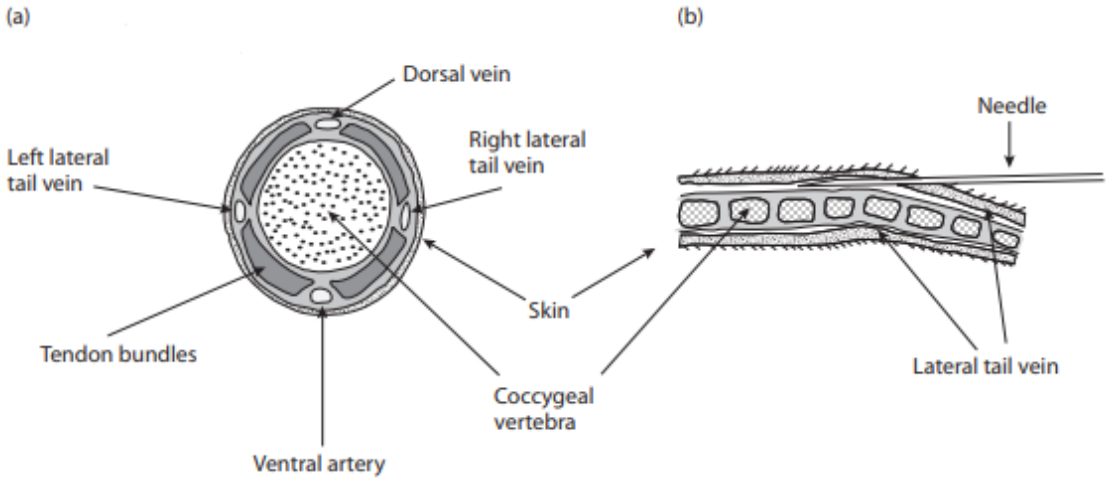

Figure 2.6: Intravenous injection into the lateral tail vein of a C57BL/6 mouse using an insulin syringe.

2.2 Blood chemistry

2.2.1 Blood glucose measurement

The mice were placed in the rodent restrainer. The tail lateral vein was punctured using a sterile lancet following site disinfection by alcohol swabs. A droplet of blood was drawn and blood glucose was measured by a glucometer (Refined CareSens N Meter, CareSens, Korea). In order to avoid diurnal variation in blood glucose, all measurements were conducted in the same time slot every week.

2.2.2 Serum preparation

The mice were culled at the designated time of the study. Blood was collected from the right ventricles by 1 ml syringe. The blood samples were left to stand for 30 min at room temperature, followed by centrifugation at 2000 rpm for 10 min at 4°C. Serum were collected and stored at -80°C until analysis.

2.2.3 Serum creatinine concentration

Serum creatinine concentration was determined by an enzymatic method (Mouse Creatinine Assay 80350; Crystal Chem, USA). This method involved a series of enzymatic reactions including enzymatic conversion of creatinine into creatine which is then converted to sarcosine (Figure 2.7). Sarcosine was oxidized to produce hydrogen peroxide (H_2O_2), which was measured at 550 nm in the presence of peroxidase. The difference in absorbance before and after the addition of peroxidase in each sample was calculated. The absorbance at 550 nm was proportional to the amount of creatinine and a standard curve was generated. The creatinine concentrations in the serum samples were quantified by interpolating their absorbance from the standard curve generated in parallel with the samples. After factoring sample dilutions, the creatinine concentrations in the original serum sample were determined.

Figure 2.7: Conversion of creatinine to hydrogen peroxide by enzymatic method

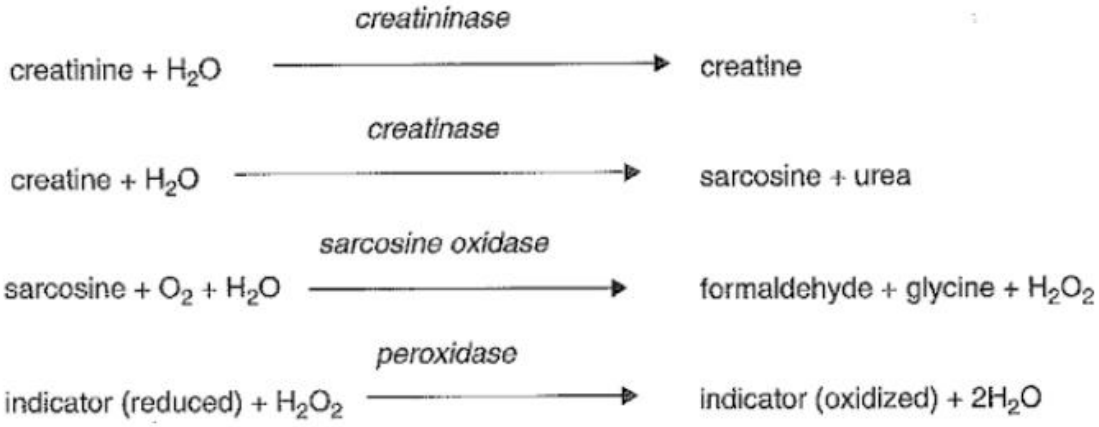

2.3 Non-invasive blood pressure (NIBP) measurement

The systolic blood pressure (SBP) measurements were made using a noninvasive blood pressure tail-cuff system (MLT125/M, ADInstruments) connected to a PowerLab system (PL3508, ADInstruments). For each measurement, mice were placed in a mouse restrainer and maintained at approximately 37°C using a heating pad throughout all training periods and measurements. Minimal mechanical vibration and sound level were maintained. To ensure acclimation to the procedure, each mouse underwent 3 days of mock measurements prior to data collection. Each training day consisted of 5 SBP measurements. For SBP readings, at least 5 technical replicates were performed for each time point on each mouse. The cuff pressure at which the tail pulse first reappeared after occlusion was identified as the SBP for analysis by the software LabChart (ADInstruments). However, the murine SBP was not successfully recorded owing to the measurement limitation of the blood pressure system. The vendor has adjusted the BP system, replaced the transducer and tail cuff of smaller diameter. The BP system could successfully record the SBP of rats but mice during onsite investigation and was returned to the manufacturer. Hence, the non-invasive blood pressure measurement of mice was terminated.

2.4 Urine chemistry

2.4.1 Urine collection

The mice were individually housed in the metabolic cages (Tecniplast, Australia) for 24 hr. The total volume of urine was recorded. The urine samples were centrifuged at 1500 rpm for 10 min at 4°C. The supernatant was collected and stored at -80°C until analysis.

2.4.2 Urinary albumin concentration

Urinary albumin concentration was determined by a sandwich ELISA (Mouse Albumin ELISA Kit BETHE99-134; Bethyl Laboratories, USA) as per manufacturer's instruction. Briefly, mouse albumin present in the urine was captured by anti-mouse albumin antibody that had been pre-adsorbed on the surface of microtiter wells. After sample binding, unbound proteins and molecules were washed off, and a biotinylated detection antibody was added to the wells to bind the captured albumin. A strepavidin-conjugated horseradish peroxidase (SA-HRP) was then added to catalyze a colorimetric reaction with the chromogenic substrate TMB (3,3',5,5'-tetramethylbenzidine). A blue product was produced, which was turned yellow when the reaction was terminated by addition of dilute sulfuric acid. The absorbance of the yellow product at 450 nm was proportional to the amount of albumin present in the sample and a standard curve was generated. The albumin concentrations in the urine samples were quantified by interpolating their absorbance from the standard curve generated in parallel with the samples. After factoring sample dilutions, the albumin concentrations in the original urine sample were determined.

2.4.3 **Urinary protein concentration**

Urine protein concentration was determined by Bradford assay that involves the binding of Coomassie Brilliant Blue G-250 dye to protein. A blue colour was produced quantitatively when protein in the sample bind to the dye in Bradford reagent (Bio-Rad Protein Assay Dye Reagent Concentrate, 5000006; Bio-Rad, USA). After incubation for 5 min at room temperature for colour development, the absorbance of the blue colour at 595 nm was proportional to the amount of protein present in the sample. A standard curve was generated using bovine serum albumin (BSA) of known concentrations. The protein concentrations in the urine samples were quantified by interpolating their absorbance from the standard curve generated in parallel with the samples. After factoring sample dilutions, the protein concentrations in the original urine sample were determined.

2.4.4 **Urinary creatinine concentration**

Urine creatinine concentration was determined by Jaffe's reaction (Creatinine Assay Kit (Colorimetric) ab204537; Abcam, USA). Briefly, an orange colour was produced quantitatively when creatinine in the sample reacted with alkaline picrate. After incubation for 30 min at room temperature for colour development, the absorbance of the orange colour at 490 nm was proportional to the amount of creatinine present in the sample and a standard curve was generated. The creatinine concentrations in the urine samples were quantified by interpolating their absorbance from the standard curve generated in parallel with the samples. After factoring sample dilutions, the creatinine concentrations in the original urine sample were determined.

2.5 Calculation of urinary albumin, protein and creatinine clearance

2.5.1 **Urinary Albumin to Creatinine Ratio (UACR)**

Urinary Albumin to Creatinine Ratio is a ratio of urinary albumin to urinary creatinine.

$$\text{UACR} = \frac{\text{Urinary Albumin (µg/µl)}}{\text{Urinary Creatinine (µg/µl)}}$$

2.5.2 **Urinary Albumin Excretion (UAE)**

Urinary Albumin Excretion is the excretion of albumin in urine in 24 hrs, expressed as (µg).

$$\text{UAE (µg)} = \text{Urinary Albumin (µg/µl)} \times \text{Volume of 24-hr urine (µl)}$$

2.5.3 **Urinary Protein to Creatinine Ratio (UPCR)**

Urinary Protein to Creatinine Ratio is a ratio of urinary protein to urinary creatinine.

$$UPCR = \frac{\text{Urinary Protein (µg/µl)}}{\text{Urinary Creatinine (µg/µl)}}$$

2.5.4 **Urinary Protein Excretion (UPE)**

Urinary Protein Excretion is the excretion of protein in urine in 24 hrs, expressed as (mg).

$$\text{UPE (mg)} = \text{Urinary Protein (mg/µl)} \times \text{Volume of 24-hr urine (µl)}$$

2.5.5 **Creatinine clearance**

Creatinine clearance as an estimated measure of glomerular filtration rate (GFR), expressed as (ml/min).

$$\text{Creatinine Clearance (ml/min)} = \frac{\text{Urinary Creatinine (µg/µl)}}{\text{Serum Creatinine (µg/µl)}} \times \frac{\text{Volume of 24-hr urine (ml)}}{\text{1440 (min)}}$$

2.6 Kidney tissue harvest

At culling, the kidney tissues were harvested in two ways (with or without perfusion) for different subsequent analyses. Kidneys perfused with Dynabeads M-450 Epoxy (diameter 4.5 µm 140-11; Invitrogen, CA, USA) were used for isolation of glomeruli for mRNA expression analysis. Kidneys without perfusion were weighed and then snap-frozen for histological analysis.

2.6.1 **Kidney weight measurement**

Kidneys without perfusion were harvested. Excessive body fluid was removed before weighing. The kidney weight and the ratio of kidney to body weight were determined.

2.6.2 **Kidney histological analysis**

The non-perfused kidneys were embedded in optimal cutting temperature (OCT) embedding media (Tissue-Tek O.C.T. Compound 4583, Sakura, The Netherlands) with coolant (Frosbite Rapid Coolant 3803100, Leica, Germany). The frozen kidney sections of 4 μm thick were cut using a microtome (Leica, Germany). The sections were stained with periodic acid Schiff (PAS) and counterstained with Mayer's hematoxylin (3801582E, Leica, Germany), which was one of the standard methods to analyse the kidney tissues. The nuclei were stained dark blue while the mucopolysaccharides were stained magneta or blue purple. Briefly, the microscopic slides were emerged into 0.5% periodic acid for 10 min, rinsed with distilled water, and incubated in Schiff reagent for 30 min followed by counterstain in Mayer's hematoxylin for 2 min. After washing in running tap water for 3 min, the bluing reagent was applied for 30 sec. The slides were rinsed with distilled water and then dehydrated through graded alcohols. The coverslips were mounted onto the slides using xylene-based mounting medium (Micromount 3801731, Leica, Germany). The microscopic images were captured using Leica ICC50 HD (Leica, Germany). The glomerular area and mesangial area were semi-quantified by the Image-J software (National Institutes of Health, USA). At least 8 glomeruli were randomly selected and analysed for each sample. The results were expressed as area in μm^2.

2.6.3 **Kidney perfusion**

The Dynabeads M-450 Epoxy (diameter 4.5 μm 140-11; Invitrogen, CA, USA) used in perfusion was prepared as per manufacturer's instruction. Briefly the Dynabeads stock was vortexed for 30 sec to ensure thorough mixing and washed with equal volume of fresh phosphate-buffered saline (PBS) for three times before use. The mice were perfused with $4x10^7$ Dynabeads M-450 Epoxy diluted in 10 ml of PBS through the left ventricle of the heart with the celiac artery clipped to reduce perfusion to the liver, and the inferior vena cava was punched to release excessive pressure during perfusion. Successful

perfusion was indicated by blanched kidneys. Kidneys with and without perfusion were shown in Figure 2.8. Kidneys were then removed, immerged in the RNAprotect Tissue Reagent and kept on ice prior to subsequent isolation of glomeruli.

2.6.4 **Isolation of glomeruli**

The kidney was rinsed with ice-cold PBS and excessive fluid was removed. The kidney cortex was then harvested and minced into 1 mm^3 pieces, and digested in collagenase solution (1 mg/ml collagenase A (10103578001; Roche, Germany), 100 U/ml deoxyribonuclease I (89836; Invitrogen, CA, USA) in HBSS) at 37°C for 30 minutes with gentle agitation at 10 min intervals. The collagenase-digested tissue was gently pressed through a 100 μm cell strainer (CORNING CLS431752; Merck, Germany) using a flattened glass rod and the cell strainer was then washed with 5 ml of ice-cold HBSS. The filtered cells were passed through a new cell strainer without pressing and the cell strainer washed with 5 ml of ice-cold HBSS. The cell suspension was then centrifuged at 200 x g for 5 minutes. The supernatant was discarded, and the cell pellet was resuspended in 1 ml of ice-cold HBSS. Finally, glomeruli containing Dynabeads were isolated by a magnetic particle concentrator (DynaMag-2 Magnet 12321D; Invitrogen, CA, USA) and washed for three times with HBSS. The whole procedure was performed on ice with the exception for the collagenase digestion at 37°C. The flow chart of isolation of glomeruli was shown in Figure 2.9. A microscopic view of isolated glomerulus was shown in Figure 2.10. The isolated glomeruli were subjected to mRNA expression analysis.

Figure 2.8: Kidneys with and without perfusion.

(A) The mouse was dissected without perfusion. The kidney was highlighted in solid arrow. (B) The mouse was perfused with Dynabeads solution through the left ventricle. The blanched kidney was highlighted in dashed arrow. (C) A perfused kidney (on the left) showed a lighter colour than a non-perfused kidney (on the right).

(A)

(B)

(C)

Figure 2.9: Flow chart of the isolation of glomeruli.

(i)

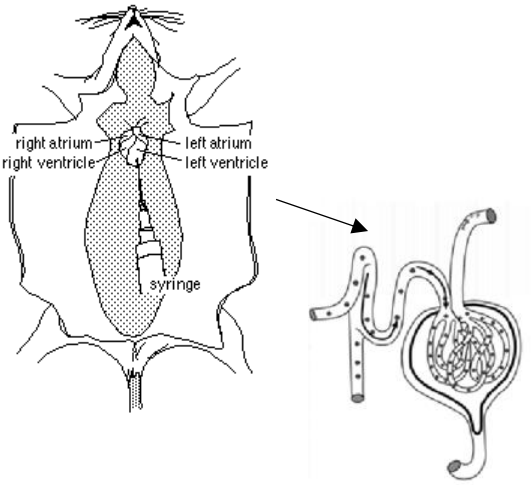

Perfusion with Dynabeads diluted in PBS through the left ventricle. Trapping of Dynabeads in the glomeruli.

(ii)

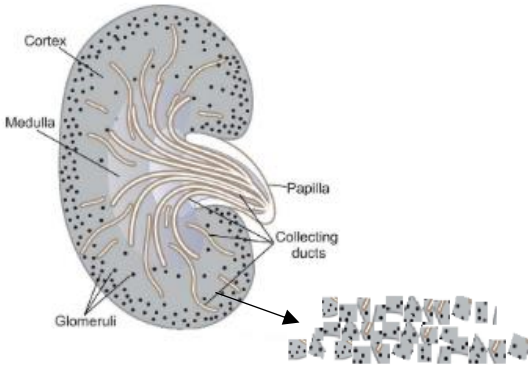

Kidney removal and subsequent processing e.g. cortex mincing into 1 mm^3 pieces.

(iii)

Digestion of kidney tissues with collagenase and deoxyribonuclease.

(iv)

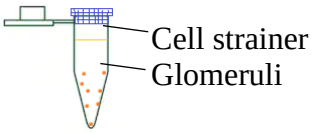

Filtration of kidney tissues with 100 µm cell strainer.

(v)

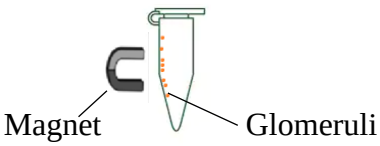

Isolation of glomeruli by a magnetic particle concentrator.

(vi)

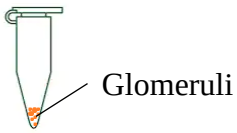

Collection of purified glomeruli.

Figure 2.10: Microscopic image of isolated glomerulus.

An isolated glomerulus containing Dynabeads was captured by Carl Zeiss microscope (100X).

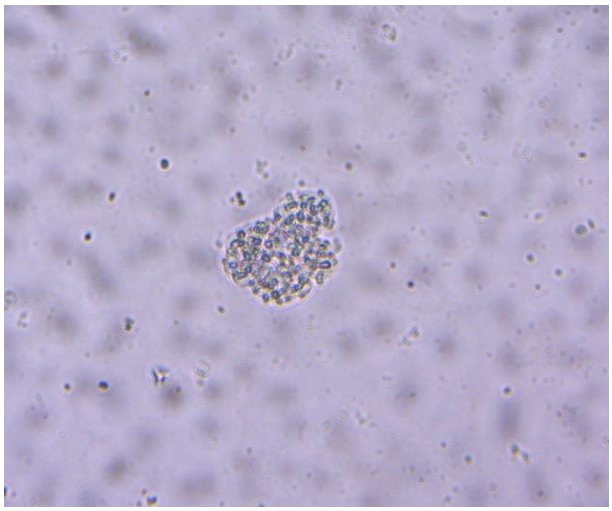

2.7 Gene expression analysis

2.7.1 RNA extraction and quantification

Total RNA from the isolated glomeruli was extracted using RNeasy Protect Mini Kit (74124; QIAGEN, USA) according to the manufacturer's instruction. Briefly, the glomeruli were lysed with the lysis buffer. The lysates together with ethanol were added to the RNeasy mini columns where the total RNA adsorbed to the silica-gel-based membrane. Following several spin washing steps, the contaminants were removed. The purified RNA was finally eluted in nuclease-free water and the samples were stored at -80°C until analysis.

The amount of RNA was quantified by Qubit RNA BR Assay Kits (Q10211; Invitrogen, CA, USA) with the Qubit Fluorometer 2.0 (Invitrogen, CA, USA). The samples were diluted with dilution buffer and transferred into Qubit Assay Tubes (Q32856; Invitrogen, CA, USA). After 2 min incubation at room temperature, the RNA concentrations were measured from the standard curve generated in parallel with the samples using the fluorometer. After factoring sample dilutions, the RNA concentrations in the original sample were determined. The result was expressed as ng/μl.

2.7.2 Reverse transcription

The cDNA was synthesized from RNA using SuperScript IV VILO Master Mix (11766050; Invitrogen, CA, USA) according the manufacturer's instruction. The total RNA (1 ng) was incubated with the gDNA digestion reaction mixture at 37°C for 2 min. It was then mixed with the master mix (containing SuperScript IV reverse transcriptase, recombinant RNase inhibitor, helper proteins, stabilizer proteins, oligo(dT)18, random hexamer primers, magnesium chloride, and dNTPs). The entire reaction mixture was

incubated at 25°C for 10 min for primer annealing, then at 50°C for 10 min for reverse transcription, and finally at 85°C for 5 min for enzyme inactivation. The resulting cDNA were stored at -80°C until analysis. Two negative controls of reverse transcription were performed to verify the absence of genomic DNA in the sample and the absence of contaminants in the master mix. The procedures were the same except for no reverse transcriptase and no RNA template were used in the reaction mixture, respectively. In both cases no cDNA were generated.

2.7.3 **Quantitative real-time polymerase chain reaction (PCR)**

The gene expression levels of PVT1, TGF-β1, PAI-1, FN1, COL4A1, BMP7 and housekeeping internal control GAPDH were quantified using real-time PCR. Briefly, total reaction mixture containing 20 ng of cDNA, 50 nM forward and reverse primers of targeted sequences (Invitrogen, CA, USA) and PowerUp SYBR Green Master Mix (A25741; Invitrogen, CA, USA) were used for running the real-time PCR on LightCycler 480 (Roche, Germany). All samples were run in duplicate using a 96-well optical plate. The thermal cycling conditions of the real-time PCR were set as Table 2.1. The forward and reverse primer sequences were shown in Table 2.2. The relative quantification of real-time PCR data was determined by the comparative threshold cycle method (delta-delta Ct method) (Table 2.3).

Table 2.1: Thermal cycling conditions of the real-time PCR

Step	Temperature	Duration	Cycles
UDG activation	50°C	2 min	Hold
Dual-Lock DNA polymerase	95°C	2 min	Hold
Denature	95°C	15 sec	50
Anneal/extend	60°C	1 min	

Table 2.2: Forward and reverse primers used in the real-time PCR

	Forward	Reverse
GADPH	GGCAAATTCAACGGCACAGT	GTCTCGCTCCTGGAAGATGG
PVT1	AGCGTTGACTTAAGAGATGCCA	GATTGCCTCCGGCATGAAGA
TGF-β1	GGACTCTCCACCTGCAAGAC	CTGGCGAGCCTTAGTTTGGA
PAI-1	CCGATGGGCTCGAGTATGAC	TTCTCAAAGGGTGCAGCGAT
FN1	ATACCGTTGTCCCAGAGGTG	GTGGAAGAGTTTAGCGGGGT
COL4A1	GGGAAATCCTGGTGACAGGG	AAGGAATGGCCGTGGTTTGA
BMP-7	GTCTGCCAGGAAAGTGTCCA	CGAGGCTTGCGATTACTCCT

Table 2.3: Relative quantification of real-time PCR data by delta-delta Ct method

$Ct_{GOI} - Ct_{Normalizer} = \Delta Ct$

$\Delta Ct_{Sample} - \Delta Ct_{Calibrator} = \Delta\Delta Ct$

Relative quantity = $2^{-\Delta\Delta Ct}$

Keys:

Ct_{GOI} : Ct gene of interest

$Ct_{Normalizer}$: Ct Normalizer (housekeeping gene)

2.8 Statistical analysis

All statistical analyses are performed using the software GraphPad Prism. Results were presented as the means ± SEM in each group. Data were analysed using unpaired student's t-test (for two data groups) or one-way ANOVA with a Tukey's Multiple Comparison post-test (for three data groups). Results were considered statistically significant if p-value < 0.05.

CHAPTER 3: EXPRESSION OF PVT1 AND ECM COMPONENTS IN C57BL/6 MICE AT DIFFERENT STAGES OF DN

3.1 Introduction

Recent genome-wide association studies suggested plasmacytoma variant translocation 1 (PVT1) is a key determinant of end stage renal disease (ESRD), which is largely accounted from DN. Some *in vitro* studies suggested PVT1 plays an important role in mediating the development of DN through the extracellular matrix (ECM) accumulation. It is hypothesized that PVT1 promotes the development of DN *in vivo*, whereas inhibition of PVT1 prevents such development through reducing ECM accumulation. The role of PVT1 in relation the ECM components on DN was discussed herein and the next chapter. In this chapter, the murine model of DN was established using a combination treatment of high fat diet and multiple low dose STZ, where blood glucose level, albuminuria, renal function and histology, and gene expression analysis (gene expressions of PVT1 and ECM components and regulators) were covered.

3.2 Plasmacytoma variant translocation 1 (PVT1)

3.2.1 Background of PVT1

PVT1 is a long noncoding RNA (lncRNA) (1.9 kb) that encodes a number of alternative transcripts but no protein product has been identified so far (Sonoki, 2014; Wu et al., 2015). Long noncoding RNAs (more than 200 nucleotides in length) is a functionally diverse set of noncoding RNAs that act as modular molecules regulating many processes including transcription and RNA expression (Leung & Natarajan, 2014). The human

PVT1 gene is homologous to the mouse plasmacytoma variant translocation gene (Colombo et al., 2015). PVT1 is strongly conserved between human and mouse (Guan et al., 2007). In mouse, PVT1 locus is a site of recurrent translocation in plasmacytomas and is a common site of tumorigenic retroviral insertion in lymphomas. In human, the region homologous to PVT1 is a site of recurrent translocation between chromosomes 2 and 8 (Guan et al., 2007). Most studies of PVT1 are related to cancers, particularly lymphomas, ovarian and breast cancers. PVT1 is known to contribute to ovarian and breast cancers when overexpressed and amplified. Silencing of PVT1 expression by RNA interference decreases cell proliferation and increases apoptosis in breast and ovarian cancer cell lines in which it was amplified and overexpressed but not in cell lines where it is not amplified and overexpressed (Guan et al., 2007). PVT1 is expressed at high levels in the kidneys, although its role is not yet well defined (Hanson et al., 2007).

3.2.2 **Genome-wide association study for DN**

Genetic susceptibility plays an important role in the pathogenesis of DN (Craig et al., 2009; Maeda, 2008). Different research approaches, such as linkage analysis, candidate gene approach, mapping by admixture linkage disequilibrium (MALD) and genome-wide association study (GWAS), are used to identify the susceptibility genes for common diseases including DN (Divers & Freedman, 2010; Freedman et al., 2007; Palmer & Freedman, 2012). GWAS scans hundreds of thousands of single nucleotide polymorphism (SNP) for association with a disease or quantitative trait, is a powerful and promising approach for identification of the susceptibility genes (Böger & Heid, 2011; Maeda, 2008; O'Seaghdha & Fox, 2012). To date, more than 100 loci for diseases including diabetes and chronic kidney disease have been identified using this approach (Garrett et al., 2010). Three GWAS for DN in Japanese, Pima Indians (native Americans), and Caucasians have been conducted (McDonough et al., 2011). A landmark GWAS, an

analysis of 115,352 SNPs in pools of 105 unrelated case subjects with ESRD and 102 unrelated control subjects who have had type 2 diabetes for 10 years or more without macroalbuminuria, was performed in Pima Indians. It indicated that SNPs showing the strongest evidence for association with ESRD were located within the PVT1 gene, which provided the first evidence supporting PVT1 as a potential gene for ESRD (Hanson et al., 2007). Another SNP genotyping study demonstrated PVT1 was associated with ESRD in Caucasians with type 1 diabetes, which was an independent and ethnically distinct population (Millis et al., 2007). Taken together, PVT1 is suggested to be a key determinant of ESRD across populations.

3.2.3 *In vitro* studies

Expression of PVT1 was found in human renal cells such as epithelial cells, mesangial cells, cortical epithelial cells and proximal tubule epithelial cells (Millis et al., 2007). In response to high glucose conditions for 96 hr, gene expression of PVT1 was significantly upregulated up to 5-fold in human mesangial cells when compared to those under normal glucose conditions. The increase of secreted collagen type IV alpha 1 (COL4A1) and TGF-β1 were 25% and 40% higher in mesangial cells under hyperglycemic conditions, and a 2-fold increase in secreted fibronectin 1 (FN1) and PAI-1 were observed. Inhibition of PVT1 expression using RNA interference showed significant decreases in both mRNA and protein levels of fibronectin, collagen type IV alpha 1, TGF-β1 and PAI-1. Of note, PVT1 knockdown in mesangial cells led to a significantly higher and more rapid reduction in levels of secreted FN1, COL4A1, and PAI-1 compared with TGF-β1. This finding suggested that PVT1 may regulate expression of ECM proteins at least in part independent of TGF-β1 (Alvarez & DiStefano, 2011). PVT1 is the host of a cluster of miRNAs (also known as microRNAs, small noncoding RNAs) that regulate gene expression through post-transcriptional repression of target coding RNAs (Huppi et al.,

2012; McKnight et al., 2010). There are at least six known miRNAs mapping to the PVT1 locus (Huppi et al., 2008). These PVT1-derived miRNAs were expressed in human mesangial cells, proximal tubule epithelial cells as well as podocytes. The mostly abundant miRNA, miR-1207-5p, was significantly upregulated by 2-fold in mesangial cells under hyperglycemic conditions. It also responded to exogenous TGF-β1 in a dose- and time-dependent manner. Overexpression of miR-1207-5p in mesangial cells led to marked increases in the levels of secreted PAI-1, TGF-β1 and fibronectin 1, whereas knockdown of miR-1207-5p abolished the increases. Interestingly, knockdown of PVT1 resulted in a 60% decrease in PVT1 in mesangial cells while miR-1207-5p mRNA remained unchanged. This finding suggested miR-1207-5p and its host gene PVT1 acted independently but both contributed to the ECM accumulation (Alvarez et al., 2013). These *in vitro* studies suggested that PVT1 plays an important role in mediating the development of DN through ECM, and at least some of its effects may be mediated through the actions of miRNAs (Alvarez & DiStefano, 2011, 2013). A recent study has shown the PVT1 expression is upregulated in human mesangial cells and PVT1 inhibition has ameliorated the high glucose-induced proliferation and fibrosis of the cells (W. Zhong et al, 2020). Similarly, PVT1 is highly expressed in primary mouse podocytes in high glucose concentration and PVT1 inhibition prevents the high glucose-induced podocyte damage and apoptosis (D. Liu et al, 2019).

3.2.4 ***In vivo* studies**

PVT1 is crucial to normal development as PVT1 knockouts cause embryonic lethality in mice (M. Cui et al, 2016). PVT1 expression is significantly higher in patients with DN (D.-W. Liu et al., 2019; Zhong, Zeng, Xue, Du, & Xu, 2020). In some disease models of DN (J. Li et al., 2020), acute kidney injury (AKI) (X. Zhu et al, 2018), sepsis (F. Feng et al, 2018), liver fibrosis (J. Zheng et al, 2016) and atrial fibrillation (F. Cao et al, 2019),

the PVT1 is highly expressed. Several studies have shown PVT1 knockdown by PVT1-siRNA or -shRNA ameliorated the diseases. For example, silencing PVT1 attenuated elevation of plasma urea nitrogen, urine protein to creatinine ratio, renal weight to body weight ratio and urine volume in mice with DN, which alleviated DN (D. Liu et al, 2019). The vancomycin-induced acute kidney injury was alleviated by PVT1 knockdown by reducing blood urea nitrogen (BUN), serum creatinine, epithelial degenerative changes and cell apoptosis in kidney cells, and Bax (pro-apoptosis protein) and increasing Bcl-2 (anti-apoptosis protein) in AKI mice through inactivation of NF-κB signalling (X. Zhu et al, 2018). PVT1 regulates MAPK/ NF-κB pathway that is crucial in inflammatory response, in which downregulated PVT1 markedly reduced the expression of inflammatory cytokines (TNF-α, IL-1β, IL-6, IL-10, IL-10, and IFN-γ) (F. Feng et al, 2018). PVT1 inhibition resulted in reduced hepatic accumulation of type I collagen and α-SMA (α-smooth muscle actin) in carbon tetrachloride (CCl_4)-induced liver fibrosis mice (J. Zheng et al, 2016). PVT1 expression was increased in atrial muscle tissues from atrial fibrillation patients and was positively correlated with type I collagen and type III collagen gene expression. PVT1 knockdown attenuated the Ang-II-induced atrial fibrosis in mice through supressing protein expression of type I collagen, type III collagen and TGF-β1 (F. Cao et al, 2019). Unilateral ureteral obstruction (UUO)-induced renal fibrosis was suppressed by PVT1 knockdown, in which PVT1 expression, serum creatinine, BUN, and protein expression of fibronectin, TGF-βRI and p-Smad3 were greatly reduced (L. Cao et al, 2020).

3.3 ECM components and regulators

3.3.1 Fibronectin & type IV collagen

The mesangial matrix consists predominantly of type IV and V collagen, laminin, fibronectin and several proteoglycans (Floege et al., 1991). Biochemical and

immunohistochemical studies have indicated marked increase in type IV collagen and fibronectin (FN) in DN (Makino et al., 1995). Type IV collagen is the predominant ECM protein found in healthy and diabetic glomeruli. Fibronectin is one of the ECM proteins increases in the early stages of DN. High glucose-induced type IV collagen deposition is shown to be dependent on the FN matrix assembly (binding of FN dimers to α5β1 integrins to promote FN matrix formation), which suggested a role for FN as a mediator of ECM accumulation (Miller et al., 2014; Singh et al., 2010). ECM accumulation is modulated by several different cytokines, growth factors and matrix-degrading proteases, which includes transforming growth factor-β1 (TGF-β1), plasminogen activator inhibitor-1 (PAI-1), angiotensin II (Ang II), connective tissue growth factor (CTGF) and tissue inhibitors of metalloproteinases (TIMPs) (Mason & Wahab, 2003). The mediators, TGF-β1, PAI-1 and BMP7, are discussed in detailed below.

3.3.2 **Transforming growth factor-β (TGF-β)**

3.3.2.1 Background of TGF-β

It is evident that TGF-β plays an integral role in the pathogenesis of DN (S. V. Mclennan et al., 2000). TGF-β is a prototype member of cytokines (Border et al., 1996). Virtually every cell in the body produces TGF-β, including several renal cell types, and has receptors for it (Border et al., 1996; Epstein et al., 2000; Ziyadeh et al., 1994). It consists of three isoforms TGF-β1, -β2 and -β3 which are structurally and functionally closely related to each other (Border & Ruoslahti, 1992). Among all isoforms, TGF-β1 is the most important in fibrosis (Reeves & Andreoli, 2000). TGF-β plays an essential role in tissue repair, in which its excessive action can result in tissue damage caused by scarring in many serious diseases including DN (Border & Ruoslahti, 1992). It is upregulated in diabetes and has been proven to mediate virtually all of the pathological changes of DN (S. Chen et al., 2001). Almost all of the molecular mediators and intracellular signalling

pathways that have been identified in diabetic kidney injury have also been found to stimulate the renal TGF-β activity as an intermediate step (Ziyadeh, 2004). TGF-β system mediates the renal hypertrophy, glomerulosclerosis, and tubulointerstitial fibrosis of DN (S. Chen, Jim, et al., 2003).

3.3.2.2 Actions of TGF-β

Pathologic accumulation of extracellular matrix is a pivot event of DN (Nicholas et al., 2005). TGF-β promotes accumulation of extracellular matrix in four ways. First, TGF-β directly upregulates the genes of most matrix proteins leading to their increased synthesis. The key matrix proteins include type I collagen, type IV collagen, fibronectin, laminin, proteoglycans, and tenascin (Border & Ruoslahti, 1992; Ziyadeh, 2004). Second, TGF-β decreases matrix degradation by inhibiting the synthesis of proteases (e.g. plasminogen activator, collagenases, elastase, and stromelysin) and activating the protease inhibitors (e.g. plasminogen activator inhibitor-1 (PAI-1) and tissue inhibitors of metalloproteinases (TIMPs)) (S. Chen et al., 2001; Ziyadeh, 2004). Third, TGF-β modulates the expression of integrins on the cell‘s surface in a manner that facilitates attachment to the newly synthesized matrix (Border et al., 1996). Finally TGF-β autoinduces its own production, which greatly amplifies its actions (Border et al., 1996).

3.3.2.3 *In vitro* studies

Extensive evidence in cell culture, animal and human studies have indicated TGF-β is an important mediator of DN. TGF-β mRNA and protein expressions were significantly upregulated in the glomeruli and tubulointerstitium in diabetic animals and patients under hyperglycemia (Mason & Wahab, 2003; Reeves & Andreoli, 2000) as well as in the cultured mesangial cells (Border et al., 1996). Glomeruli from patients with DN showed

a striking increase in immunoreactive TGF-β protein and fibronectin, whereas those from normal individuals or from patients with other glomerular diseases (where extracellular matrix accumulation is not a feature) were negative or barely positive (Yamamoto et al., 1993). Normal kidneys showed trace mRNA expression and staining for TGF-β (Border et al., 1996; Mason & Wahab, 2003; Yamamoto et al., 1996). Treatment of cultured mesangial cells with exogenous TGF-β has shown to increase the levels of type I collagen, type IV collagen, fibronectin, laminin, proteoglycans, which are major ECM components (Border et al., 1990; Takamichi Nakamura et al., 1992; Ziyadeh et al., 1994). The concentration of exogenous TGF-β increased the proteoglycans (biglycan and decorin) dose-dependently (Border et al., 1990). Furthermore, exposure of TGF-β to cultured mesangial cells increased the levels of PAI-1 dose-dependently and markedly decreased the conversion of latent metalloproteinase-2 (MMP-2) to active MMP-2 (Baricos et al., 1999). The inhibition in matrix degradation is caused by both increasing the level of protease inhibitor and decreasing the activation of proteases for degradation. Addition of TGF-β has markedly increased the synthesis of subunits of β1 integrins in cultured glomeruli, which contributed to matrix accumulation by providing increased numbers of receptors for binding of matrix components to the glomerular cell surface and for the deposition of these components into the extracellular matrix (Border et al., 1996). Furthermore, TGF-β induces podocyte apoptosis by the activation of MAPK p38 and classic effector caspase-3 (Schiffer et al, 2001). High glucose significantly upregulates the expression of TGF-βRII in the cultured mouse podocytes, which makes the podocytes more sensitive to elevated levels of TGF-β and thus more prone to apoptosis (Iglesias-de la Cruz et al, 2002; Wolfet al, 2005, Wang et al, 2000).

3.3.2.4 *In vivo* studies

In STZ-induced diabetic rats, glomerular TGF-β1 mRNA and protein levels increased markedly after onset of hyperglycemia (Shankland et al., 1994). Glomerular TGF-β mRNA expression was significantly increased by 5.2-fold in STZ-induced diabetic rats when compared with the controls after 24 weeks of diabetes (Tsukasa Nakamura et al., 1993). The increase was most significant among growth factors investigated in the same study and was partially ameliorated by insulin treatment. Similarly TGF-β1 mRNA level was increased 3-fold in the kidneys of models of spontaneous type 1 diabetes, biobreeding (BB) rats and nonobese diabetic (NOD) mice, after 3 to 9 days of diabetes (Pankewycz et al., 1994; Sharma & Ziyadeh, 1994). In db/db mice, a genetic model of type 2 diabetes, mRNA and protein expressions of both TGF-β1 and its receptor TGF-β Type II receptor were significantly upregulated in the glomerular and tubular compartments (Hong et al., 2001). Sustained elevation of mRNA and protein levels of TGF-β Type II receptor was observed as early as 1 week of diabetes in STZ-induced mice (Isono et al., 2000). All TGF-β isoforms and the TGF-β type II receptor were reported to be upregulated in the diabetic models (Hill et al., 2000; Mason & Wahab, 2003). In transgenic mice overexpressing TGF-β1, the podocytes undergo apoptosis in situ shortly after the sclerotic lesion appears in the glomerulus (Schiffer et al, 2001). The TGF-β1 expression is enhanced in podocytes in patients with progressive podocyte diseases including membranous nephropathy and focal segmental glomerulosclerosis (Lopez-Hernandez & Lopez-Novoa, 2012). Furthermore, TGF-β1 has been shown to mediate several key tubular pathological events during chronic kidney disease, namely interstitial fibrosis, epithelial to mesenchymal transition (EMT) and epithelial cell death. The *in vivo* inhibition of TGF-β reduces the extent of tubular cell death in animal models of chronic kidney disease (Lopez-Hernandez & Lopez-Novoa, 2012).

Administration of neutralizing anti-TGF-β antibodies to STZ-induced diabetic mice prevented glomerular hypertrophy and attenuated the increase in mRNA expressions of TGF-β1, α1 chain of type IV collagen, and fibronectin (Sharma et al., 1996). Long-term antibody therapy in the db/db mice, virtually prevented mesangial matrix expansion and preserved creatinine clearance (Ziyadeh, 2004; Ziyadeh et al., 2000). Furthermore antibody therapy significantly reduced GBM thickness and mesangial matrix accumulation in db/db mice, approaching the non-diabetic norm (S. Chen, Iglesias-de la Cruz, et al., 2003). The results demonstrated inhibiting renal TGF-β activity can partially reverse the GBM thickening and mesangial matrix expansion. However, the antibody therapy did not reduce albuminuria. Treatment of diabetic rats with soluble TGF-β type II receptor significantly decreased albuminuria and type IV collagen deposition, which decreased the progression of DN (Russo et al., 2007). Using knockout mouse models for TGF-β type II receptor, the importance and signalling of TGF-β is well demonstrated. In heterozygous mice for TGF-βIIR gene, expression of TGF-β type II receptor was significantly reduced and the mice were resistant to progression of STZ-induced DN through inhibiting the Smad signalling pathway (H. W. Kim et al., 2004).

3.3.3 **Plasminogen activator inhibitor-1 (PAI-1)**

3.3.3.1 Background of PAI-1

Plasminogen activator inhibitor-1 (PAI-1), a 50 kDa single chain glycoprotein, is a serine protease inhibitor (SERPIN). It is the primary physiological inhibitor of tissue-type and urokinase-type plasminogen activators (tPA and uPA, respectively). It irreversibly forms complexes with active plasminogen activators (PA), which are subsequently endocytozed and degraded (Rerolle et al., 2000). Within blood vessels, PAI-1 blocks tPA-dependent plasmin generation and degradation of fibrin clots. In extravascular areas, PAI-1 impairs matrix turnover by inhibiting uPA-dependent activation of plasminogen. Plasmin, the

active form of plasminogen, is a broad-spectrum protease that degrades fibrin clots and various extracellular matrix proteins (type IV collagen, fibronectin, laminin, and proteoglycan) (H. B. Lee & Ha, 2005). It also activates matrix metalloproteinases (MMPs) from their latent forms. These components are part of the two main enzyme systems, PA/plasmin/PAI system and MMP/TIMP system, involved in ECM degradation. PAI-1 interferes with the generation of plasmin and activation of MMP by blocking PA (E. A. Lee et al., 2005).

3.3.3.2 *In vitro* study

Elevated plasma PAI-1 levels are observed in individuals with insulin-resistant states, obesity, hypertension and diabetes (Collins et al., 2006; Eddy, 2002). PAI-1 is overexpressed in pathologic conditions associated with renal fibrosis including DN, while it is undetectable in normal human kidneys (Nicholas et al., 2005). PAI-1 protein is prominent in areas of severe lesions, i.e. Kimmelstiel-Wilson nodules in the kidney (Eddy & Fogo, 2006; Paueksakon et al., 2002). PAI-1 expression in glomerular mesangial cells and in renal tubular epithelial cells is induced by high ambient glucose levels, TGF-β and angiotensin (Ha et al., 2009). Both mRNA and protein expressions of PAI-1 are upregulated by high glucose and TGF-β1 in a dose-dependent manner and resulted in decreased plasmin activity in glomerular mesangial cells (Ha & Lee, 2003; E. A. Lee et al., 2005).

3.3.3.3 *In vivo* study

PAI-1 knockout mice developed fewer glomerular crescents, glomerular fibrin deposits and reduced collagen accumulation, whereas extensive collagen accumulation was found in mice with overexpression of PAI-1 (Eddy & Fogo, 2006). In PAI-1 knockout mice,

treatment of high fat diet failed to induce obesity, hyperglycemia, and hyperinsulinemia while such diabetic phenotypes were obvious in wild-type mice. Insulin sensitivity, metabolic rate and glucose uptake by primary adipose cells were enhanced in PAI-1 knockout mice (L. J. Ma et al., 2004). Treatment of STZ did not result in albuminuria in PAI-1 knockout mice as it did in wild-type mice. TGF-β and fibronectin mRNA and protein expressions were significantly lower in diabetic PAI-1 knockout mice than in diabetic wild-type. In addition, TGF-β expression was upregulated in primary mesangial cells from rats with administration of recombinant PAI-1 via mitogen-activated protein kinase (MAPK) pathway, and that anti-uPAR antibody abolished PAI-1 induced TGF-β1 expression in cultured mesangial cells (Nicholas et al., 2005). PAI-1 deficiency in db/db mice has improved nephropathy in terms of albumin to creatinine ratio and glomerular ECM area compared to db/db mice (Collins et al., 2006). Administration of a PAI-1 mutant (PAI-1R, that reduce endogenous PAI-1 activity by competing with native PAI-1 for vitronectin binding sites) markedly reduced the increases in proteinuria, collagens and fibronectin expression, as well as restored plasmin activity (Huang et al., 2008). These findings suggested that PAI-1 is an important regulator of ECM remodelling and PAI-1 deficiency prevent DN in diabetic subjects.

3.3.4 **Bone morphogenetic protein 7 (BMP7)**

3.3.4.1 Background of BMP7

Bone morphogenetic protein 7, formerly called osteogenic protein 1 (OP 1), is one of over twenty currently known BMPs which are within the TGF-β superfamily of secreted growth factors (Katagiri & Watabe, 2016; G. Mitu & Hirschberg, 2008; Zeisberg et al., 2004). BMPs are highly conserved across animal species and mature human and mouse BMP7 share 98% amino acid sequence identity (Ozkaynak et al., 1990; Zeisberg, 2006). BMP7 has vital functions during kidney and eye development (Godin et al., 1998). Mice

deficient for BMP7 gene have very small kidneys and die shortly after birth from renal failure (Dudley et al., 1995; Hogan, 1996; Luo et al., 1995). BMP7 is the most abundant BMP in fetal and adult mammalian kidney, and conversely, kidney is the most abundant site of BMP7 production (Kopp, 2000). It is specifically expressed in podocytes, distal tubules and collecting ducts (G. Mitu & Hirschberg, 2008). BMP7 expression was down regulated in patients with DN at advanced stage (Ivanac-Janković et al., 2015). The reduction in renal BMP7 is observed early at the onset of DN in rodents and is paralleled by the appearance and subsequent increase in TGF-β (G. Mitu & Hirschberg, 2008). *In vitro* and *in vivo* studies have demonstrated BMP7 plays a role in protecting the kidney from injury which counteract TGF-β1 mediated fibrosis (Patel & Dressler, 2005; Zeisberg et al., 2004).

3.3.4.2 ***In vitro*** **studies**

The anti-fibrotic activity of BMP7 have shown in different renal cells, including mesangial cells, podocytes and tubular cells. Mesangial cells do not express BMP7 but express BMP7-binding receptors. Incubation with TGF-β1 induced overexpression of several extracellular matrix genes in murine mesangial cells. Co-incubation with recombinant human BMP7 reduced the increase of type IV collagen, fibronectin, secreted soluble type IV collagen, thrombospondin (TSP) and connective tissue growth factor (CTGF). BMP7 inhibited PAI-1 secretion while increased matrix metalloprotease 2 (MMP2) activity, which contributing to proteolytic degradation of several extracellular matrix proteins (including collagens, fibronectin, laminin and elastin) and proteolytic activation of several other MMPs (Shinong Wang & Hirschberg, 2003). These findings indicated BMP7 antagonized TGF-β1 induced fibrogenesis in mesangial cells. DN is characterised by podocyte injury and apoptosis. Incubation with high glucose or recombinant human TGF-β1 reduced BMP7 secretion by podocytes. Treatment of high

glucose or TGF-β1 transformed the murine podocytes into a more rounded shape, loosened their close connections with the neighbouring cells partially through structural changes in actin cytoskeleton, and significantly reduced cell survival. The cytoskeleton change, injury and apoptosis of podocytes were largely inhibited by BMP7. Moreover, the podocytes expressed BMP7 as well as BMP7 receptors, which gave rise to autocrine and paracrine actions (G. M. Mitu et al., 2007). BMP7 was crucial to podocyte differentiation and survival, which could reduce podocyte loss and albuminuria. Neutralization of endogenous BMP7 in murine proximal tubular cells significantly increased the expression of fibronectin. The loss of BMP7 activity per se is profibrogenic in tubular cells (S.-N. Wang et al., 2001).

3.3.4.3 ***In vivo*** **studies**

BMP7 expression declined early during DN. At 15 wk of STZ-induced diabetes, the tubular BMP7 expression was decreased by about half and was further decreased to less than 10% by 30 wk when compared with the timed controls. Renal expression of the high affinity BMP type II receptor (BMP-RII) was significantly decreased while the secreted gremlin (a BMP antagonist) was significantly increased (S.-N. Wang et al., 2001). These changes in the renal expressions of BMP7, BMP type II receptor and its antagonist coincided with the expression TGF-β1, which suggested the TGF-β1 down-regulated BMP7 or the BMP7 loss stimulated in TGF-β1 overexpression. Other studies have reported similar findings in diabetic rats, including decline in renal expression of BMP7 and BMP-RII, and increase expression of TGF-β1 and type I collagen (Q. Yang et al., 2007; Yeh et al., 2009). Intravenous administration of BMP7 to diabetic rat models had partially reversed diabetic-induced kidney hypertrophy, restored glomerular filtration rate, urine albumin excretion, and glomerular histology towards normal in a dose-dependent manner. BMP7 treatment was more effectively than enalapril, an angiotensin-converting

enzyme (ACE) inhibitor, on prevention of glomerulosclerosis (Song Wang et al., 2003). Restoration of BMP7 expression was associated with a successful repair reaction and a reversal of the ill-fated injury response. Similarly, BMP7 therapy inhibited progression of fibrosis in different murine models of renal fibrogenesis (T. Li et al., 2004; Zeisberg & Kalluri, 2008). Transgenic expression of BMP7 in podocytes and proximal tubules prevented podocyte loss and reductions in nephrin levels in diabetic mice. Maintenance of BMP7 also reduced albuminuria, glomerular fibrosis, and expression of type I collagen and fibronectin (Shinong Wang et al., 2006). Inhibition of gremlin by gremlin siRNA injection had significantly reduced proteinuria, serum creatinine, glomerular diameter, and renal cell apoptosis in diabetic mice (Q. Zhang et al., 2010). Taken together, BMP7 was important for renal protection in diabetic animal models.

3.4 Albuminuria

DN is clinically characterized by albuminuria and progressive renal insufficiency and is the major cause of end-stage renal disease worldwide. Albuminuria is used to stage DN, which can be determined using 24hr urine or spot urine. Urinary albumin excretion (UAE) in a 24-hr collection is considered as the gold standard method, while urinary albumin to creatinine ratio (UACR) in spot collection is widely adopted with strong association with 24-hr UAE (Dyer et al., 2004; Witte et al., 2009). Microalbuminuria is an early predictor of DN, while macroalbuminuria is usually associated with reduced glomerular filtration rate or renal insufficiency. Stages in DN is shown in Table 3.1. In this study, UAE, UACR, urinary protein excretion and urinary protein to creatinine ratio are measured.

3.5 Glomerular filtration rate, creatinine clearance & serum creatinine

Glomerular filtration of kidney is a passive process whereby an ultrafiltration of glomerular capillary blood is driven across the capillary wall into the Bowman's capsule by pressure within the glomerular capillary network. The rate of glomerular filtration was determined by the surface area, intrinsic permeability, and hydrostatic and oncotic pressure gradients across the glomerular capillary walls. Glomerular filtration rate is regarded as the best overall indicator of kidney function (Johnson, Levey, Coresh, Levin, & Eknoyan, 2004; Manjunath, Sarnak, & Levey, 2001). It is important to determine the progression of kidney disease as well as the early disease management. Glomerular filtration rate cannot be measured by direct means. It is measured as the urinary clearance of exogenous filtration markers such as inulin, ^{51}Cr-EDTA, ^{99m}Tc-DTPA, iodine-125 iothalamate and radiological contrasting agents such as iohexol (Wahab et al., 2001). Inulin is considered as an ideal filtration marker as it is freely filtered, not protein bound, and not reabsorbed, secreted nor metabolized by the kidney, which does not impact the kidney function (Yokoi et al., 2002). Despite the exogenous inulin clearance is regarded as a gold standard, it is difficult to measure. An alternative method, endogenous creatinine clearance, is thus widely used to estimate the glomerular filtration rate.

Creatinine clearance is determined based on the 24hr urine collection and serum creatinine, which is influenced by body size, age and gender. Serum creatinine level is not only affected by the renal function, but also the generation, intake and metabolism of creatinine. Creatinine is formed as a result of nonenzymatic degradation of muscle creatine. Creatine is synthesized primarily in the liver and actively transported into the muscle, which contains about 98% of total creatine pool in the body. Approximately 1.6-1.7% of the total creatine pool is converted into creatinine every day (Guha, Xu, Tung, Lanting, & Natarajan, 2007). Creatine turnover rates are relatively constant in normal individuals. In general, individuals with greater total muscle mass and dietary intake of

creatine have greater generation of creatinine. Of note, glomerular filtration rate is exceeded by creatinine clearance as creatinine is both filtered and secreted by the kidney tubules. Despite such limitation, a reduced creatinine clearance or an increase in serum creatinine concentration is an almost certain indication that glomerular filtration rate is reduced. Many studies support the similarity of creatinine clearance to glomerular filtration rate and its reciprocal relationship with serum creatinine (S. McLennan, Wang, Moreno, Yue, & Twigg, 2004; Mori et al., 1999).

There are four main ways (i.e. alkaline picrate methods, enzymatic methods, high performance liquid chromatography (HPLC) and MS-based procedures) to determine the creatinine level. The alkaline picrate methods based on Jaffe's reaction is commonly used. Creatinine combines with alkaline picrate to form a red-coloured complex or chromophore, the light absorbance of which are measured in the 490-510nm wavelength. This method is subject to interference by non-creatinine chromogens (particularly proteins), resulting in an overestimation of serum creatinine by as much as 15-25% (David, Duarte Vogel, Longo, Sanchez, & Lawson, 2014; Hilliard et al., 2017). As the non-creatinine chromogens are not retained at a reduced glomerular filtration rate, their relative effect is greater than at the lower range of levels of serum creatinine. The enzymatic methods make use of the sequential enzymatic conversion from creatinine to formation of hydrogen peroxide, which is then measured spectrophotometrically. While enzymatic methods do not detect the non-creatinine chromogens, they generally have improved specificity with fewer interferences than Jaffe method and yield lower values for serum creatinine. The enzymatic method performs better or without bias in creatinine determination in samples spiked with major interferents such as albumin, glucose and pyruvate, whereas the Jaffe method record an overestimation by 20% approximately (Hilliard et al., 2017). Serum glucose is a strong positive bias whereas albumin acts as a

negative bias in Jaffe method (David et al., 2014). The HPLC and MS-based methods are not widely used despite having greater analytical specificity and accuracy than conventional methods. Based on the enzymatic method is less affected by serum glucose and protein, it is employed in determining serum creatinine concentration in this study.

3.6 Aims

This study aims to study the role of PVT1 in murine models of DN. The specific aims of this chapter are:

(1) To establish early, intermediate and relatively advanced stages of DN in C57BL/6 mice using a combination treatment of high fat diet and low dose STZ
(2) To study expression levels of PVT1 and extracellular matrix (ECM) components at early, intermediate and relatively advanced stages of DN in C57BL/6 mice.

3.7 Experiment overview

The male C57BL/6 mice were used in this study. After weaning, they were randomly allocated into either diabetic or control groups. The diabetic and control groups were fed with high fat diet (HFD, 60% kcal from fat; TD06414, Enivgo, Madison, WI) and low fat control diet (LFD, 10% kcal from fat; TD08806, Enivgo, Madison, WI) respectively. At 5 weeks of age, the HFD-fed mice were intraperitoneally administered with low-dose STZ (40 mg/kg of body weight per day) for three consecutive days after 4 hr fasting, while the LFD-fed mice were administered with vehicle (sodium citrate buffer). Type 2 diabetes was induced by the combined treatment of HFD and STZ. The diabetic group

and normal control group were represented by the HFD-STZ-treated mice and the LFD-vehicle-treated mice, respectively.

All mice were housed in the animal facility maintained on constant temperature (22-25 °C), relative humidity (55-65%), 12 hr light/12 hr dark cycles, and were supplied with tap water *ad libitum*. Body weights and blood glucose were measured weekly on the commence of the study. The mice were culled at around the age of 9 (young), 16 (middle-aged) or 24 (old) weeks old which represented early, intermediate and relatively advanced stages of diabetes. Samples (e.g. blood, urine, and kidneys) were collected on or before culling.

Evaluations at functional level (e.g. UAE, UACR, UPE, UPCR, creatinine clearance and serum creatinine), histological level (e.g. kidney hypertrophy, glomerular area and mesangial area) and molecular level (e.g. gene expressions of PVT1, TGF-β1, PAI-1, FN1, COL4A1 and BMP-7), as well as body weight and blood glucose, were conducted according to the methods described in Chapter 2.

3.8 Results

3.8.1 Body weight

The initial body weight (i.e. the weight at 4-week-old) was measured to determine if the age-matched mice were of similar weight at the beginning of the experiment. It was also used as the baseline to calculate the change of body weight at the end of experiment.

The initial body weight of diabetic and control mice of different age groups were shown in Figure 3.1. The initial body weights were not statistically different between diabetic

and control mice in all young, middle-aged and old groups. There was no significant difference in initial body weight among different age groups within the same treatment.

The final body weight of diabetic and control mice of different age groups were shown in Figure 3.2. The final body weight in diabetic mice was higher than in age-matched control mice. Statistical significance was observed in young and middle-aged groups (*$p < 0.05$).

The body weight growth curve of diabetic and control mice of different age groups was shown in Figure 3.3. The body weight growth was faster in the diabetic mice than in the control mice in all young, middle-aged and old groups. The diabetic mice were heavier than the control mice from 7-week-old till the end of experiment in all age groups.

The change in body weight of diabetic and control mice of different age groups was shown in Figure 3.4. It was calculated as: difference between final body weight and initial body weight / initial body weight x 100%. The diabetic mice had greater body weight gain than the control mice in all young (by 40%), middle-aged (by 37%) and old (by 18%) groups. Statistical significance was observed in young and middle-aged groups (*$p < 0.05$).

Figure 3.1: The initial body weight of diabetic and control mice of different age groups. Results were expressed in mean ± SEM, n = 6. A p-value < 0.05 was considered statistically significant using unpaired student's t-test between age-matched individual groups.

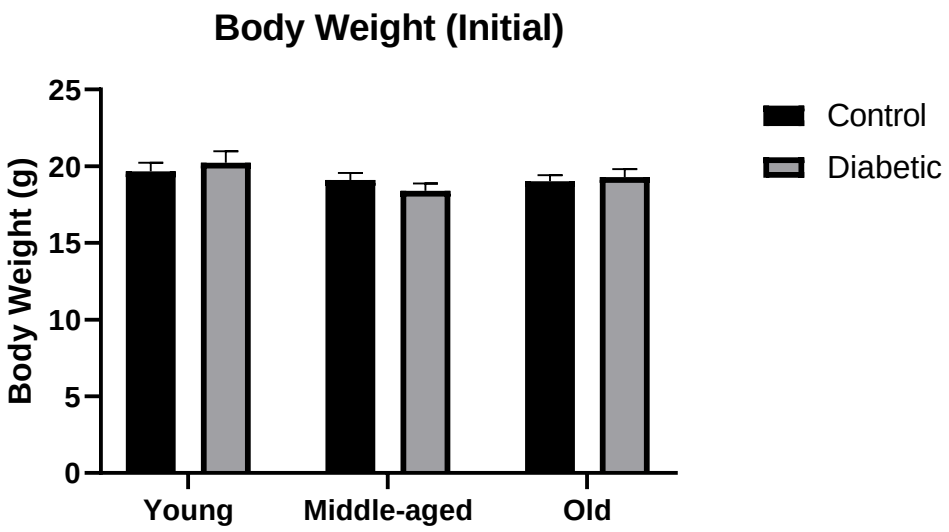

Figure 3.2: The final body weight of diabetic and control mice of different age groups. Results were expressed in mean ± SEM, n = 6. A p-value < 0.05 was considered statistically significant using unpaired student's t-test between age-matched individual groups (*$p < 0.05$) or one-way ANOVA among different age groups within the same treatment ($^{\#}p < 0.05$, $^{\#\#}p < 0.01$, $^{\#\#\#}p < 0.001$).

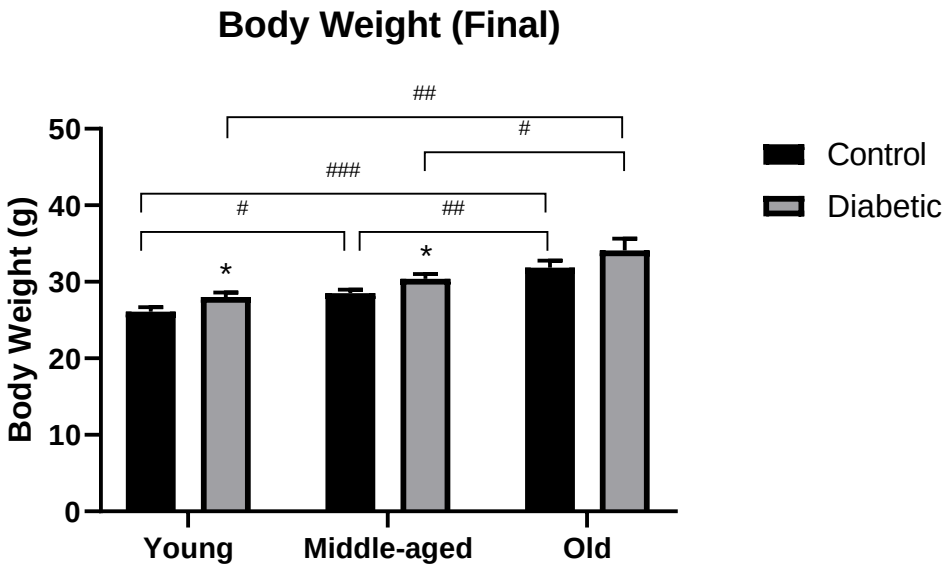

Figure 3.3: The body weight growth curve of diabetic and control mice of different age groups, (A) young, (B) middle-aged and (C) old.

Results were expressed in mean ± SEM, n = 6. A p-value < 0.05 was considered statistically significant using unpaired student's t-test between age-matched individual groups (*p < 0.05).

(A)

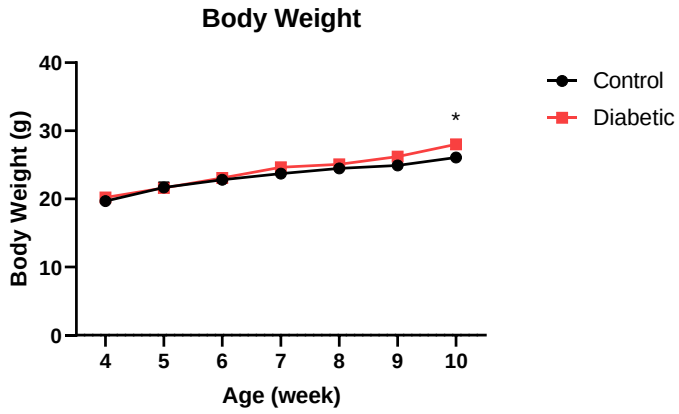

(B)

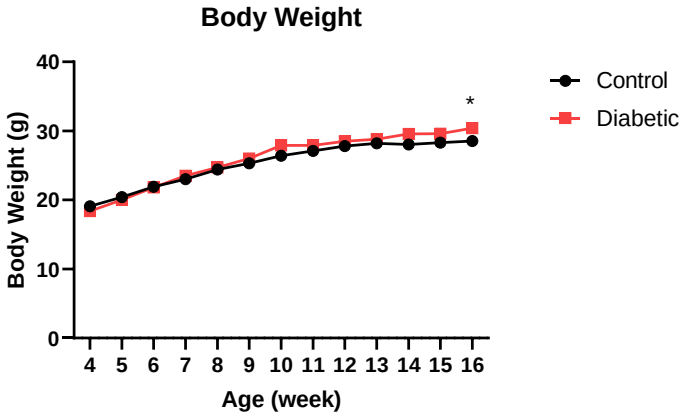

(C)

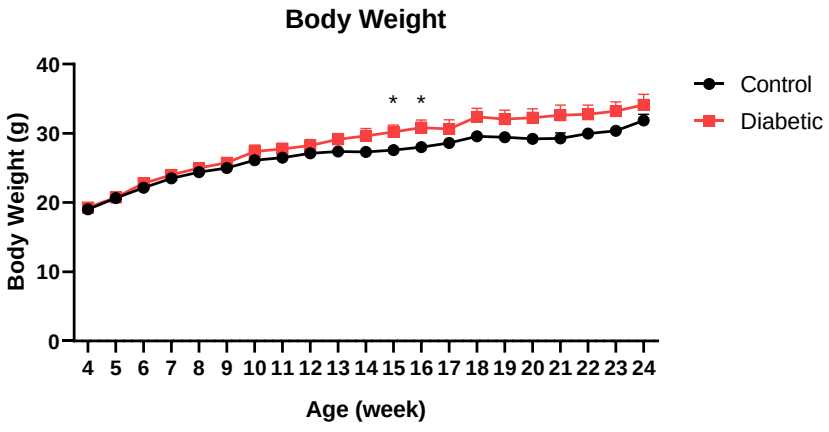

Figure 3.4: The change in body weight of diabetic and control mice of different age groups.

Results were expressed in mean ± SEM, n = 6. A p-value < 0.05 was considered statistically significant using unpaired student's t-test between age-matched individual groups (*$p < 0.05$) or one-way ANOVA among different age groups within the same treatment ($^{\#}p < 0.05$, $^{\#\#}p < 0.01$, $^{\#\#\#}p < 0.001$).

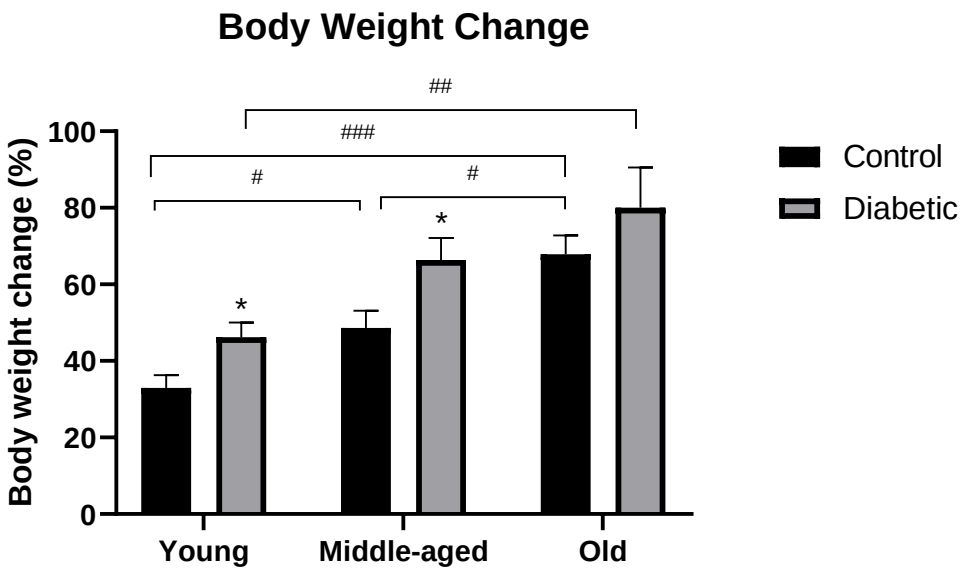

3.8.2 **Blood glucose**

At the beginning of the study, the initial blood glucose (at 4-week-old) was measured to determine if the age-matched mice were of normal blood glucose. Blood glucose was measured weekly to evaluate the status of diabetes. Mice with chronic elevation of blood glucose concentration over 17 mmol/L was considered to be diabetic.

The initial blood glucose of diabetic and control mice of different age groups were shown in Figure 3.5. The initial blood glucose was similar between diabetic and control mice in all age groups. All mice were with normal blood glucose levels when the experiment commenced. As the experiment proceeded, hyperglycaemia was gradually developed in diabetic mice as a result of the combined treatment of high fat diet and low dose STZ.

The final blood glucose of diabetic and control mice of different age groups were shown in Figure 3.6. Blood glucose of diabetic mice was significantly higher than those of control mice in all young (2.37-fold), middle-aged (2.28-fold) and old (2.34-fold) groups (***$p < 0.001$).

The weekly blood glucose of diabetic and control mice of different age groups was shown in Figure 3.7. In general, the blood glucose increased gradually from 5-week-old in diabetic mice. It remained steadily high from 10-week-old till the end of the experiment in middle-aged and old groups. Compared to the control mice, blood glucose was significantly higher in diabetic mice from 6-week-old till the end of the experiment in all age groups (***$p < 0.001$).

Figure 3.5 The initial blood glucose of diabetic and control mice of different age groups. Results were expressed in mean ± SEM, n = 6. A p-value < 0.05 was considered statistically significant using unpaired student's t-test between age-matched individual groups or one-way ANOVA among different age groups within the same treatment.

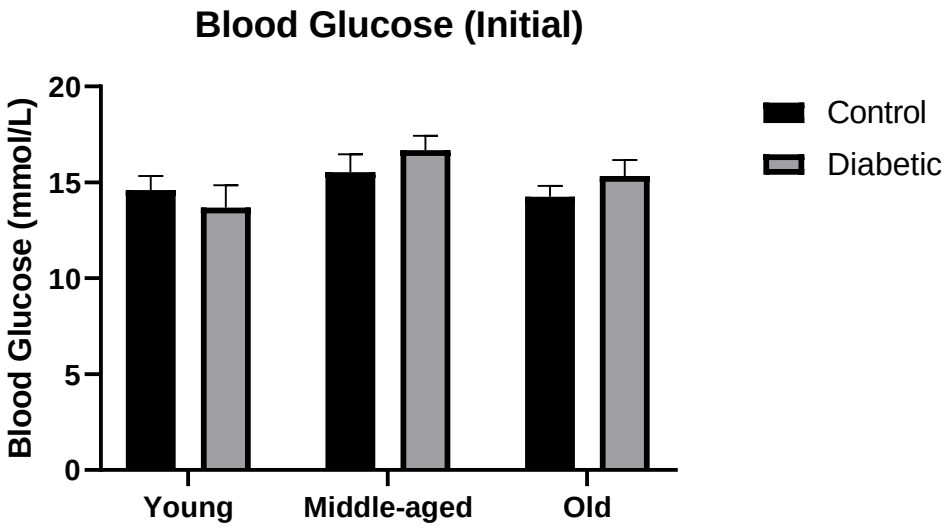

Figure 3.6: The final blood glucose of diabetic and control mice of different age groups. Results were expressed in mean ± SEM, n = 6. A p-value < 0.05 was considered statistically significant using unpaired student's t-test between age-matched individual groups (*$p < 0.05$, **$p < 0.01$, ***$p < 0.001$) or one-way ANOVA among different age groups within the same treatment.

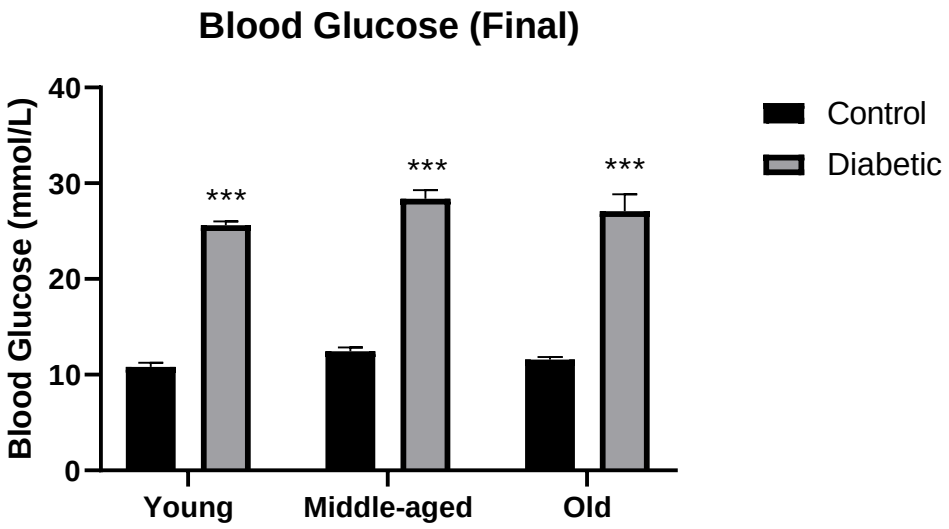

Figure 3.7: The weekly blood glucose of diabetic and control mice of different age groups, (A) young, (B) middle-aged and (C) old.

Results were expressed in mean ± SEM, n = 6. A p-value < 0.05 was considered statistically significant using unpaired student's t-test between age-matched individual groups (*p < 0.05, **p < 0.01, ***p < 0.001).

(A)

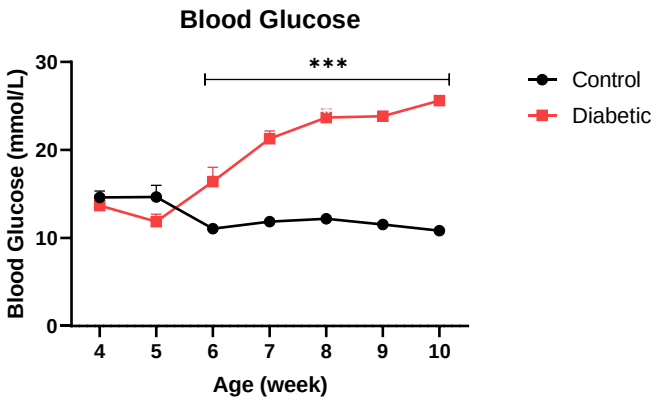

(B)

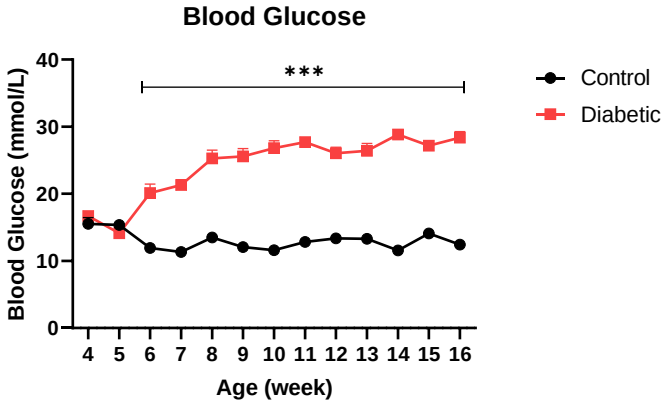

(C)

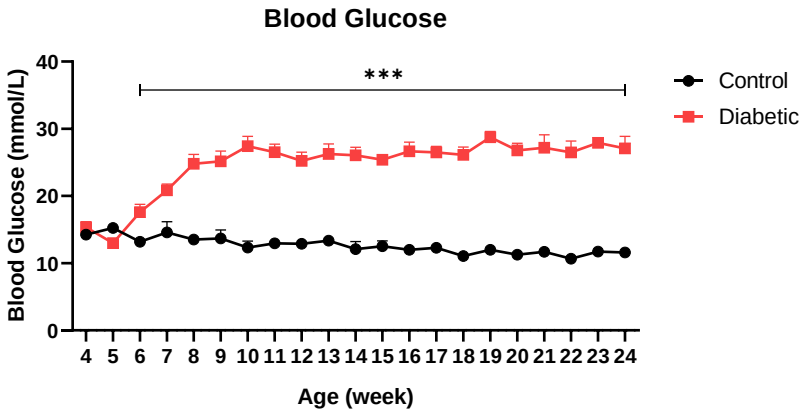

3.8.3 **Kidney weight**

Renal hypertrophy is a consistent manifestation in diabetic patients and murine models. The kidney weight was used as an index of renal hypertrophy in this study. The kidney weight of diabetic and control mice of different age groups was shown in Figure 3.8. The kidney weight remained similar in the control mice of different ages. Compared to the age-matched control mice, the kidney was heavier in diabetic mice in all young (by 18%), middle-aged (by 22%) and old (16%) groups.

The kidney to body weight ratio of diabetic and control mice of different age groups was shown in Figure 3.9. As the mice grow older and gained weight, the kidney to body weight ratio tended to decrease with age in both diabetic and control mice. Compared to the age-matched control mice, the kidney to body weight ratio was increased in diabetic mice in all young (by 13%), middle-aged (by 21%) and old (9%) groups.

Figure 3.8: The kidney weight of diabetic and control mice of different age groups. Results were expressed in mean ± SEM, n = 6. A p-value < 0.05 was considered statistically significant using unpaired student's t-test between age-matched individual groups (*p < 0.05) or one-way ANOVA among different age groups within the same treatment.

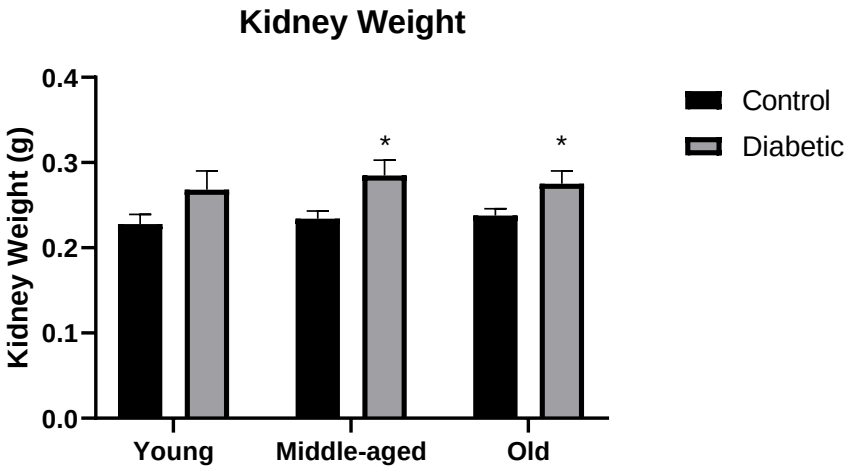

Figure 3.9: The kidney to body weight ratio of diabetic and control mice of different age groups.

Results were expressed in mean ± SEM, n = 6. A p-value < 0.05 was considered statistically significant using unpaired student's t-test between age-matched individual groups (*p < 0.05) or one-way ANOVA among different age groups within the same treatment.

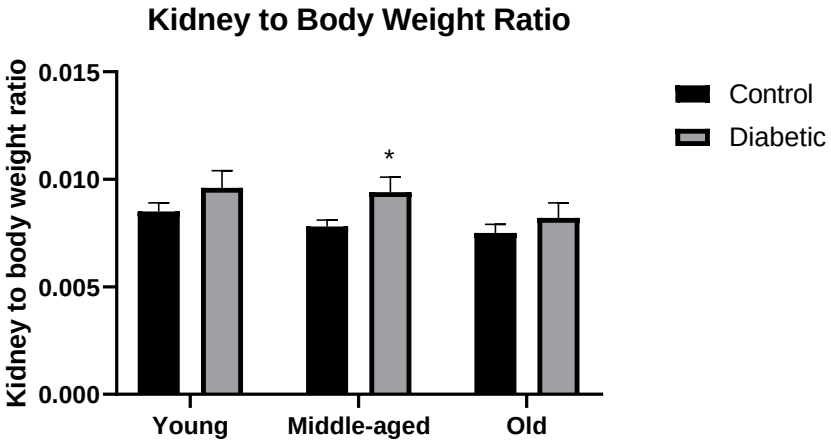

3.8.4 **Urinary albumin excretion and urine protein excretion**

The urinary albumin to creatinine ratio of diabetic and control mice of different age groups was shown in Figure 3.10. The UACR was significantly increased in diabetic mice of young (by 53%), middle-aged (by 208%) and old (by 249%) group when compared to the age-matched control mice. The UACR was slightly increased from young to old ages in control group. In contrast, the UACR was significantly elevated as the diabetic mice aged. A greater magnitude of increase was observed among the diabetic mice in an order of young < middle-aged < old age. The old diabetic mice had doubled the UACR as their young ones, and the middle-aged had about intermediate UACR among all groups.

The urinary albumin excretion of diabetic and control mice of different age groups was shown in Figure 3.11. The UAE was significantly increased in diabetic mice of young (by 206%), middle-aged (by 299%) and old (by 329%) group when compared to the age-matched control mice. The UAE was slightly increased from young to old ages in control group. In contrast, the UAE was significantly elevated as the diabetic mice aged. A greater magnitude of increase was observed among the diabetic mice in an order of young < middle-aged < old age. The old and middle-aged diabetic mice had almost triple and double the UAE as their young ones, respectively.

The urinary protein to creatinine ratio of diabetic and control mice of different age groups was shown in Figure 3.12. The UPCR remained steady among the control mice of different ages, while it gradually increased in diabetic groups over time. The UPCR was significantly increased in diabetic mice of young (by 32%), middle-aged (by 41%) and old (by 52%) group when compared to the age-matched controls.

The urinary protein excretion of diabetic and control mice of different age groups was shown in Figure 3.13. Similar to the UPCR, the UPE remained steady among the control

mice, while it increased gradually from young to old ages of diabetic mice. The UPE was increased in diabetic mice of young (by 52%), middle-aged (by 86%) and old (by 203%) group when compared to the age-matched controls.

Figure 3.10: The urinary albumin to creatinine ratio of diabetic and control mice of different age groups.

Results were expressed in mean ± SEM, n = 6. A p-value < 0.05 was considered statistically significant using unpaired student's t-test between age-matched individual groups (*p < 0.05, **p < 0.01, ***p < 0.001) or one-way ANOVA among different age groups within the same treatment (^p < 0.05, ^^p < 0.01, ^^^p < 0.001).

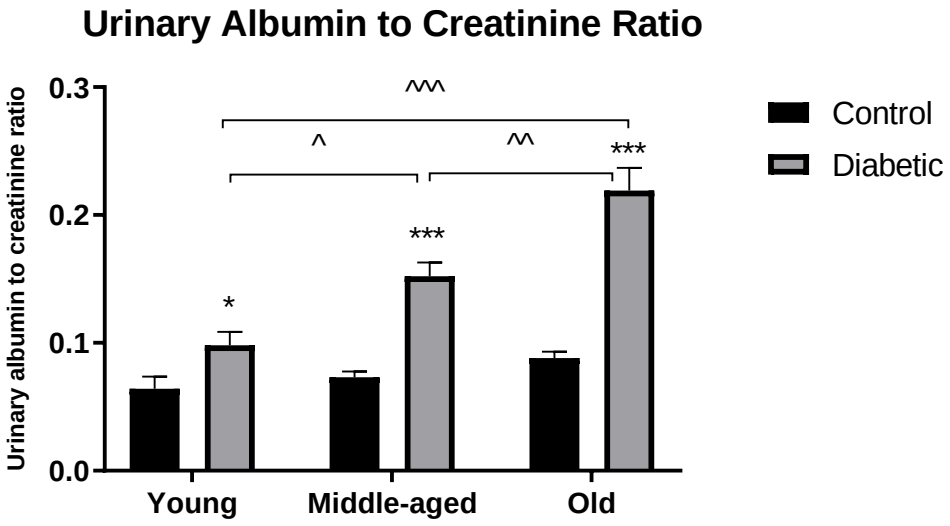

Figure 3.11: The urinary albumin excretion of diabetic and control mice of different age groups.

Results were expressed in mean ± SEM, n = 6. A p-value < 0.05 was considered statistically significant using unpaired student's t-test between age-matched individual groups (*p < 0.05, **p < 0.01, ***p < 0.001) or one-way ANOVA among different age groups within the same treatment (^p < 0.05, ^^p < 0.01, ^^^p < 0.001).

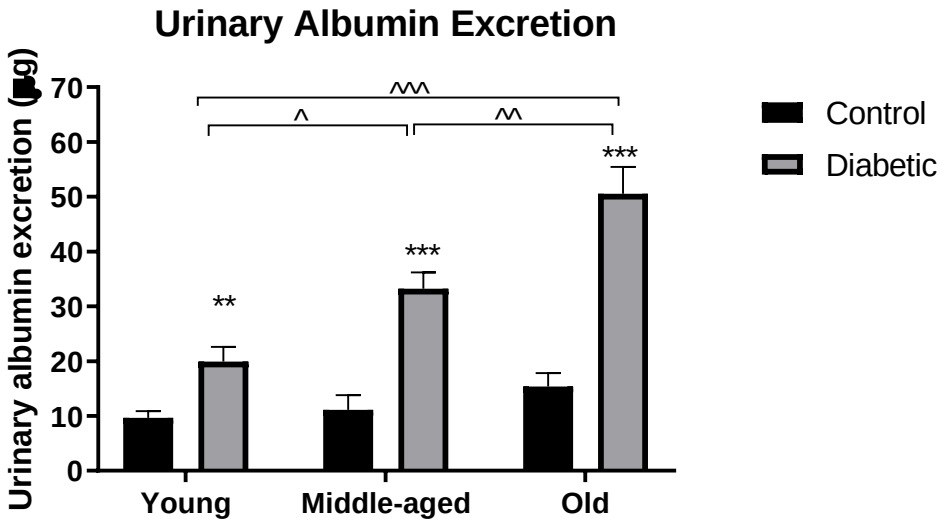

Figure 3.12: The urinary protein to creatinine ratio of diabetic and control mice of different age groups.

Results were expressed in mean ± SEM, n = 6. A p-value < 0.05 was considered statistically significant using unpaired student's t-test between age-matched individual groups (*$p < 0.05$, **$p < 0.01$) or one-way ANOVA among different age groups within the same treatment.

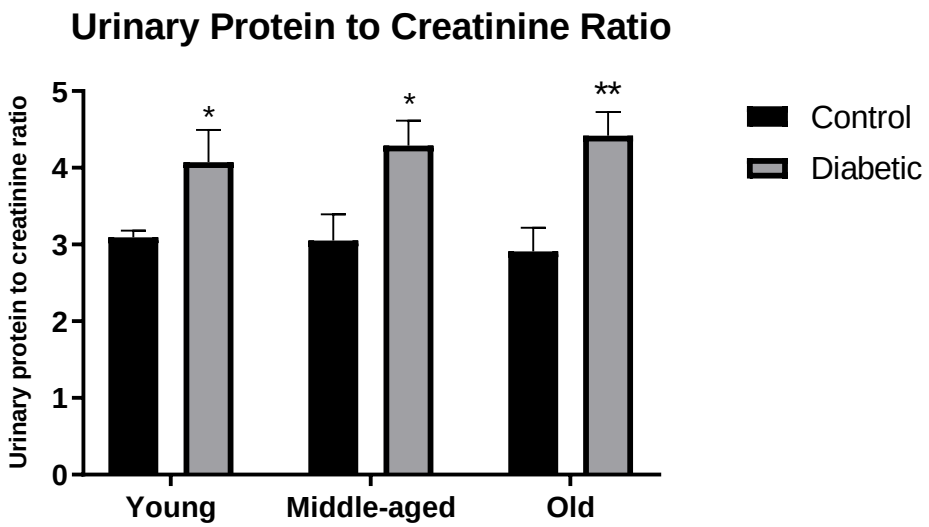

Figure 3.13: The urinary protein excretion of diabetic and control mice of different age groups.

Results were expressed in mean ± SEM, n = 6. A p-value < 0.05 was considered statistically significant using unpaired student's t-test between age-matched individual groups (*p < 0.05) or one-way ANOVA among different age groups with the same treatment.

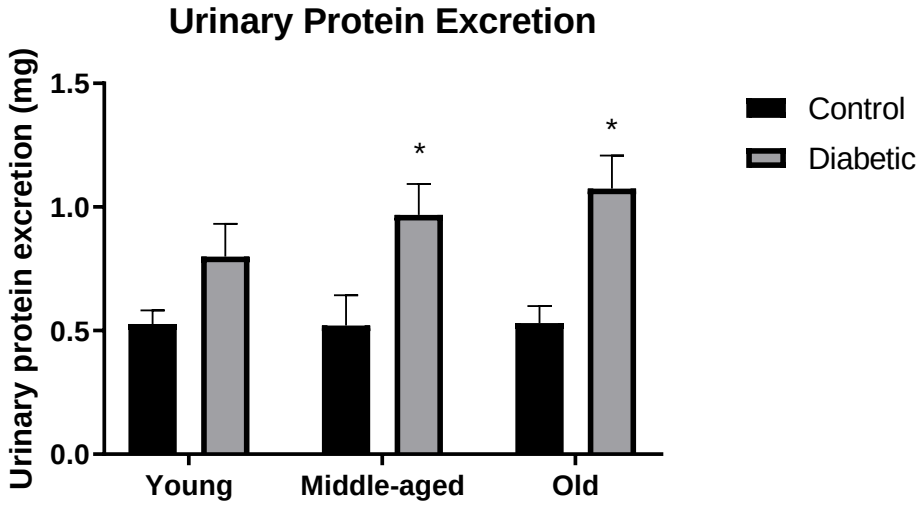

3.8.5 **Creatinine clearance**

The creatinine clearance of diabetic and control mice of different age groups was shown in Figure 3.14. At young age, the creatinine clearance was slightly lower in diabetic mice than that in control mice. The creatinine clearance was significantly declined in diabetic mice of middle-aged (by 38%) and old (by 46%) age when compared to the age-matched controls. Both groups of old mice had their lowest level of creatinine clearance. The diabetic mice had lower creatinine clearance over time and the level was significantly decreased in old mice when compared to young mice.

3.8.6 **Serum creatinine**

Serum creatinine is an important clinical marker for renal clearance. The serum creatinine concentration of diabetic and control mice of different age groups was shown in Figure 3.15. Compared to the control mice, the serum creatinine concentration was significantly increased in diabetic mice in all young (by 53%), middle-aged (by 63%) and old (by 64%) groups. The serum creatinine level was shown to increase with ages in diabetic and control mice, with a larger magnitude in the former.

Figure 3.14: The creatinine clearance of diabetic and control mice of different age groups. Results were expressed in mean ± SEM, n = 6. A p-value < 0.05 was considered statistically significant using unpaired student's t-test between age-matched individual groups (*$p < 0.05$, **$p < 0.01$) or one-way ANOVA among different age groups within the same treatment (^$p < 0.05$).

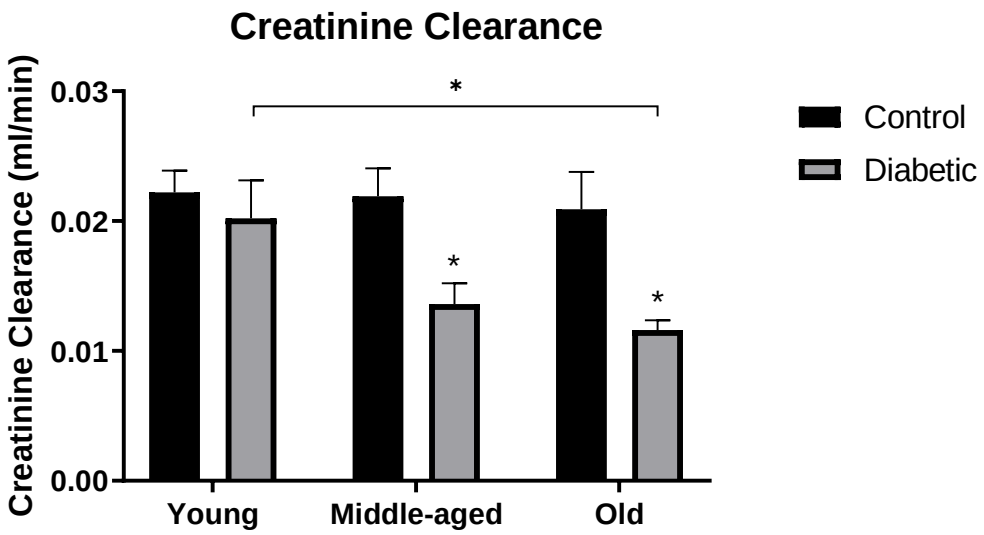

Figure 3.15: The serum creatinine of diabetic and control mice of different age groups. Results were expressed in mean ± SEM, n = 6. A p-value < 0.05 was considered statistically significant using unpaired student's t-test between age-matched individual groups (*p < 0.05) or one-way ANOVA among different age groups within the same treatment.

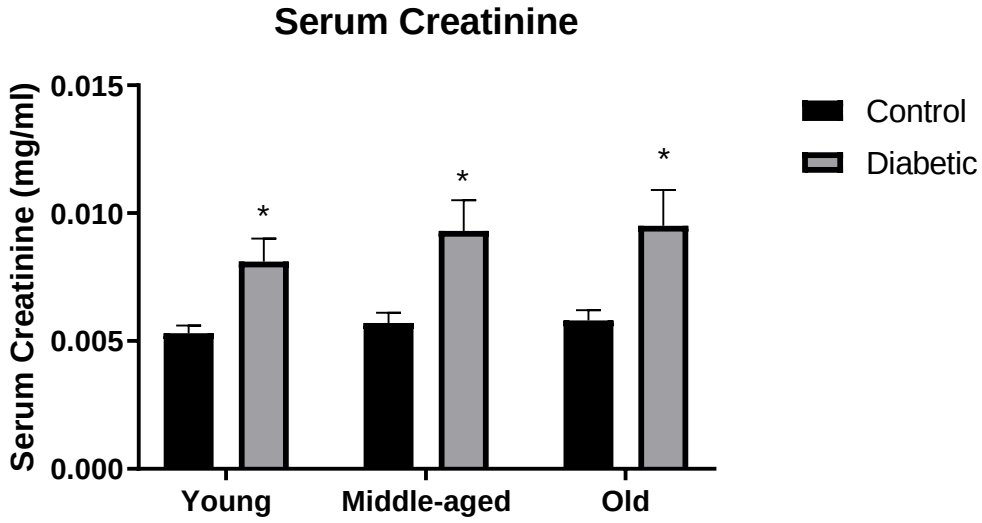

3.8.7 **Histological analysis**

The glomerular area of diabetic and control mice of different age groups was shown in Figure 3.16. The glomerular area was significantly increased in diabetic mice of young (by 33%), middle-aged (by 48%) and old (by 50%) group when compared to the age-matched controls. The glomerular area remained almost unchanged among the control mice of different ages. In contrast, the glomerular area was enlarged gradually as the diabetic mice aged, with a significant difference between young and old group.

The mesangial area of diabetic and control mice of different age groups was shown in Figure 3.17. The mesangial area was significantly increased in diabetic mice of young (by 44%), middle-aged (by 62%) and old (by 59%) group when compared to the age-matched controls. The mesangial area tended to increase slightly in control mice over time. The mesangial area was increased gradually as the diabetic mice aged, with a significant difference between young and old group. A representative of microscopic images of kidney sections from diabetic and control mice of different ages was shown in Figure 3.18.

Figure 3.16: The glomerular area of diabetic and control mice of different age groups. Results were expressed in mean ± SEM, n = 6. A p-value < 0.05 was considered statistically significant using unpaired student's t-test between age-matched individual groups (*$p < 0.05$, **$p < 0.01$, ***$p < 0.001$) or one-way ANOVA among different age groups within the same treatment (*$p < 0.05$).

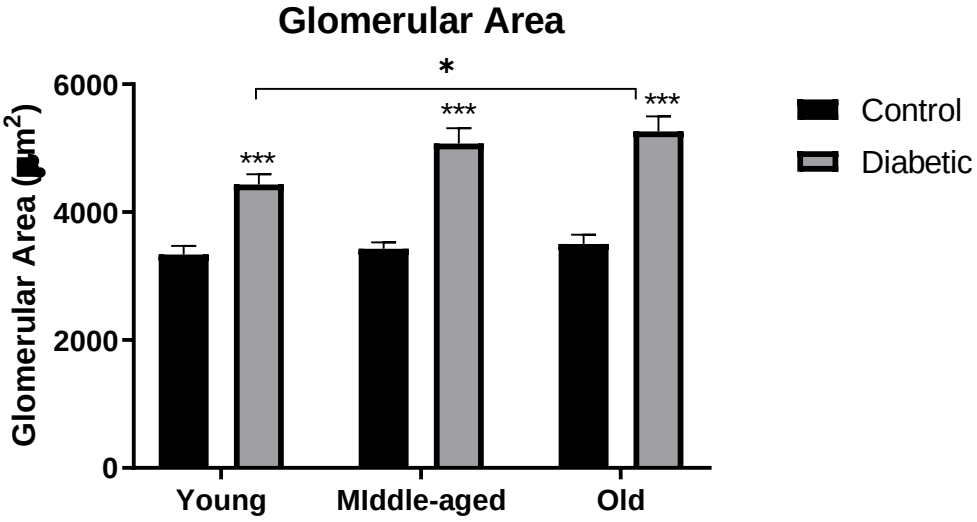

Figure 3.17: The mesangial area of diabetic and control mice of different age groups. Results were expressed in mean ± SEM, n = 6. A p-value < 0.05 was considered statistically significant using unpaired student's t-test between age-matched individual groups (*p < 0.05, **p < 0.01, ***p < 0.001) or one-way ANOVA among different age groups within the same treatment (*p < 0.05).

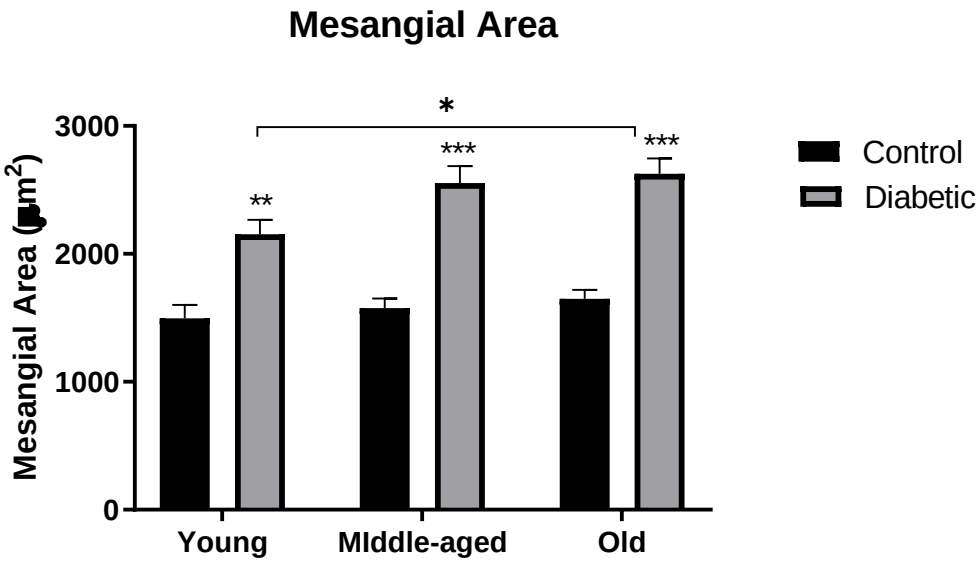

Figure 3.18: The microscopic images of kidney sections from diabetic and control mice of different age groups, (A) young, (B) middle-aged and (C) old.

The kidney sections were stained with periodic acid Schiff (PAS) and counterstained with Mayer's hematoxylin, and viewed under 40X.

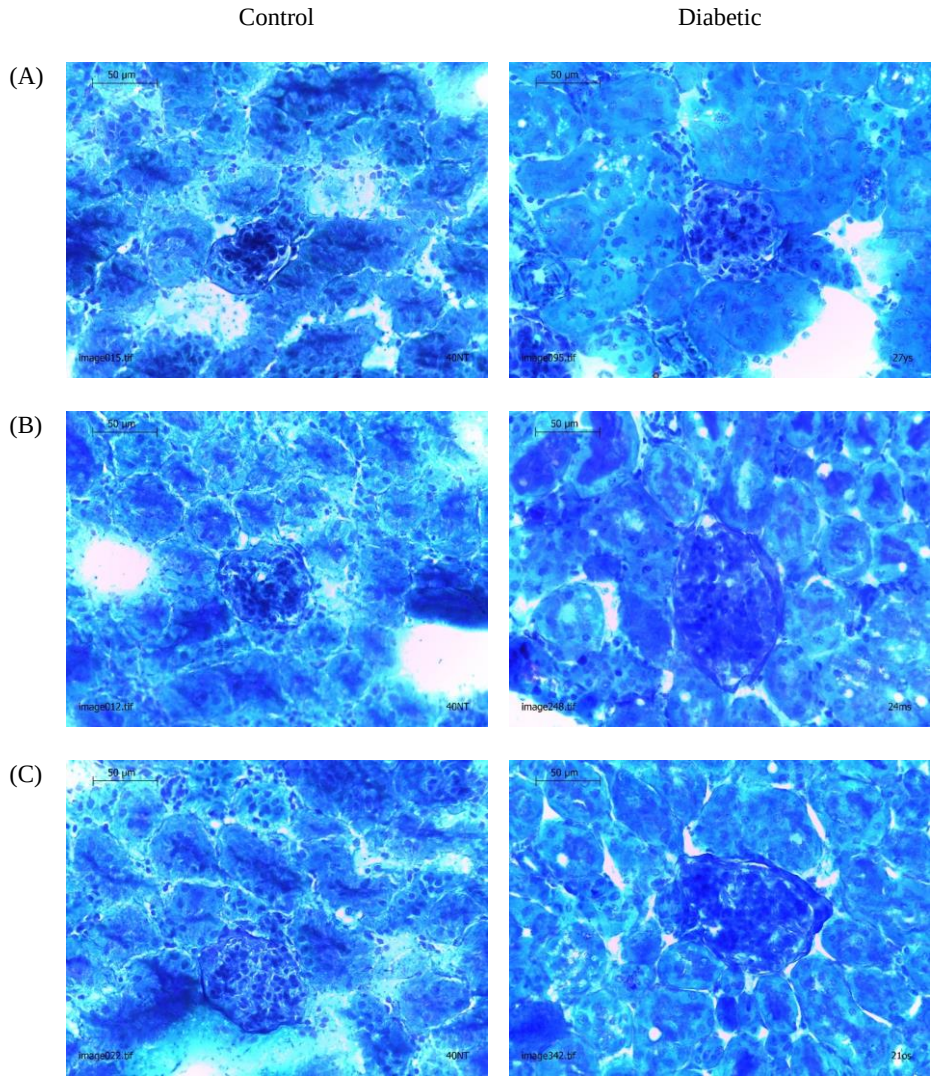

3.8.8 **Gene expression analysis**

The gene expressions of PVT1 (Figure 3.19), TGF-β1 (Figure 3.20), PAI-1 (Figure 3.21), FN1 (Figure 3.22), COL4A1 (Figure 3.23) and BMP7 (Figure 3.24) of diabetic and control mice of different age groups were shown in the corresponding figures. All these gene expressions except BMP7 were increased with time in the diabetic mice. The PVT1 expression was increased significantly in diabetic mice of young (by 89%, $p < 0.05$), middle-aged (by 106%, $p < 0.05$) and old (by 156%, $p < 0.001$) group when compared to the age-matched controls. The TGF-β1 mRNA expression was increased significantly in diabetic mice of young (by 87%, $p < 0.05$), middle-aged (by 154%, $p < 0.05$) and old (by 441%, $p < 0.001$) group when compared to the age-matched controls. The PAI-1 mRNA expression was increased significantly in diabetic mice of young (by 139%, $p < 0.01$), middle-aged (by 187%, $p < 0.001$) and old (by 250%, $p < 0.01$) group when compared to the age-matched controls. The FN1 mRNA expression was increased significantly in diabetic mice of young (by 55%, $p < 0.05$), middle-aged (by 179%, $p < 0.001$) and old (by 184%, $p < 0.01$) group when compared to the age-matched controls. The COL4A1 mRNA expression was increased significantly in diabetic mice of young (by 85%, $p < 0.01$), middle-aged (by 124%, $p < 0.01$) and old (by 382%, $p < 0.001$) group when compared to the age-matched controls. In contrast to the PVT1 and ECM components mentioned above, the BMP7 mRNA expression was reduced in diabetic mice of young (by 34%, $p > 0.05$), middle-aged (by 43%, $p < 0.01$) and old (by 54%, $p < 0.001$) group when compared to the age-matched controls.

Figure 3.19: The PVT1 expression of diabetic and control mice of different age groups. Results were expressed in mean ± SEM, n = 6. A p-value < 0.05 was considered statistically significant using unpaired student's t-test between age-matched individual groups (*p < 0.05, **p < 0.01, ***p < 0.001).

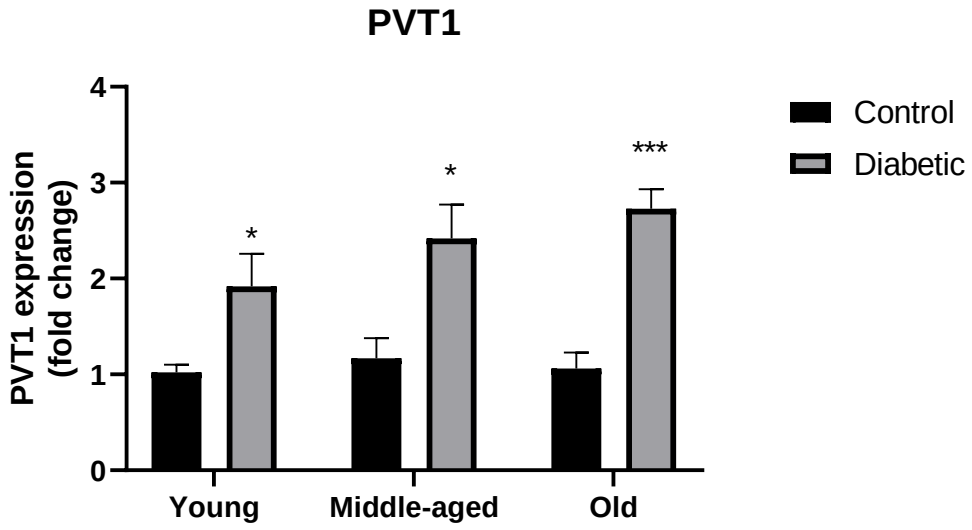

Figure 3.20: The TGF-β1 mRNA expression of diabetic and control mice of different age groups.

Results were expressed in mean ± SEM, n = 6. A p-value < 0.05 was considered statistically significant using unpaired student's t-test between age-matched individual groups (*p < 0.05, **p < 0.01, ***p < 0.001).

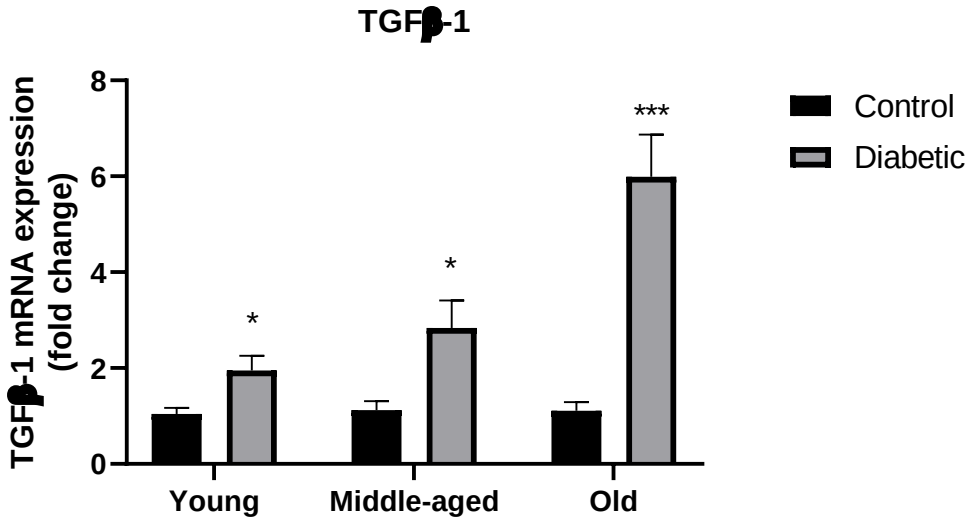

Figure 3.21: The PAI-1 mRNA expression of diabetic and control mice of different age groups.

Results were expressed in mean ± SEM, n = 6. A p-value < 0.05 was considered statistically significant using unpaired student's t-test between age-matched individual groups (*p < 0.05, **p < 0.01, ***p < 0.001).

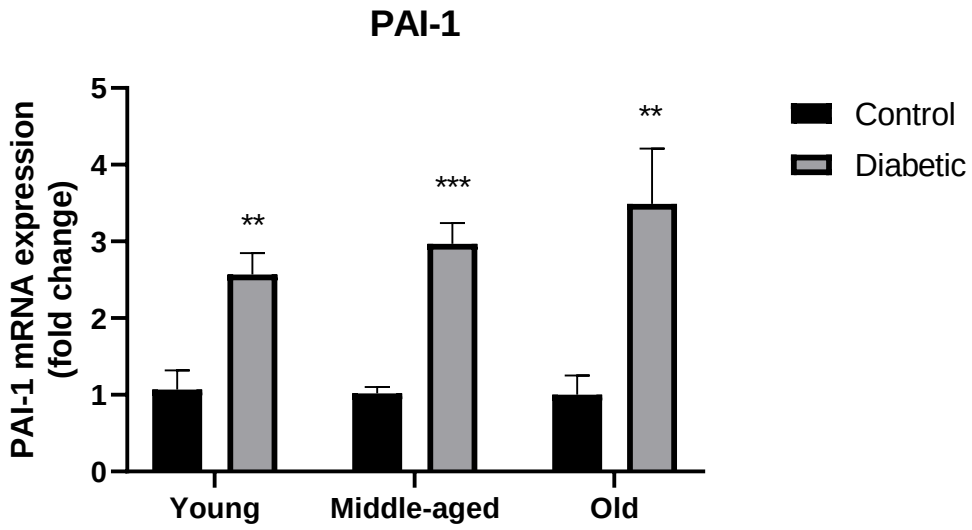

Figure 3.22: The FN1 mRNA expression of diabetic and control mice of different age groups.

Results were expressed in mean ± SEM, n = 6. A p-value < 0.05 was considered statistically significant using unpaired student's t-test between age-matched individual groups (*p < 0.05, **p < 0.01, ***p < 0.001).

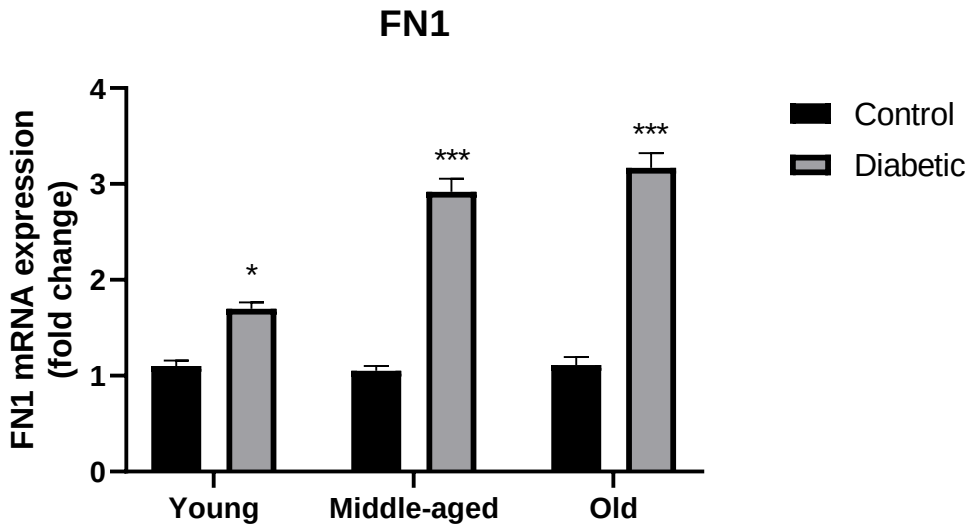

Figure 3.23: The COL4A1 mRNA expression of diabetic and control mice of different age groups.

Results were expressed in mean ± SEM, n = 6. A p-value < 0.05 was considered statistically significant using unpaired student's t-test between age-matched individual groups (*p < 0.05, **p < 0.01, ***p < 0.001).

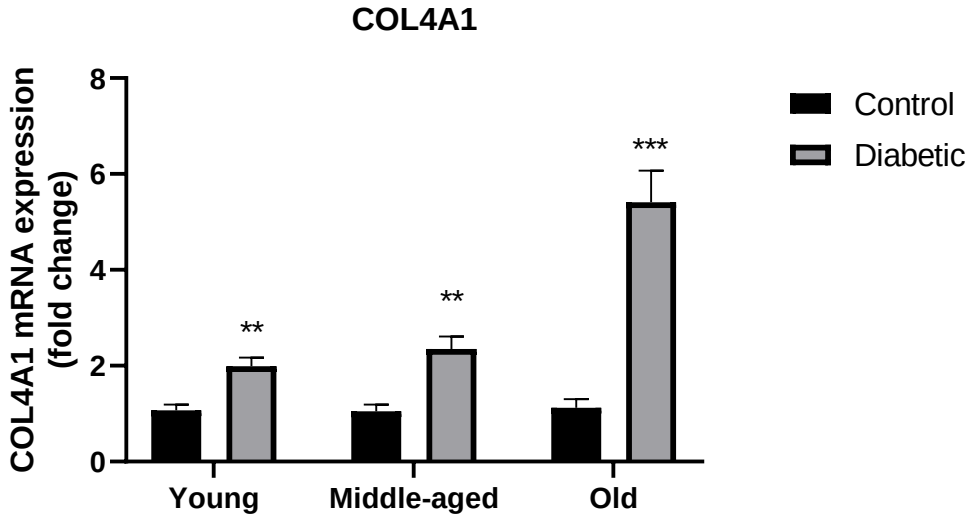

Figure 3.24: The BMP7 mRNA expression of diabetic and control mice of different age groups.

Results were expressed in mean ± SEM, n = 6. A p-value < 0.05 was considered statistically significant using unpaired student's t-test between age-matched individual groups (*p < 0.05, **p < 0.01, ***p < 0.001).

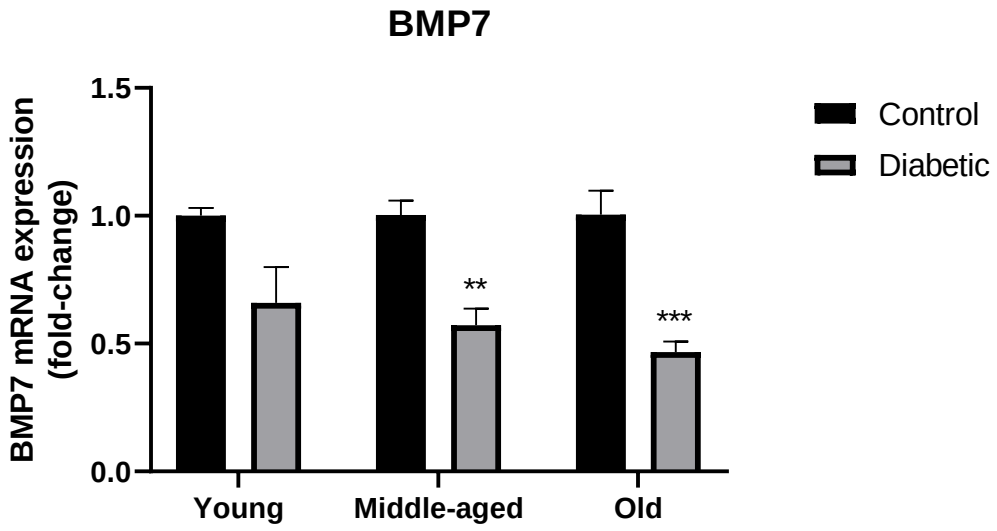

3.9 Discussions

Diabetic nephropathy is a common complication in patients with type 1 or 2 diabetes mellitus. Type 2 diabetes is a complex heterogenetic disease that its development involves a combination of genetic and environmental factors. Establishing an appropriate murine model of DN relied primarily on the induction and maintenance of diabetes. A combination of high fat diet (60% kcal from fat) and three consecutive low dose STZ (40mg/kg of body weight) was shown to be suitable for induction of type 2 diabetes rather than either treatment alone. Previous *in vivo* studies had demonstrated high fat diet induced a gradual increase in insulin resistance and hyperinsulinemia, which were characteristics of many obese people. The high fat diet caused body weight gain, stable hyperglycemia, albuminuria and mesangial expansion with increased extracellular matrix proteins (fibronectin and type IV collagen) over time (Jiang et al., 2005; Winzell & Ahrén, 2004). Administration of low dose STZ caused a partial destruction of pancreatic β cell, which reduced insulin secretion to maintain normoglycemia and resulted in hyperglycemia over time. It was reported that there was a 60% reduction in relative pancreatic β cell volume in obese type 2 diabetes patients and 40% reduction in obese individuals with impaired fasting blood glucose levels (Phanish, Winn, & Dockrell, 2009). Mice injected with three dosages of STZ resulted in about 50% destruction of islets, which was similar to the amount lost β cells observed in type 2 diabetic patients (Gilbert, Fu, & Liu, 2011). The combination treatment had incorporated the advantages of both high fat diet and STZ, which offered a metabolic profile resembling type 2 diabetes. In addition to cost effectiveness, it minimized the variability of diet-induced diabetes development and thus provide better experimental controls for evaluating diabetic treatment strategies.

As expected, a murine model of DN was successfully developed using the combination of high fat diet and low dose STZ in this study. A series of hallmark of DN (such as hyperglycemia, kidney hypertrophy, albuminuria, reduced creatinine clearance, and glomerular mesangial expansion) was observed in the diabetic mice. The diabetic mice were heavier than the age-matched controls. The difference in the percentage of body weight gain between the diabetic and control mice became smaller as the animals aged, which might be due to the heterogeneity of the response to high fat diet within the inbred C57BL/6 strain. It was reported that while all C57BL/6 mice fed with high fat diet were insulin resistant in a study, approximately 50% of them became obese and diabetic, 10% lean and diabetic, 10% lean and nondiabetic, and 30% displayed intermediate phenotype. The body weight gain of those mice was widely scattered at 6 and 9 months old, with values lower, similar, or higher than the body weights of the control mice (Burns et al., 2006).

Blood glucose concentration is the most common end-point measurement to evaluate the treatment effectiveness in diabetic subjects. Since different species tend to have different blood glucose concentrations than humans, extra attention should be paid when defining if the animal models are considered diabetic. It was reported that mice tend to have higher blood glucose concentrations than humans, the non-fasting blood glucose concentration over 13.8mmol/L (250mg/dL) or preferably a chronic elevation over 16.7mmol/L (300mg/dL) is appropriate to consider a mouse diabetic (King, 2012). In our study, the mice received high fat diet and STZ became diabetic after 2 weeks post-injection. The blood glucose level gradually increased and remained steadily high from 10-week-old till the end of the experiment in middle-aged and old groups. The chronic hyperglycemia present in diabetic mice had suggested the diabetes was effectively induced and maintained through the combination treatment of high fat diet and low dose STZ. The

control mice treated with low fat diet and vehicle injection remained non-diabetic throughout their life. The significant difference (about 2.3-fold) in blood glucose concentration between the diabetic and control mice at all ages (young, middle-aged and old) had suggested that these murine models were useful for evaluating treatment of diabetes and associated DN.

Renal hypertrophy is a consistent finding in the early stage of type 1 diabetes mellitus in humans and in the STZ-diabetes model (Weston, Wahab, & Mason, 2003). Kidney weight is measured as an index of renal hypertrophy (Sharma & Ziyadeh, 1994). In our study, the diabetic mice had higher kidney weight and kidney to body weight ratio than the age-matched controls at all age groups, which indicated the presence of renal hypertrophy in diabetic models.

Similar to many studies in the literature, the UAE (2.06-fold, 3.00-fold, 3.29-fold vs control at young, middle-aged, old, respectively) and UACR (1.53-fold, 2.08-fold, 2.49-fold vs control at young, middle-aged, old, respectively) were significantly higher than the age-matched controls. Albuminuria became more severe as the diabetic mice aged, which showed progression of DN continued if the diabetic condition was not intervened, while the UAE and UACR remained unchanged in controls over time. This suggested these sets of diabetic and control models provided a good platform for studying the treatment of DN in the next chapter. Previous study had demonstrated that the urine total protein measurement is less robust at low levels of protein than is urine albumin measurement and it is insufficiently sensitive to detect all clinically important concentrations of urine albumin (Moon, Moss-Morris, Hunter, & Hughes, 2017). This was agreed with our results on UPE and UPCR, which the significant difference in UPE

was not observed in the young group, the fold-change increases were smaller than that in UAE and UACR, and both UPE and UPCR were not significantly different across time. The UAE and UACR remained to be the important and reliable markers for assessing proteinuria.

The marked decline in creatinine clearance in diabetic mice at middle-aged and old age when compared with age-matched controls had indicated that the GFR was significantly reduced. The greater the decline, the greater the loss of glomerular filtration and the more likely to have end-stage renal disease. The significant difference in creatinine clearance between the diabetic mice of young and old age had suggested a progression of DN. It was worthy to note that the creatinine clearance in young diabetic mice was only slightly reduced when compared with its control. This could be explained by the compensatory changes in surviving nephrons after the nephron loss in kidney injury, which are commonly observed in the clinical practice. This leads to a lesser loss of total renal function than anticipated by the extent of anatomic damage. In fact, the earliest nephron losses are likely to be invisible due to functional compensation, which would bring GFR back into the normal range. For example, a loss of half the functioning nephrons leads to a decrease in GFR of only 20–30%, rather than the anticipated 50% (Yokoi et al., 2002). As the well-known reciprocal relationship between serum creatinine and GFR, serum creatinine was considered an index of kidney injury as well. The marked elevation of serum creatinine concentration in diabetic mice suggested a progressive kidney injury and renal function deterioration.

Albuminuria and decreased GFR were correlated strongly to mesangial expansion (Mauer et al., 1984). Mesangial matrix expansion appears to be the main cause of declining renal

function in DN (Steffes et al., 1989). The GMB thickening and mesangial expansion do not completely explain the decline in renal function as some patients with persistent proteinuria did not have diabetic glomerulopathy (Dalla Vestra et al., 2003) or vice versa (Caramori et al., 2003; MacIsaac et al., 2004). Other structural changes, such as podocyte foot process effacement, decrease in podocyte number and density, are involved, in which podocyte injury leads directly to proteinuria (Dronavalli et al., 2008; Jefferson et al., 2008; Wolf et al., 2005). Despite so, our study showed marked increases in glomerular and mesangial matrix areas in diabetic mice with relative to their age-matched controls in all age groups, which paralleled with elevated albuminuria and reduced creatinine clearance. Both glomerular and mesangial areas were significantly different between the young and old diabetic mice, suggesting a progression of DN.

Our study showed that the gene expression of ECM major components FN1 and COL4A1, and regulators such as TGF-β1 and PAI-1, were significantly increased in diabetic mice at all ages. The expression of PVT1, TGF-β1, PAI-1, FN1 and COL4A1 became higher in diabetic mice as they aged, which indicated a continual ECM accumulation in the glomeruli. TGF-β1 is a well-known strong regulator to promote fibrogenesis, which increases production of fibronectin and type IV collagen as well as decreases their degradation through increasing the activity of PAI-1. Some studies reported the renal mRNA expression of TGF-β1 increased up to 3-fold and 5.2-fold approximately in type 1 diabetic models of young and old age respectively (Tsukasa Nakamura et al., 1993; Pankewycz et al., 1994; Sharma & Ziyadeh, 1994). Similarly, the TGF-β1 mRNA expression was increased up to around 1.8-fold, 2.5-fold and 5.4-fold in diabetic mice of young, middle-aged and old age, respectively. The autocrine action of TGF-β1 that stimulates its own production might partly account for the higher expression level of TGF-β1. The PVT1 expression was increased up to about 2.6-fold in diabetic mice, which

suggested the diabetic or hyperglycemic condition induced the upregulation of PVT1 expression, in line with many previous studies. One study showed an approximate 3-fold increase in PVT1 expression in C57BL/6 mice which were uninephrectomised, fed with high fat high sugar diet, and injected with five consecutive low dose STZ (55mg/kg of body weight), and culled at ages over 37 week-old (D.-W. Liu et al., 2019). Another study showed PVT1 expression increased up to 5-fold in db/db mice, which was a well-established murine model of type 2 diabetes susceptible to DN (J. Li, Zhao, Jin, Li, & Song, 2020). Taking the more rigorous method to establish DN and the more susceptible genetic background into consideration, the magnitude of upregulation of PVT1 expression in our study might be comparable to that in the two studies. In contrast, BMP7 expression was decreased in diabetic mice at all ages. The decrease might be resulted from the overexpression of TGF-β1 that exerted inhibitory effects on BMP7 as well as due to the diabetic condition, as reported in other studies (S.-N. Wang et al., 2001; Shinong Wang & Hirschberg, 2003; Q. Yang et al., 2007; Yeh et al., 2009). The downregulation of BMP7 might fail to counteract the fibrotic actions of TGF-β1, to reduce the action of PAI-1 directly or indirectly through TGF-β1, which in turn promoted the ECM accumulation as well as to glomerular podocytes apoptosis in diabetic mice. Of note, the upregulation of PVT1 expression paralleled with the increase in TGF-β1, PAI-1, FN1 and COL4A1, and decrease in BMP7, which suggested an interrelationship among each other. The study on the effect of PVT1 inhibition in relation to the ECM components and regulators was conducted and discussed in the next chapter. Taken together, the continual ECM accumulation might partly account for the increased albuminuria and reduced creatinine clearance in diabetic mice, which promoted the progression of DN. These findings were in agreement with many previous *in vitro* and *in vivo* studies, which suggested that the PVT1 might play a key role in ECM accumulation contributing to

development of DN (Alvarez & DiStefano, 2011; Dean, 2012; J. Li et al., 2020). Targeting PVT1 might be a potential strategy for treating DN.

3.10 Conclusions

The murine model of DN was successfully established using a combination treatment of high fat diet and low dose STZ in male C57BL/6 mice. Hyperglycemia, kidney hypertrophy, albuminuria, reduced creatinine clearance, elevated serum creatinine, and increased glomerular and mesangial areas were observed in these diabetic mice. These conditions were intensified as the diabetic mice aged and were significantly different from the age-matched controls. The results had suggested that this nongenetic and relatively inexpensive murine model that mimicked the DN in humans was appropriate for future studies aimed at developing prevention and treatment of DN.

In this study, the gene expression of PVT1 was upregulated along with that of TGF-β1, PAI-1, FN1, COL4A1 while BMP7 was downregulated in diabetic model, and were significantly different from the age-matched controls of young, middle-aged and old age. The findings were in agreement with many *in vitro* studies in which the PVT1 expression was associated with increased expression of TGF-β1 and PAI-1 as well as production of ECM proteins such as collagen and fibronectin. It was suggested that the PVT1 might play a key role in modulation of ECM accumulation leading to deterioration of renal function. Therefore, PVT1 was suggested as a potential target for treatment of DN.

CHAPTER 4: EFFECT OF PVT1 INHIBITION IN DIABETIC C57BL/6 MICE AT DIFFERENT STAGES OF DN

4.1 Introduction

Following the previous chapter, we had successfully established a murine model of DN which exhibited some hallmarks similar to that observed in humans with DN. In addition to kidney hypertrophy, albuminuria, reduced creatinine clearance and glomerular mesangial expansion, the gene expression of key ECM components (FN1 and COL4A1) and regulators (TGF-β1, PAI-1 and BMP7) were modulated to increase ECM accumulation, which were paralleled to upregulation of PVT1 expression in diabetic mice. These manifestations were worsened as the diabetic mice aged. In order to elucidate the role of PVT1 in ECM accumulation leading to the progression of DN, the inhibition of PVT1 expression was conducted in diabetic mice using RNA interference (RNAi).

4.2 Long noncoding RNAs, PVT1 and DN

For decades the focus of gene regulatory system has been mainly relied on the protein encoding genes, whereas genomic analyses have determined that approximately 90% of the noncoding sequences of the human genome are transcribed into noncoding RNAs (Z. Yang et al., 2019). Long noncoding RNAs (lncRNAs) is a class of RNAs with length of over 200 nucleotides that do not encode any proteins. Like mRNAs, most lncRNAs have their own promoters, are RNA polymerase II transcribed, 5'-capped, polyadenylated and subjected to splicing. LncRNA genes are dispersed throughout the genome. They can be inter- or intragenic. In the latter case, they are positioned in sense or antisense direction, inside exons, introns or overlapping both (Ignarski, Islam, & Müller, 2019). Despite they

have been regarded as “noises or wastes” from transcription for a long time, emerging evidence have shown lncRNAs play critical regulatory roles in multiple biological processes at all levels (i.e. transcriptional, post-transcriptional and post-translational). They may act (i) as sponges for microRNA or as naturally competing endogenous RNAs (ceRNAs), (ii) as host genes for microRNAs, (iii) as scaffolds to bring protein complexes together, (iv) as controllers of mRNA decay, DNA sequestration of transcription factors, and epigenetic regulation of chromatin compaction, and (v) as stabilizers of mRNA through miRNA binding site masking (Raut & Khullar, 2018). Often, a single lncRNA may have more than one function, which varies based on cell type, stimuli, and cellular localization (Z. Yang et al., 2019). Through their influence on gene expression, lncRNAs are increasingly recognized as players with essential roles in molecular and cellular process such as proliferation, differentiation, apoptosis and senescence (J. Kim et al., 2016).

Recent studies have shown the dysfunction of several long noncoding RNAs in DN, retinopathy, neuropathy and cardiomyopathy suggesting their potential role in the pathogenesis, and hence a potential therapeutic target of diabetes-induced microvascular complications. A schematic model showing functional role of lncRNAs in DN was shown in Figure 4.1 (Raut & Khullar, 2018). For instance, PVT1 is the first lncRNA gene being identified as a key determinant of ESRD in human (Hanson et al., 2007). It is one of the lncRNAs that promotes ECM accumulation in mesangial cells (Alvarez & DiStefano, 2011), and as a host for miR-1207-5p that upregulates renal TGF-β1, PAI-1, FN1 and COL4A1 expression independently of PVT1 (Alvarez et al., 2013). This indicates PVT1 plays a crucial role in the pathogenesis and progression of DN. The upregulated lncRNAs have a common function in promoting the ECM accumulation, glomerular sclerosis, renal interstitial fibrosis, and inflammation and thickening of mesangial cells, while the

downregulated lncRNAs appear to function as the protective factor against DN (Y. Li et al., 2019). At present, most of the evidence linking lncRNAs and ECM accumulation and subsequent fibrosis is *in vitro* data. Thus, further investigation on the role of lncRNAs and their modes of actions in the development of DN *in vivo* is needed to pave the way for early diagnosis as well as better prevention and treatment options including RNAi-based therapeutics.

4.3 Challenges of RNAi *in vivo*

RNAi refers to a post-transcriptional gene silencing tool to neutralize or silence the pathological protein via activating RNA-induced silencing complex (RISC), endogenously. Gene silencing is made feasible *in vitro*, *in vivo* and in humans with the use of siRNA, which are synthetic RNA duplex designed to specifically knockdown the gene to treat a disease at cellular and molecular levels. Effective delivery of siRNA is the most challenging hurdle in RNAi *in vivo* (de Fougerolles et al., 2007). Despite quite efficient and reliable gene silencing *in vitro*, only limited RNAi has been achieved *in vivo* because of rapid enzymatic degradation by endogenous nucleases, uptake by phagocytes, aggregation with serum proteins, poor cellular uptake of siRNA, and kidney filtration (Shim & Kwon, 2010). Initially, the viral vectors have been employed to deliver siRNA into the cell. However, the stimulation of the immune system through the activation of viral pathogens was found to be the foremost hurdle. Tremendous efforts were made to develop a non-viral and clinically translatable approach for the intracellular transfection of siRNA (Raval, Jogi, Gondaliya, Kalia, & Tekade, 2019).

In order to enhance RNAi efficacy, delivery strategy (local or systemic), delivery system (chemical modification or transfection agents/ siRNA carriers) and siRNA design, must

be carefully considered. The route of administration depends on the types of target tissues and cells. Systemic delivery via intravenous (i.v.) or intraperitoneal (i.p.) is widely applicable when the target sites are not locally confined or not readily accessible, such as kidneys. Systemic siRNA delivery imposes additional barriers that the siRNA should remain in its active form during circulation and reach target tissues after passing through multiple barrier organs (e.g. liver, kidney and lymphoid organs) (Shim & Kwon, 2010). The naked siRNA has large molecular weight (about 13 kDa) and polyanionic nature (about 40 negative phosphate charges), and hence it does not freely cross the cell membrane (Akhtar & Benter, 2007). In addition, siRNA has relatively short half-life in vivo due to rapid degradation by endogenous enzymes. Therefore, delivery systems or chemical modification of siRNA are required to facilitate its access to the target cells. Judicious use of chemical modifications can improve the stability of a siRNA duplex, decrease the likelihood of triggering an innate immune response, lower the incidence of off-target effects (OTEs), and improve pharmacodynamics. However chemical modifications can alter the potency of the siRNA and frequently a chemically modified siRNA will show lower potency than the unmodified one of the same sequence, especially when extensively modified (Behlke, 2008). To date, several types of delivery systems have been developed to facilitate siRNA delivery *in vivo*, which includes liposomes, cationic polymers, cationic liposomes (Whitehead, Langer, & Anderson, 2009). Complex formation with cationic polymers or incorporation into liposomes are a promising approach for delivery of siRNAs because they are prevented from being excreted from the kidney due to their size. In addition, the positive charge of the complex of siRNAs and carriers could enhance cellular uptake through electrostatic interaction with the negative charge on the cell membrane. Moreover, surface modification of cationic compounds with polyethyleneimine (PEG) and/or ligands enables the cell-selective targeting of siRNAs *in vivo* (Kawakami & Hashida, 2007).

The effectiveness of RNAi also relies on the design of siRNA. Effective gene silencing comes with perfect or near-perfect Watson-Crick base pairing between the mRNA transcript and the antisense or guide strand of the siRNA, which results in cleavage of the mRNA by the RISC (D. H. Kim & Rossi, 2007). It is reported at least eight specific determinants of siRNA functionality have been identified through analysing thermodynamic characteristics of the siRNA test panel. Three criteria are particularly important for siRNA functionality, which includes moderate to low G/C content, low internal stability of the sense 3'-end (5' antisense) and a lack of internal repeats or palindromes that may form internal fold-back structures to reducing the effective concentration and silencing potential of the siRNA. The remaining five criteria describe base preferences at specific positions (positions 3, 10, 13 and 19) of the sense strand. (Reynolds et al., 2004).

4.4 Hydrodynamic approach for systemic delivery of siRNA

Hydrodynamic approach has proven to be simple and useful for siRNA delivering *in vivo* (Lewis & Wolff, 2007; Sørensen et al., 2003). It involves the rapid intravenous injection of siRNA in a large volume (i.e. equivalent of about one time the animal's blood volume) of vehicle solution to achieve effective localization of siRNA mainly in the liver, and to a less extent in the kidney, lung, and pancreas (Akhtar & Benter, 2007; Wesche-Soldato et al., 2005). Previous studies demonstrated hydrodynamic injection were successful in delivery and uptake of siRNA by the kidneys (Lewis et al., 2002; D. Ma et al., 2009; Van de Water et al., 2006; Wesche-Soldato et al., 2005). The original study, from which the hydrodynamic delivery method is developed, investigated the transfection in mice by systemic administration of plasmid DNA via tail vein. It demonstrated that level of gene

expression is related to the volume of DNA solution administered as well as the injection time. The optimal injection volume is approximately 8-12% of the body weight. The level of gene expression is found to decrease with increasing injection time. (F. Liu et al., 1999). A separate study, used siRNA encapsulated in the cationic liposomal agent DOTAP, demonstrated hydrodynamic injection was more effective than standard injection (Larson et al., 2007). Of note, younger animals have a smaller cardiac output, a smaller injected volume is sufficient to reach the hydrostatic pressure required for a high level of gene expression. Generally, an injection volume was used of 10% of the body weight of the experimental animal in a relatively short time (15–30 s), whereas a volume of 50–100 μl is the generally accepted average for intravenous injections in mouse tail veins. The sudden increase in hydrostatic pressure may induce a severe, but transient capillary dysfunction, and may result in capillary 'leakage' leading to exposure of parenchymal tissue cells (in the case of the kidney the tubular epithelium) to the siRNA (Geurt Stokman, 2010). Although some minor liver damage as indicated by transient elevation of alanine aminotransferase (ALT) was observed, the mice recovered quickly afterwards. Previous studies demonstrated hydrodynamic injection were successful in delivery and uptake of siRNA by the kidneys (Lewis et al., 2002; D. Ma et al., 2009; Van de Water et al., 2006; Wesche-Soldato et al., 2005). Furthermore, gene silencing effect of siRNA is transient in mammalian cells as the intracellular concentrations of siRNA are diluted over the course of successive cell divisions (Hannon, 2002; D. H. Kim & Rossi, 2007; Sørensen et al., 2003). The peak level of gene expression can be regained by repeated injection of siRNA but a similar reduction pattern is observed over time (F. Liu et al., 1999).

4.5 Current progress of RNAi-based therapeutics in clinical trials

RNAi-based therapeutics have emerged for the treatment of cancer, infectious diseases, and other diseases associated with specific gene disorders. Since the discovery of RNAi,

there have been more than 30 clinical trials involving 21 different siRNAs or the precursors to siRNAs known as short hairpin RNA (shRNAs) (Burnett et al., 2011). The delivery methods of siRNA-based therapeutics continue to improve when maximizing the specificity while minimizing the toxicity and the degradation of the therapeutics. The delivery systems can be classified into *ex vivo* delivery and systemic delivery. *Ex vivo* delivery makes use of a procedure called autologous cell therapy in which the removed cells from the patients are modified with siRNA/shRNA and then reimplanted/reinfused into the patients. For example, three clinical trials that has delivered lentiviral-delivered shRNA for the treatment of HIV/AIDS, an antitumor bifunctional siRNA (bi-shRNA), and siRNA for the treatment of metastatic melanoma. Systemic delivery of siRNA/shRNA therapeutics includes different administration routes by intravenous injection, intravitreal injection, oral, inhalation, and topical application. Among all, intravenous injection is the most commonly used method of systemic delivery. One clinical trial has used intravenous injection of siRNA for acute kidney injury and delayed graft function, which has proceeded to phase II trials with favourable safety data (Watts & Corey, 2010).

Figure 4.1: Schematic model showing functional role of long noncoding RNAs in DN (adapted from Raut & Khullar, 2018)

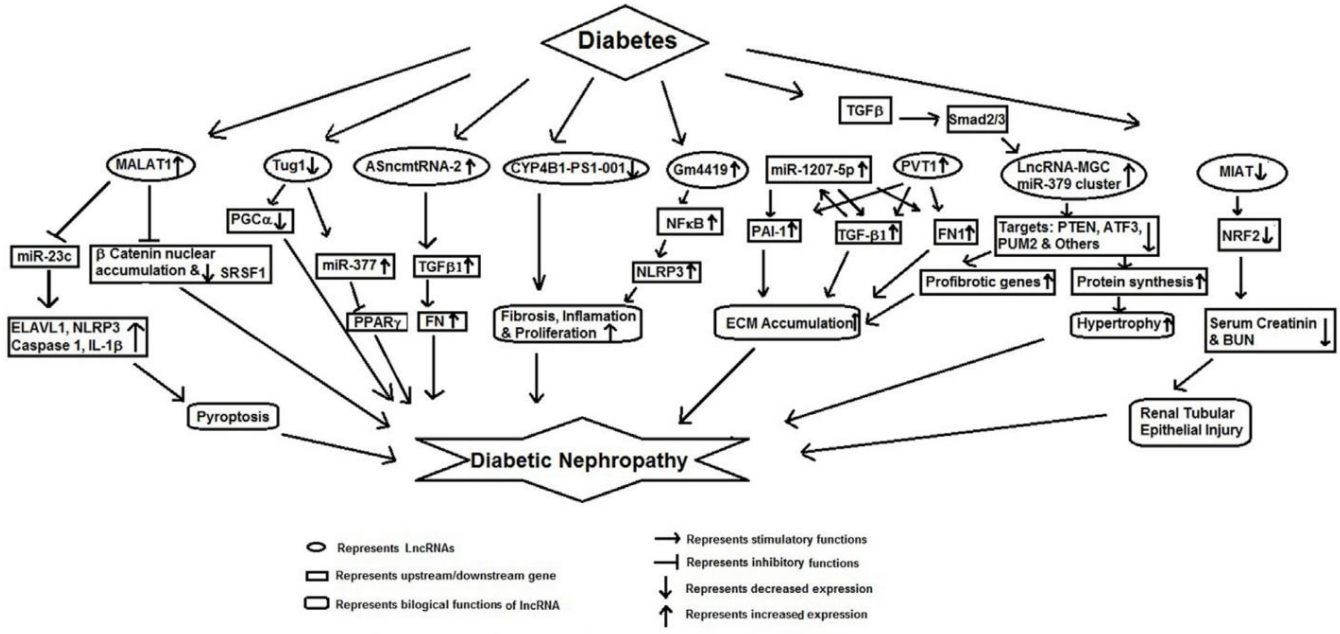

4.6 Aims

This project aims to study the role of PVT1 in a DN murine model. The specific aims of this chapter are:

(1) to study the effectiveness of PVT1 inhibition in C57BL/6 mice using RNAi; and

(2) to study the effect of PVT1 inhibition on progression of DN in diabetic C57BL/6 mice at early, intermediate and relatively advanced ages.

4.7 Experimental overview

The male C57BL/6 mice were used in this study. After weaning, they were randomly allocated into either diabetic or control groups. The diabetic and control groups were fed with high fat diet (HFD, 60% kcal from fat; TD06414, Enivgo, Madison, WI) and low fat diet (LFD, 10% kcal from fat; TD08806, Enivgo, Madison, WI) respectively. At 5 week of age, the HFD-fed mice were intraperitoneally administered with low-dose STZ (40 mg/kg of body weight per day) for three consecutive days after 4 hr fasting, while the LFD-fed mice were administered with vehicle (sodium citrate buffer). Type 2 diabetes was induced by the combined treatment of HFD and STZ. The diabetic group and normal control group were represented by the HFD-STZ-treated mice and the LFD-vehicle-treated mice, respectively. The diabetic mice were divided into two groups, which were treated with scramble siRNA (DM+siRNA(scramble) or PVT1 siRNA (DM+siRNA(PVT1)). The DM+siRNA(PVT1) group was compared with the DM+siRNA(scramble) group for effects of PVT1 inhibition, while the normal control group served as a reference. A pilot study on the effectiveness of PVT1 inhibition was conducted in control and diabetic mice two days after siRNA-injection, which gene expressions of PVT1 and ECM components and regulators were evaluated. Successful

inhibition on PVT1 using siRNA would substantiate further study on its effect on progression of DN in mice at three different ages, which detailed evaluation at functional, histological and molecular levels was covered.

All mice were housed in the animal facility maintained on constant temperature (22-25 °C), relative humidity (55-65%), 12 hr light/12 hr dark cycles, and were supplied with tap water *ad libitum*. Body weights and blood glucose were measured weekly on the commence of the study. The mice were culled at around the age of 9 (young), 16 (middle-aged) or 24 (old) weeks old which represented early, intermediate and relatively advanced stages of diabetes. Samples (e.g. blood, urine, and kidneys) were collected on or before culling.

Evaluations at functional level (e.g. UAE, UACR, UPE, UPCR, creatinine clearance and serum creatinine), histological level (e.g. kidney hypertrophy, glomerular area and mesangial area) and molecular level (e.g. gene expressions of PVT1, TGF-β1, PAI-1, FN1, COL4A1 and BMP-7), as well as body weight and blood glucose, were conducted according to the methods described in Chapter 2.

4.8 Results

4.8.1 Pilot study on PVT1 inhibition

The effectiveness of PVT1 inhibition using *in vivo* delivery of PVT1-siRNA was evaluated by the relative reduction on PVT1 expression in both diabetic and control mice. The gene expressions of PVT1 (Figure 4.2), TGF-β1 (Figure 4.3), PAI-1 (Figure 4.4), FN1 (Figure 4.5), COL4A1 (Figure 4.6) and BMP7 (Figure 4.7) of diabetic and control mice were shown in the corresponding figures. As shown in Figure 4.2, the expression of PVT1 was significantly decreased (by 50%) in diabetic mice with PVT1-siRNA when compared with diabetic mice with scramble-siRNA. In the control mice, the gene

expression of PVT1 was significantly decreased (by 67%) after the PVT1-siRNA treatment. These results had demonstrated the effective inhibition on PVT1 expression in the C57BL/6 mice. The effect of PVT1 inhibition on progression of DN was further studied in the diabetic mice as described in the sections below.

In summary, treatment with PVT1-siRNA had significantly suppressed gene expressions of PVT1, TGF-β1, PAI-1, FN1 and COL4A1 in both diabetic mice and control, while that of BMP7 remained unchanged. In control mice, decrease in mRNA expressions of TGF-β1 (by 67%), PAI-1 (57%), FN1 (67%) and COL4A1 (65%) were observed in PVT1-siRNA treatment. A comparable decrease in mRNA expressions of TGF-β1 (by 44%), PAI-1 (43%), FN1 (50%) and COL4A1 (40%) were observed in diabetic mice treated with PVT1-siRNA.

Figure 4.2: The expression of PVT1 in (A) diabetic and (B) control mice two days post siRNA injection.

(A) Diabetic mice were treated with either scramble-siRNA (DM+siRNA(scramble)) or PVT1-siRNA (DM+siRNA(PVT1)). (B) Control mice were treated with either scramble-siRNA (Control+siRNA(scramble)) or PVT1-siRNA (Control+siRNA(PVT1)). Results were expressed in mean ± sem, n = 3. A p-value < 0.05 was considered statistically significant using unpaired student's t-test (*p < 0.05, **p < 0.01, ***p < 0.001 vs diabetic or control treated with scramble-siRNA).

(A)

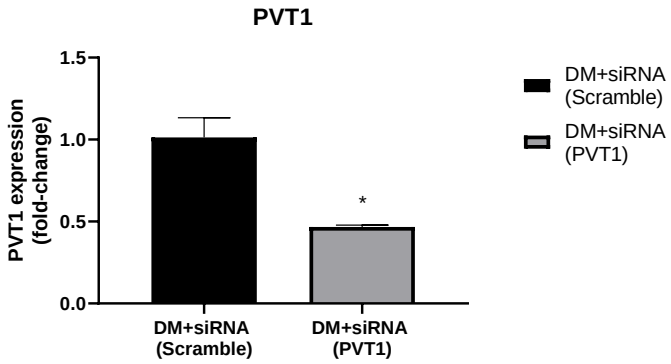

(B)

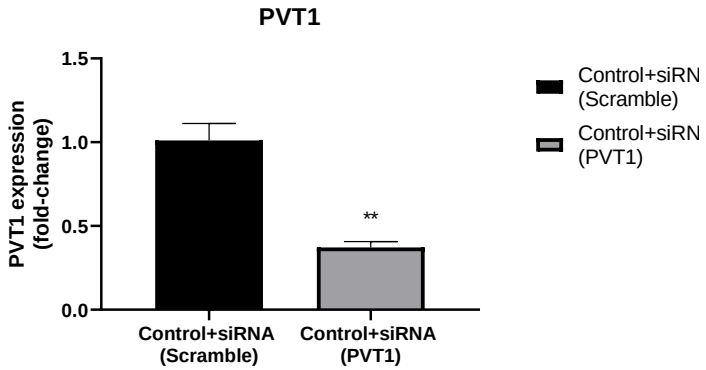

Figure 4.3: The mRNA expression of TGF-β1 in (A) diabetic and (B) control mice two days post siRNA injection.

(A) Diabetic mice were treated with either scramble-siRNA (DM+siRNA(scramble)) or PVT1-siRNA (DM+siRNA(PVT1)). (B) Control mice were treated with either scramble-siRNA (Control+siRNA(scramble)) or PVT1-siRNA (Control+siRNA(PVT1)). Results were expressed in mean ± sem, n = 3. A p-value < 0.05 was considered statistically significant using unpaired student's t-test (*p < 0.05, **p < 0.01, ***p < 0.001 vs diabetic or control treated with scramble-siRNA).

(A)

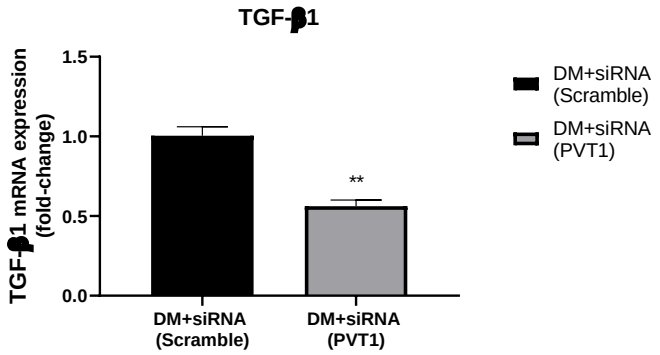

(B)

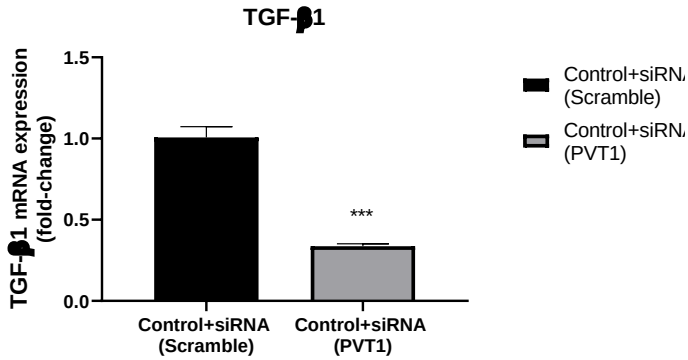

Figure 4.4: The mRNA expression of PAI-1 in (A) diabetic and (B) control mice two days post siRNA injection.

(A) Diabetic mice were treated with either scramble-siRNA (DM+siRNA(scramble)) or PVT1-siRNA (DM+siRNA(PVT1)). (B) Control mice were treated with either scramble-siRNA (Control+siRNA(scramble)) or PVT1-siRNA (Control+siRNA(PVT1)). Results were expressed in mean ± SEM, n = 3. A p-value < 0.05 was considered statistically significant using unpaired student's t-test (*p < 0.05, **p < 0.01, ***p < 0.001 vs diabetic or control treated with scramble-siRNA).

(A)

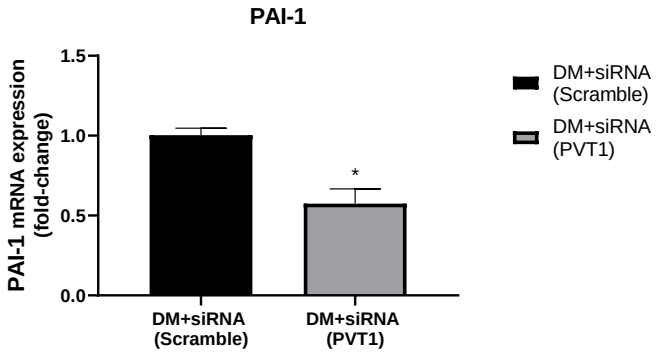

(B)

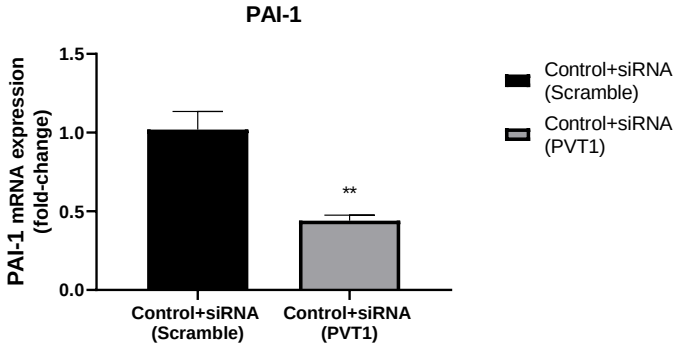

Figure 4.5: The mRNA expression of FN1 in (A) diabetic and (B) control mice two days post siRNA injection.

(A) Diabetic mice were treated with either scramble-siRNA (DM+siRNA(scramble)) or PVT1-siRNA (DM+siRNA(PVT1)). (B) Control mice were treated with either scramble-siRNA (Control+siRNA(scramble)) or PVT1-siRNA (Control+siRNA(PVT1)). Results were expressed in mean ± SEM, n = 3. A p-value < 0.05 was considered statistically significant using unpaired student's t-test (*p < 0.05, **p < 0.01, ***p < 0.001 vs diabetic or control treated with scramble-siRNA).

(A)

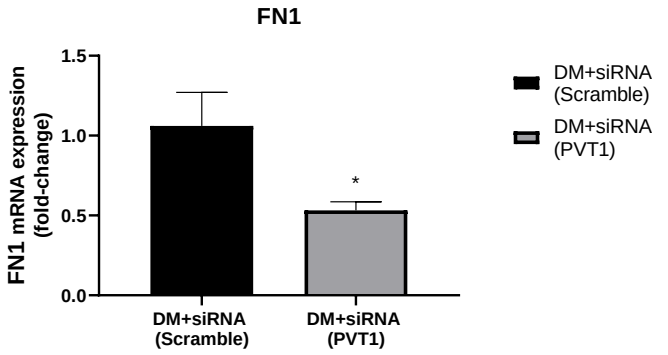

(B)

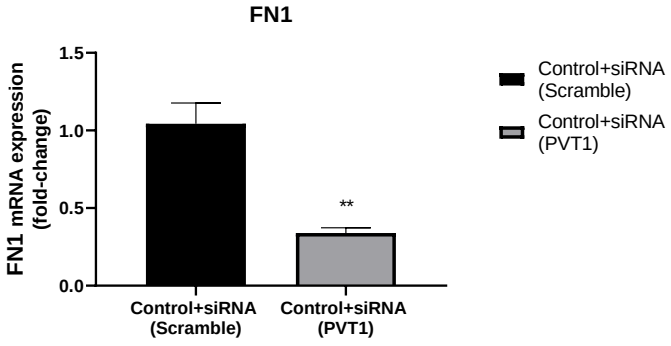

Figure 4.6: The mRNA expression of COL4A1 in (A) diabetic and (B) control mice two days post siRNA injection.

(A) Diabetic mice were treated with either scramble-siRNA (DM+siRNA(scramble)) or PVT1-siRNA (DM+siRNA(PVT1)). (B) Control mice were treated with either scramble-siRNA (Control+siRNA(scramble)) or PVT1-siRNA (Control+siRNA(PVT1)). Results were expressed in mean ± SEM, n = 3. A p-value < 0.05 was considered statistically significant using unpaired student's t-test (*p < 0.05, **p < 0.01, ***p < 0.001 vs diabetic or control treated with scramble-siRNA).

(A)

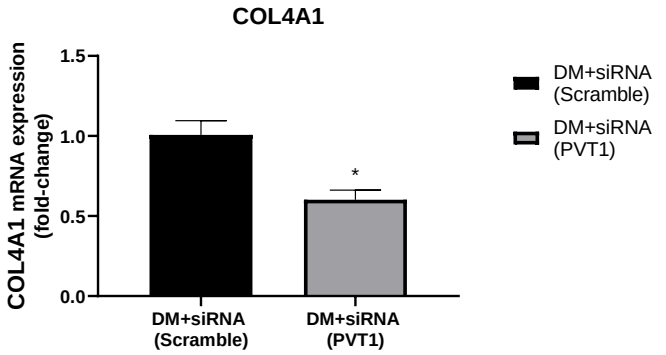

(B)

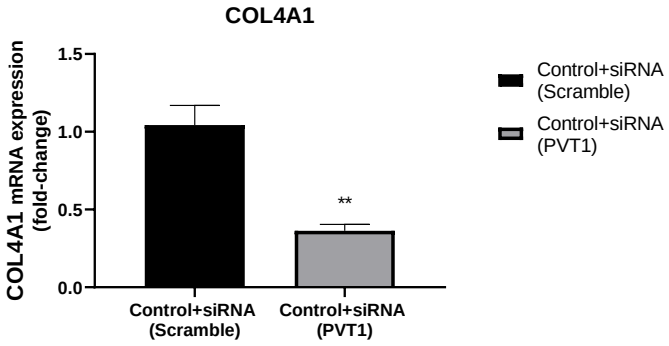

Figure 4.7: The mRNA expression of BMP7 in (A) diabetic and (B) control mice two days post siRNA injection.

(A) Diabetic mice were treated with either scramble-siRNA (DM+siRNA(scramble)) or PVT1-siRNA (DM+siRNA(PVT1)). (B) Control mice were treated with either scramble-siRNA (Control+siRNA(scramble)) or PVT1-siRNA (Control+siRNA(PVT1)). Results were expressed in mean ± SEM, n = 3. A p-value < 0.05 was considered statistically significant using unpaired student's t-test (*p < 0.05, **p < 0.01, ***p < 0.001 vs diabetic or control treated with scramble-siRNA).

(A)

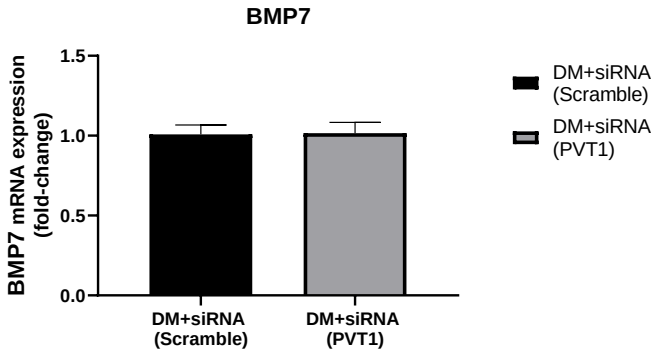

(B)

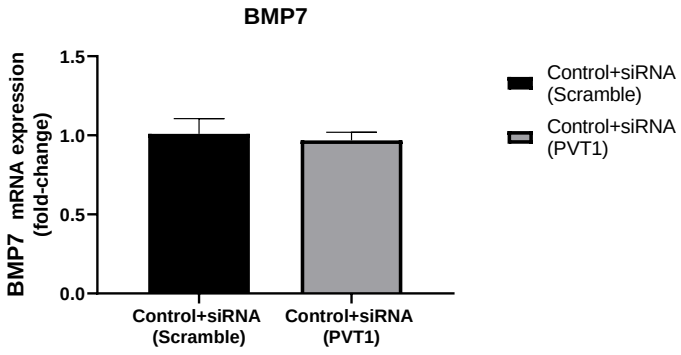

4.8.2 **Body weight**

The initial body weight (i.e. the weight at 4-week-old) was measured to determine if the age-matched mice were of similar weight at the beginning of the experiment. It was also used as the baseline to calculate the change of body weight at the end of experiment.

The initial body weight of control, diabetic mice with scramble-siRNA and diabetic mice with PVT1-siRNA of different age groups were shown in Figure 4.8. The initial body weights were not statistically different among all three groups of different treatments. Mice were of similar weight at the beginning of each age-matched experiment, despite the mice used for the old group experiment were of lighter body weight.

The final body weight of control, diabetic mice with scramble-siRNA and diabetic mice with PVT1-siRNA of different age groups were shown in Figure 4.9. Both diabetic mice with scramble-siRNA or PVT1-siRNA were significantly heavier (*$p < 0.05$) than the control mice at young age. In the middle-aged group, diabetic mice with scramble-siRNA was significantly heavier (*$p < 0.05$) than control and diabetic mice with PVT1-siRNA, while the latter two were of similar weight. At old age, the final body weight was similar among all three groups.

The body weight growth curve of siRNA-treated diabetic and control mice of different age groups was shown in Figure 4.10. The body weight gain was faster in the diabetic mice than in the control mice in all young, middle-aged and old groups. The change in body weight of diabetic and control mice of different age groups was shown in Figure 4.11. It was calculated as: difference between final body weight and initial body weight / initial body weight x 100%. The diabetic mice with scramble-siRNA had the greatest body weight gain among all at young and middle-aged groups. Moderate weight gain was observed in diabetic mice with PVT1-siRNA at young age (**$p < 0.01$ vs control; ^$p <$

0.05 vs DM+siRNA(scramble)) and middle-aged (^^p < 0.01 vs DM+siRNA(scramble)). The weight gain became similar in all mice at old age.

Figure 4.8: The initial body weight of siRNA-treated diabetic and control mice of different age groups.

Diabetic mice were treated with either scramble-siRNA (DM+siRNA(scramble)) or PVT1-siRNA (DM+siRNA(PVT1)), whereas control mice were normal mice without siRNA injection (Control). Results were expressed in mean ± SEM, n = 6. A p-value < 0.05 was considered statistically significant using one-way ANOVA.

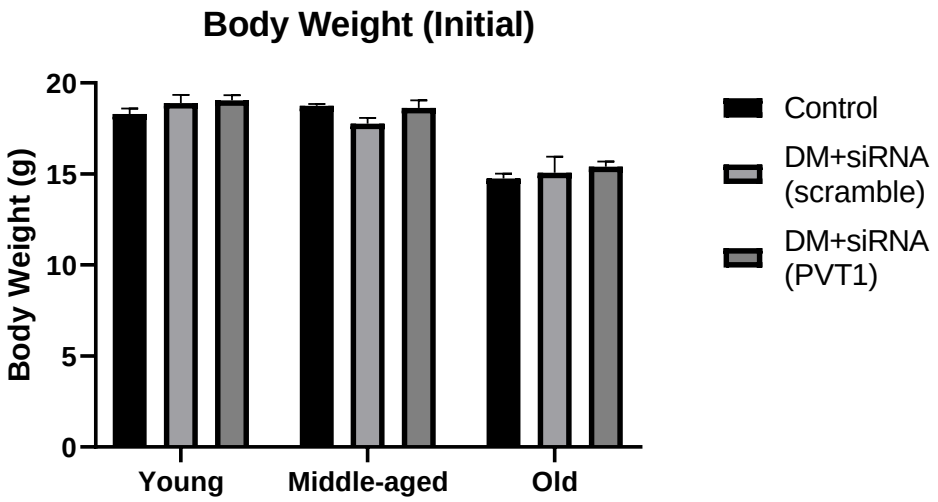

Figure 4.9: The final body weight of siRNA-treated diabetic and control mice of different age groups.

Diabetic mice were treated with either scramble-siRNA (DM+siRNA(scramble)) or PVT1-siRNA (DM+siRNA(PVT1)), whereas control mice were normal mice without siRNA injection (Control). Results were expressed in mean ± SEM, n = 6. A p-value < 0.05 was considered statistically significant using one-way ANOVA with Tukey post-test (*p < 0.05 vs control; ^p < 0.05 vs DM+siRNA(scramble)).

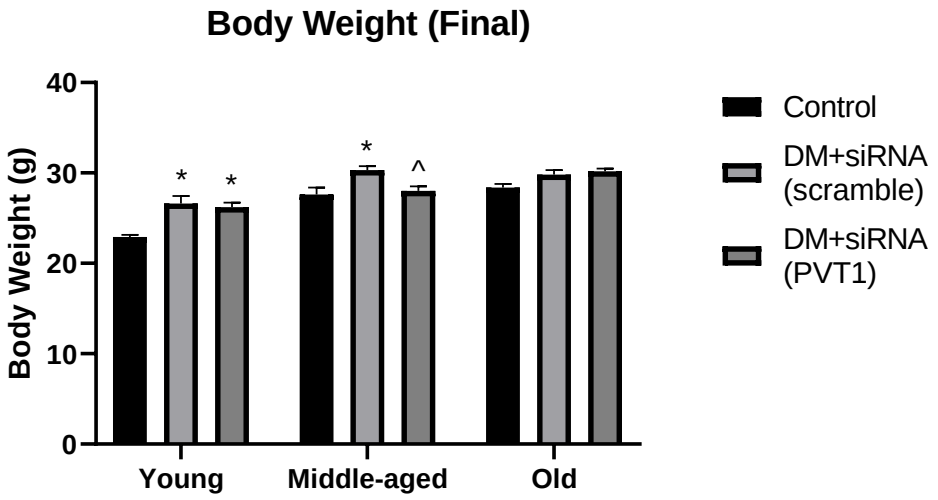

Figure 4.10: The body weight growth curve of siRNA-treated diabetic and control mice of different age groups, (A) young, (B) middle-aged and (C) old.

Diabetic mice were treated with either scramble-siRNA (DM+siRNA(scramble)) or PVT1-siRNA (DM+siRNA(PVT1)), whereas control mice were normal mice without siRNA injection (Control). Results were expressed in mean ± SEM, n = 6. A p-value < 0.05 was considered statistically significant using one-way ANOVA with Tukey post-test (*p < 0.05, **p < 0.01 vs control; ^p < 0.05 vs DM+siRNA(scramble)).

(A)

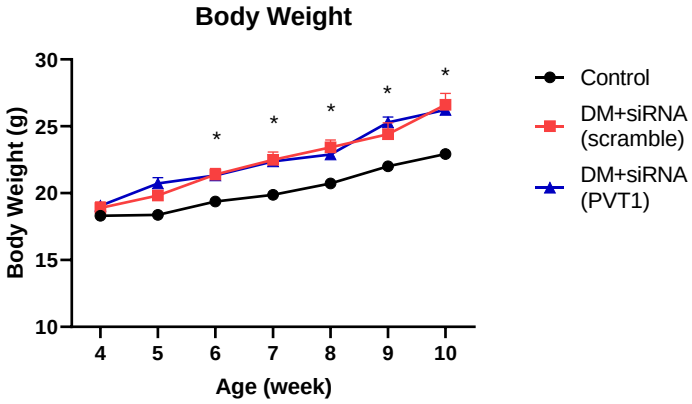

(B)

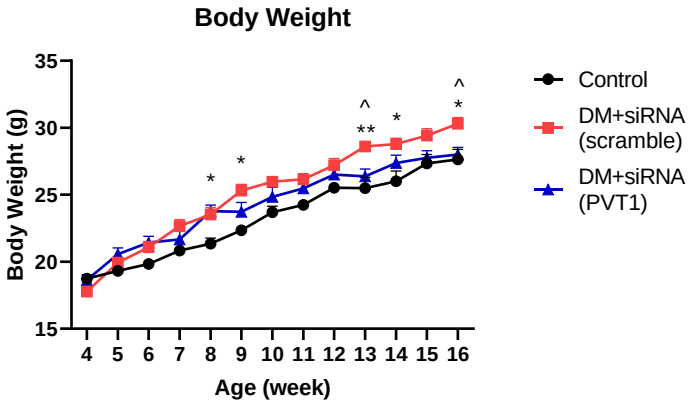

(C)

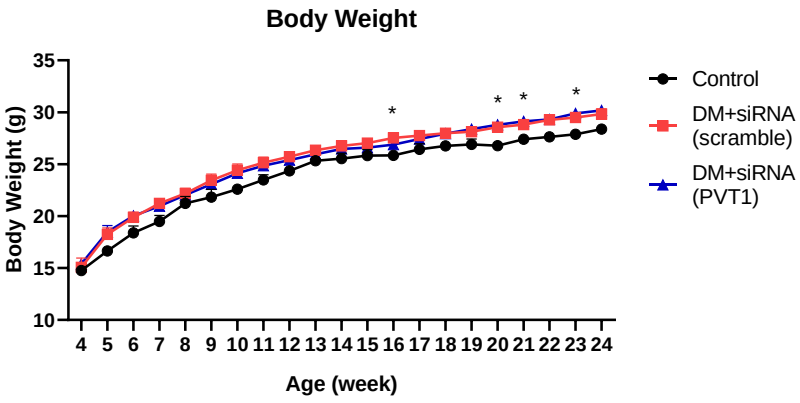

Figure 4.11: The change in body weight of siRNA-treated diabetic and control mice of different age groups.

Diabetic mice were treated with either scramble-siRNA (DM+siRNA(scramble)) or PVT1-siRNA (DM+siRNA(PVT1)), whereas control mice were normal mice without siRNA injection (Control). Results were expressed in mean ± SEM, n = 6. A p-value < 0.05 was considered statistically significant using one-way ANOVA with Tukey post-test (*p < 0.05, **p < 0.01, ***p < 0.001 vs control; ^p < 0.05, ^^p < 0.01 vs DM+siRNA(scramble)).

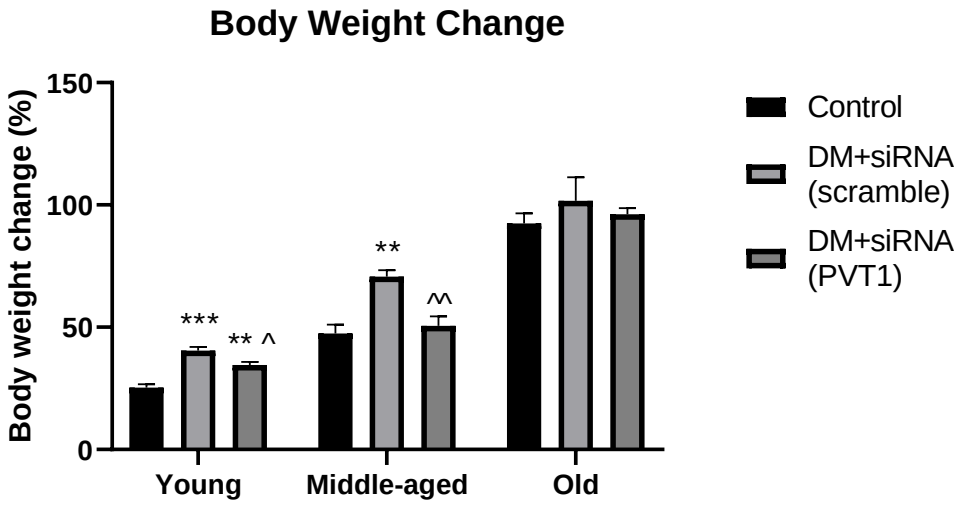

4.8.3 **Blood glucose**

At the beginning of the study, the initial blood glucose (at 4-week-old) was measured to determine if the age-matched mice were of normal blood glucose. Blood glucose was measured weekly to evaluate the status of diabetes. Mice with chronic elevation of blood glucose concentration over 17 mmol/L was considered to be diabetic.

The initial blood glucose of siRNA-treated diabetic and control mice of different age groups were shown in Figure 4.12. The initial blood glucose was similar among all treatment groups. All mice were with normal blood glucose levels when the experiment commenced. As the experiment proceeded, hyperglycaemia was gradually developed in diabetic mice with scramble-siRNA or PVT1-siRNA as a result of the combined treatment of high fat diet and low dose STZ. Significant increase in blood glucose was observed in diabetic mice from week 6 onwards.

The final blood glucose of siRNA-treated diabetic and control mice of different age groups were shown in Figure 4.13. Diabetic mice had significantly higher blood glucose than control mice. Blood glucose of diabetic mice with scramble-siRNA was significantly higher than those of control mice in all young (2.06-fold), middle-aged (2.50-fold) and old (2.38-fold) groups (***$p < 0.001$). Diabetic mice with PVT1-siRNA had lower blood glucose at young (not significant), middle-aged (^$p < 0.05$) and old (not significant) age when compared with diabetic mice with scramble-siRNA.

The weekly blood glucose of siRNA-treated diabetic and control mice of different age groups was shown in Figure 4.14. In general, the blood glucose increased gradually from 6-week-old in diabetic mice with scramble-siRNA or PVT1-siRNA. It remained steadily high from 11-week-old till the end of the experiment in middle-aged and old groups. The blood glucose of control mice remained normal (below 17 mmol/L) throughout the experiment at all ages.

Figure 4.12: The initial blood glucose of siRNA-treated diabetic and control mice of different age groups.

Diabetic mice were treated with either scramble-siRNA (DM+siRNA(scramble)) or PVT1-siRNA (DM+siRNA(PVT1)), whereas control mice were normal mice without siRNA injection (Control). Results were expressed in mean ± SEM, n = 6. A p-value < 0.05 was considered statistically significant using one-way ANOVA.

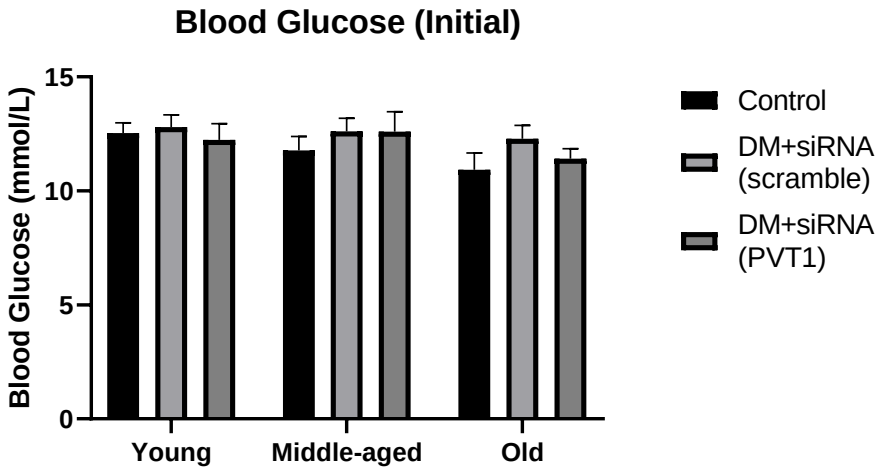

Figure 4.13: The final blood glucose of siRNA-treated diabetic and control mice of different age groups.

Diabetic mice were treated with either scramble-siRNA (DM+siRNA(scramble)) or PVT1-siRNA (DM+siRNA(PVT1)), whereas control mice were normal mice without siRNA injection (Control). Results were expressed in mean ± SEM, n = 6. A p-value < 0.05 was considered statistically significant using one-way ANOVA with Tukey post-test (*p < 0.05, **p < 0.01, ***p < 0.001 vs control; ^p < 0.05 vs DM+siRNA(scramble)).

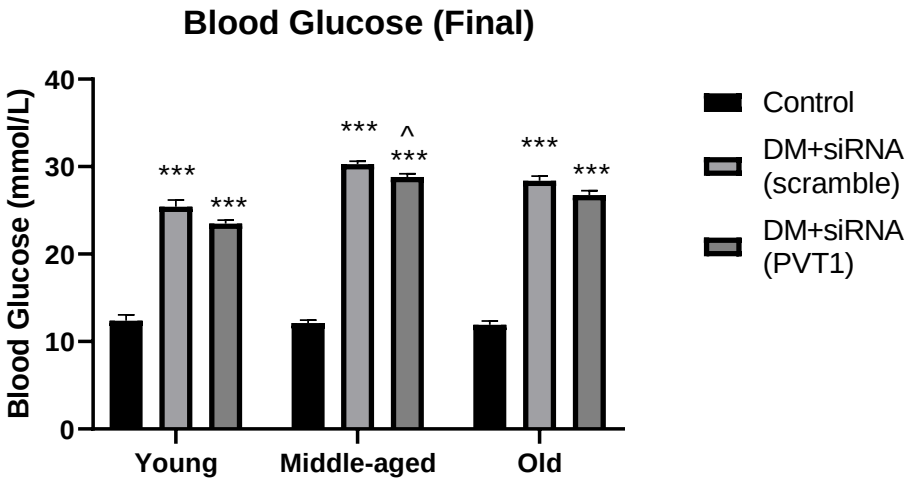

Figure 4.14: The change in blood glucose of siRNA-treated diabetic and control mice of different age groups, (A) young, (B) middle-aged, (C) old.

Diabetic mice were treated with either scramble-siRNA (DM+siRNA(scramble)) or PVT1-siRNA (DM+siRNA(PVT1)), whereas control mice were normal mice without siRNA injection (Control). Results were expressed in mean ± SEM, n = 6. A p-value < 0.05 was considered statistically significant using one-way ANOVA with Tukey post-test (*p < 0.05, **p < 0.01, ***p < 0.001 vs control).

(A)

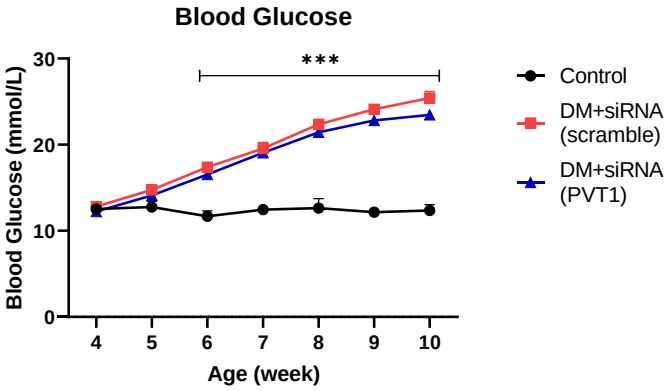

(B)

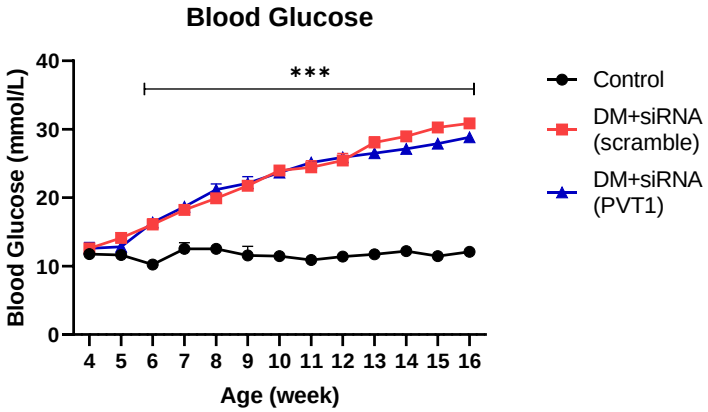

(C)

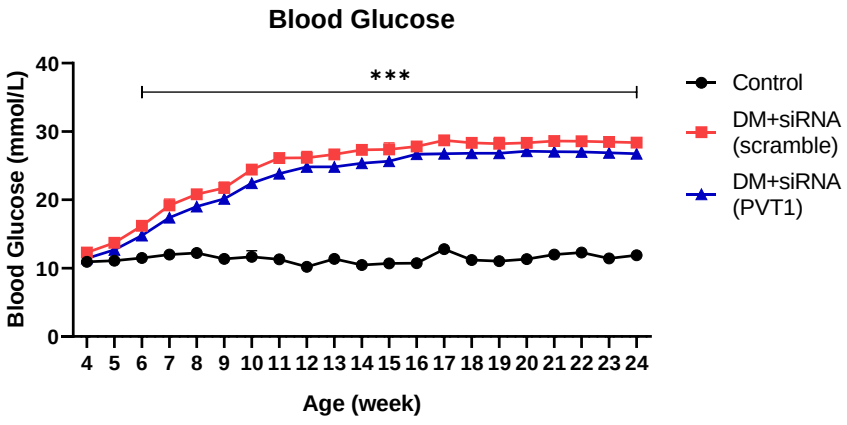

4.8.4 **Kidney weight**

Renal hypertrophy is a consistent manifestation in diabetic patients and murine models. The kidney weight was used as an index of renal hypertrophy in this study. The kidney weight of diabetic siRNA-treated mice and control mice of different age groups was shown in Figure 4.15. Diabetic mice had higher kidney weight than control mice. The kidney weight of diabetic mice with scramble-siRNA was higher than that of diabetic mice with PVT1-siRNA in all age groups.

The kidney to body weight ratio of siRNA-treated diabetic and control mice of different age groups was shown in Figure 4.16. Compared to the control mice, the kidney to body weight ratio was higher in diabetic mice with scramble-siRNA in all age groups and significant difference was observed in the middle-aged (**$p < 0.01$) and old (**$p < 0.01$) group. Diabetic mice with PVT1-siRNA had significantly lower kidney to body weight ratio than diabetic mice with scramble-siRNA at middle-aged and old age, of which the ratio were close to that of control mice.

Figure 4.15: The kidney weight of siRNA-treated diabetic and control mice of different age groups.

Diabetic mice were treated with either scramble-siRNA (DM+siRNA(scramble)) or PVT1-siRNA (DM+siRNA(PVT1)), whereas control mice were normal mice without siRNA injection (Control). Results were expressed in mean ± SEM, n = 6. A p-value < 0.05 was considered statistically significant using one-way ANOVA.

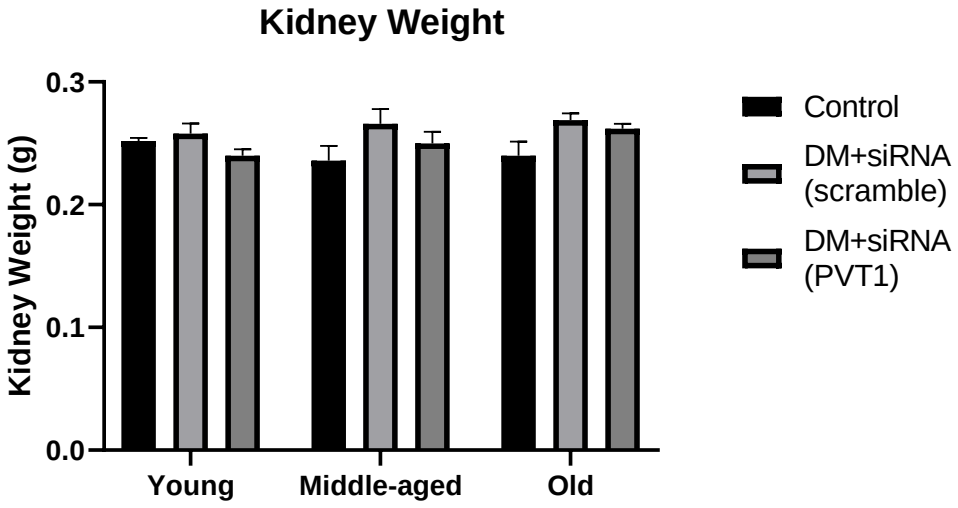

Figure 4.16: The kidney to body weight ratio of siRNA-treated diabetic and control mice of different age groups.

Diabetic mice were treated with either scramble-siRNA (DM+siRNA(scramble)) or PVT1-siRNA (DM+siRNA(PVT1)), whereas control mice were normal mice without siRNA injection (Control). Results were expressed in mean ± SEM, n = 6. A p-value < 0.05 was considered statistically significant using one-way ANOVA with Tukey post-test (*p < 0.05, **p < 0.01, ***p < 0.001 vs control; ^p < 0.05, ^^p < 0.01, ^^^p < 0.001 vs DM+siRNA(scramble)).

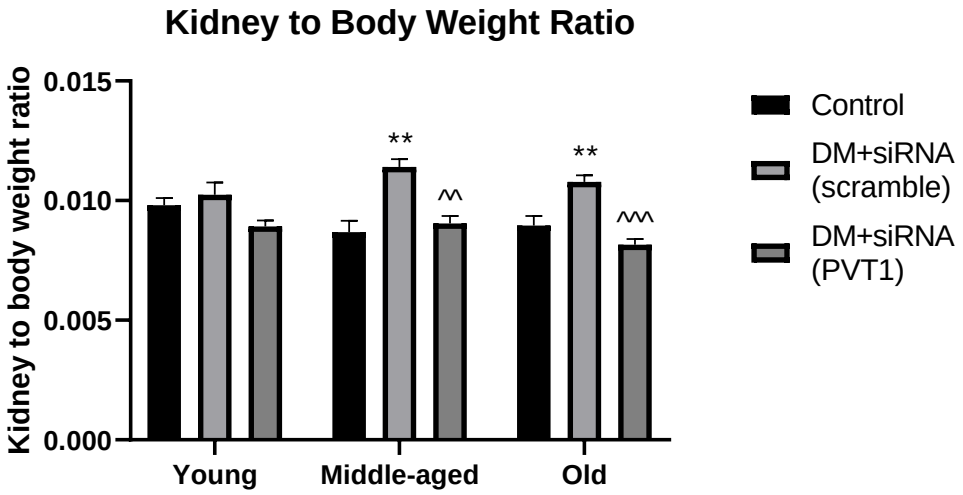

4.8.5 **Urinary albumin excretion and urine protein excretion**

The urinary albumin to creatinine ratio of siRNA-treated diabetic and control mice of different age groups was shown in Figure 4.17. The UACR was slightly increased from young to old ages in control group. In contrast, the UACR was significantly elevated as the diabetic mice with scramble-siRNA aged. In all age groups, the UACR was increased in an order of control mice < diabetic mice with PVT1-siRNA < diabetic mice with scramble-siRNA. When compared to the age-matched control mice, the UACR was significantly increased in diabetic mice with scramble-siRNA of young (by 2.02 fold), middle-aged (by 2.01 fold) and old (by 2.48 fold) group, while moderate increase (by 4 to 41%) was observed in diabetic mice with PVT1-siRNA. The UACR was significantly lowered in diabetic mice with PVT1-siRNA of young (by 49%), middle-aged (by 32%) and old (by 43%) when compared with the diabetic mice with scramble-siRNA.

The urinary albumin excretion of siRNA-treated diabetic and control mice of different age groups was shown in Figure 4.18. The UAE was slightly increased from young to old ages in control group. In contrast, the UAE was significantly elevated as the diabetic mice aged. In all age groups, the UAE was increased in an order of control mice < diabetic mice with PVT1-siRNA < diabetic mice with scramble-siRNA. The UAE was significantly increased in diabetic mice with scramble-siRNA of young (by 2.20 fold), middle-aged (by 2.97 fold) and old (by 3.05 fold) group when compared to the age-matched control mice. Moderate increase in UAE (by 38 to 70%) was observed in diabetic mice with PVT1-siRNA. When compared with the diabetic mice with scramble-siRNA, the UAE was significantly lowered in diabetic mice with PVT1-siRNA of young (by 37%), middle-aged (by 43%) and old (by 44%).

The urinary protein to creatinine ratio of siRNA-treated diabetic and control mice of different age groups was shown in Figure 4.19. In all age groups, the UPCR was increased in an order of control < diabetic mice with PVT1-siRNA < diabetic mice with scramble-siRNA. The UPCR remained steady among the control mice of different ages. When compared to the age-matched control mice, the UPCR was significantly increased in diabetic mice with scramble-siRNA of middle-aged (by 26%) and old (by 38%) group, while moderate increase (by 5-11%) was observed in diabetic mice with PVT1-siRNA. The UPCR in diabetic mice with PVT1-siRNA was lower (by 10-21%) than that in diabetic mice with scramble-siRNA.

The urinary protein excretion of siRNA-treated diabetic and control mice of different age groups was shown in Figure 4.20. The UPE was slightly increased from young to old ages in control group. In contrast, the UPE was significantly elevated as the diabetic mice with scramble-siRNA aged. In all age groups, the UPE was increased in an order of control mice < diabetic mice with PVT1-siRNA < diabetic mice with scramble-siRNA. The UPE was significantly increased in diabetic mice with scramble-siRNA of young (by 1.22 fold), middle-aged (by 1.84 fold) and old (by 1.98 fold) group when compared to the age-matched control mice. Moderate increase in UPE (by 3 to 37%) was observed in diabetic mice with PVT1-siRNA. When compared with the diabetic mice with scramble-siRNA, the UPE was significantly lowered in diabetic mice with PVT1-siRNA of young (by 16%), middle-aged (by 40%) and old (by 31%) group.

Figure 4.17: The urinary albumin to creatinine ratio of siRNA-treated diabetic and control mice of different age groups.

Diabetic mice were treated with either scramble-siRNA (DM+siRNA(scramble)) or PVT1-siRNA (DM+siRNA(PVT1)), whereas control mice were normal mice without siRNA injection (Control). Results were expressed in mean ± SEM, n = 6. A p-value < 0.05 was considered statistically significant using one-way ANOVA with Tukey post-test (*p < 0.05, **p < 0.01, ***p < 0.001 vs control; ^p < 0.05, ^^p < 0.01 vs DM+siRNA(scramble); $^{\#}$p < 0.05, $^{\#\#}$p < 0.01 vs specified groups).

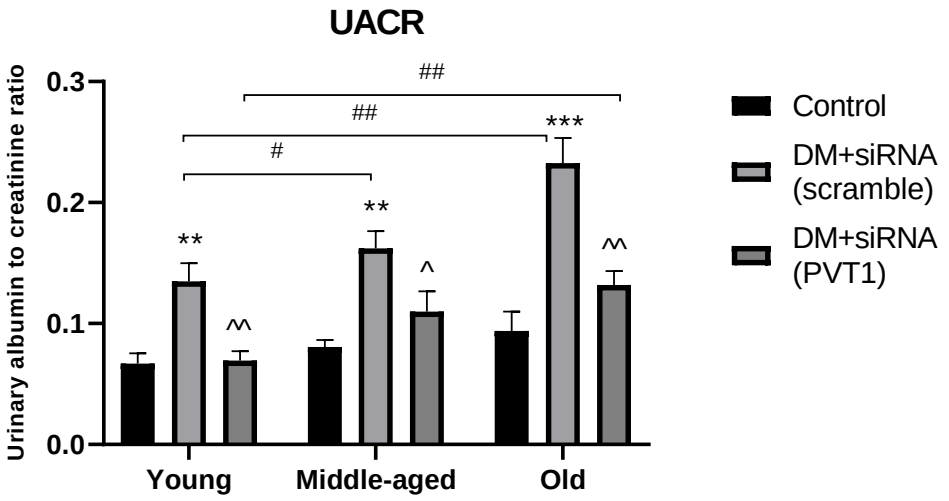

Figure 4.18: The urinary albumin excretion of siRNA-treated diabetic and control mice of different age groups.

Diabetic mice were treated with either scramble-siRNA (DM+siRNA(scramble)) or PVT1-siRNA (DM+siRNA(PVT1)), whereas control mice were normal mice without siRNA injection (Control). Results were expressed in mean ± SEM, n = 6. A p-value < 0.05 was considered statistically significant using one-way ANOVA with Tukey post-test (*$p < 0.05$, **$p < 0.01$, ***$p < 0.001$ vs control; ^$p < 0.05$, ^^$p < 0.01$, ^^^$p < 0.001$ vs DM+siRNA(scramble); $^{\#}p < 0.05$, $^{\#\#}p < 0.01$vs specified groups).

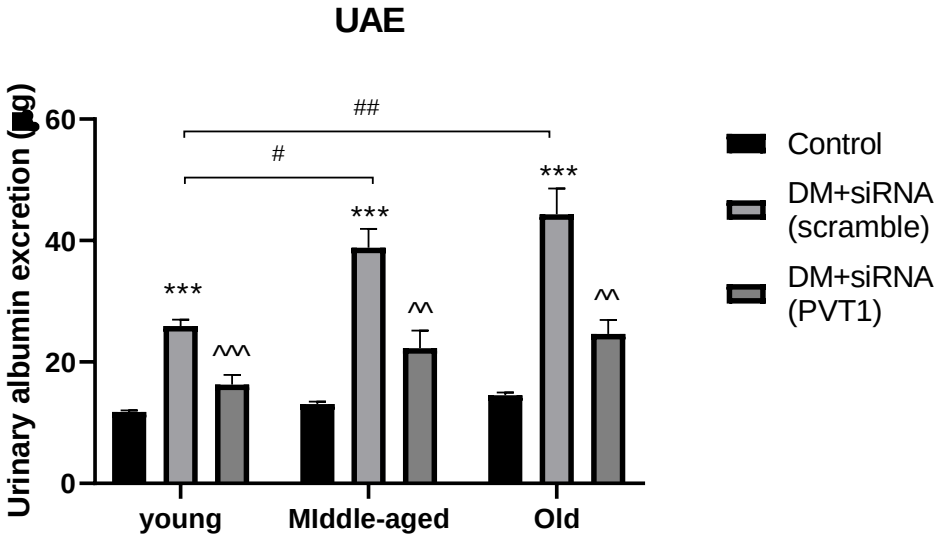

Figure 4.19: The urinary protein to creatinine ratio of siRNA-treated diabetic and control mice of different age groups.

Diabetic mice were treated with either scramble-siRNA (DM+siRNA(scramble)) or PVT1-siRNA (DM+siRNA(PVT1)), whereas control mice were normal mice without siRNA injection (Control). Results were expressed in mean ± SEM, n = 6. A p-value < 0.05 was considered statistically significant using one-way ANOVA with Tukey post-test (*p < 0.05 vs control).

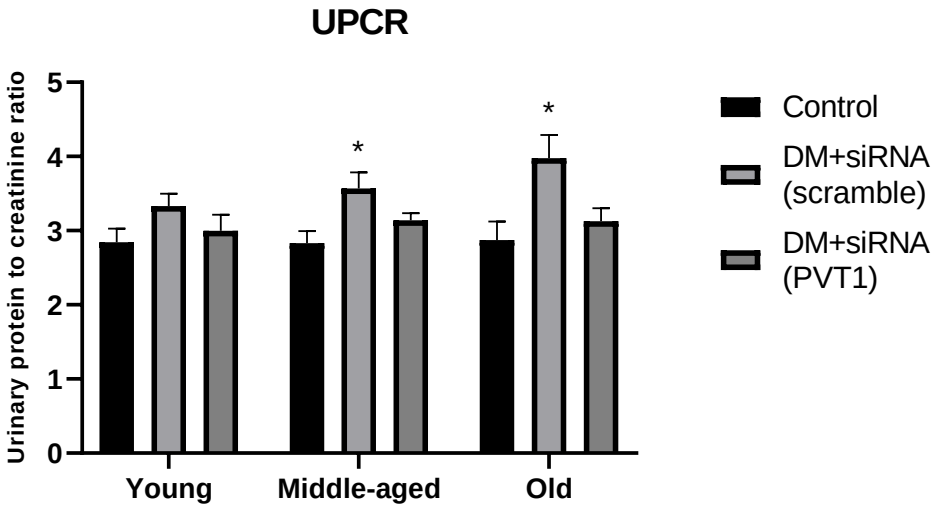

Figure 4.20: The urinary protein excretion of siRNA-treated diabetic and control mice of different age groups.

Diabetic mice were treated with either scramble-siRNA (DM+siRNA(scramble)) or PVT1-siRNA (DM+siRNA(PVT1)), whereas control mice were normal mice without siRNA injection (Control). Results were expressed in mean ± SEM, n = 6. A p-value < 0.05 was considered statistically significant using one-way ANOVA with Tukey post-test (*$p < 0.05$, **$p < 0.01$ vs control; ^$p < 0.05$, ^^$p < 0.01$ vs DM+siRNA(scramble); $^{\#}p < 0.05$, $^{\#\#}p < 0.01$, $^{\#\#\#}p < 0.001$ vs specified groups).

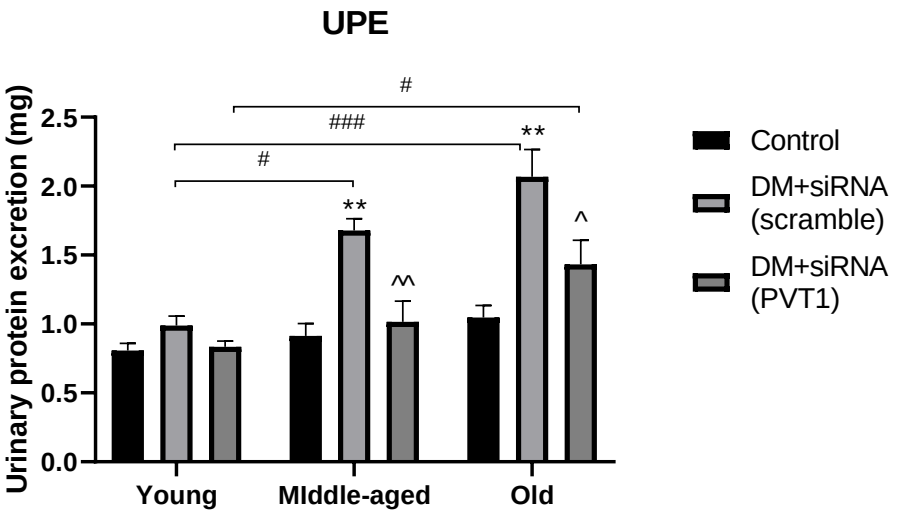

4.8.6 **Creatinine clearance**

The creatinine clearance of siRNA-treated diabetic and control mice of different age groups was shown in Figure 4.21. The creatinine clearance decreased gradually in diabetic mice with scramble-siRNA or PVT1-siRNA, while it remained steady in control mice as they aged. At young age, the creatinine clearance was slightly lower in siRNA-treated diabetic mice than that in control mice. The creatinine clearance was significantly declined in diabetic mice of middle-aged (by 41%) and old (by 50%) age when compared to the age-matched control mice, while smaller decrease (by 12-20%) was observed in diabetic mice with PVT1-siRNA. When compared with diabetic mice with scramble-siRNA, the creatinine clearance was improved by 50% at middle-aged and 60% at old age of diabetic mice with PVT1-siRNA.

4.8.7 **Serum creatinine**

The serum creatinine concentration of siRNA-treated diabetic and control mice of different age groups was shown in Figure 4.22. The serum creatinine concentration remained steady in control mice of different ages. In all age groups, the serum creatinine was increased in an order of control mice < diabetic mice with PVT1-siRNA < diabetic mice with scramble-siRNA. When compared to the age-matched control mice, the serum creatinine was significantly increased in diabetic mice with scramble-siRNA of young (by 52%), middle-aged (by 88%) and old (by 73%) group, while moderate increase (by 25-41%) was observed in diabetic mice with PVT1-siRNA. The serum creatinine was significantly lowered in diabetic mice with PVT1-siRNA of young (by 18%), middle-aged (by 25%) and old (by 26%) when compared with the diabetic mice with scramble-siRNA.

Figure 4.21: The creatinine clearance of siRNA-treated diabetic and control mice of different age groups.

Diabetic mice were treated with either scramble-siRNA (DM+siRNA(scramble)) or PVT1-siRNA (DM+siRNA(PVT1)), whereas control mice were normal mice without siRNA injection (Control). Results were expressed in mean ± SEM, n = 6. A p-value < 0.05 was considered statistically significant using one-way ANOVA with Tukey post-test (*$p < 0.05$, **$p < 0.01$ vs control; ^$p < 0.05$ vs DM+siRNA(scramble); $^{\#}p < 0.05$, $^{\#\#}p < 0.01$, $^{\#\#\#}p < 0.001$ vs specified groups).

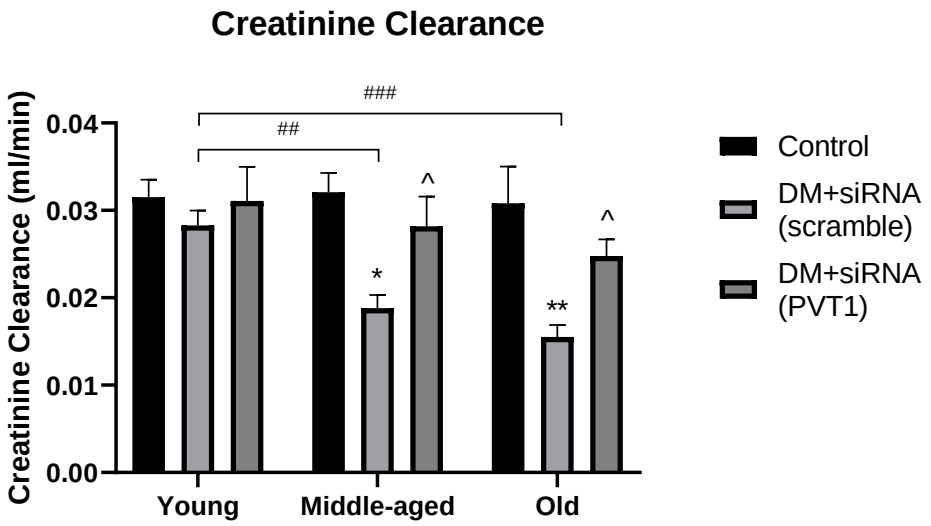

Figure 4.22: The serum creatinine of siRNA-treated diabetic and control mice of different age groups.

Diabetic mice were treated with either scramble-siRNA (DM+siRNA(scramble)) or PVT1-siRNA (DM+siRNA(PVT1)), whereas control mice were normal mice without siRNA injection (Control). Results were expressed in mean ± SEM, n = 6. A p-value < 0.05 was considered statistically significant using one-way ANOVA with Tukey post-test (*p < 0.05, **p < 0.01, ***p < 0.001 vs control; ^p < 0.05 vs DM+siRNA(scramble)).

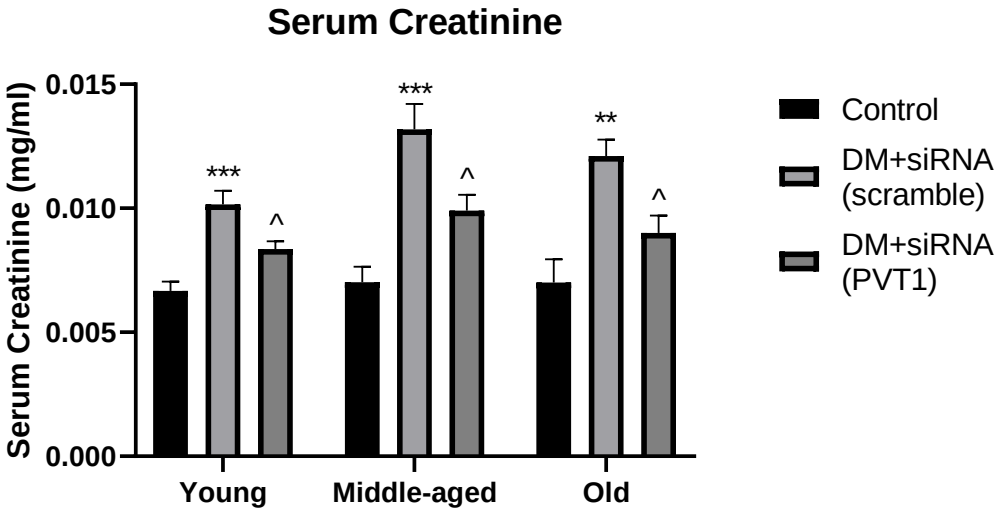

4.8.8 **Histological analysis**

The glomerular area of siRNA-treated diabetic and control mice of different age groups was shown in Figure 4.23. The glomerular area was increased with a different degree as the mice aged. The control mice had a slight increase in glomerular area, while the diabetic mice with PVT1-siRNA had a moderate increase followed by a significant increase in diabetic mice with scramble-siRNA. The glomerular area was significantly increased in diabetic mice with scramble-siRNA of young (by 36%), middle-aged (by 56%) and old (by 61%) group when compared to the age-matched control mice. The diabetic mice with PVT1-siRNA had a moderate increase in glomerular area by 13-16%. When compared with the diabetic mice with scramble-siRNA, the glomerular area was decreased in the diabetic mice with PVT1-siRNA at young (17%), middle-aged (28%) and old (28%) group.

The mesangial area of siRNA-treated diabetic and control mice of different age groups was shown in Figure 4.24. Like the glomerular area, the mesangial area was increased in an order of control mice < diabetic mice with PVT1-siRNA < diabetic mice with scramble-siRNA. The mesangial area was significantly increased in diabetic mice with scramble-siRNA of young (by 52%), middle-aged (by 70%) and old (by 71%) group when compared to the age-matched control mice, while the diabetic mice with PVT1-siRNA showed a moderate increase by 18-20%. When compared with the diabetic mice with scramble-siRNA, the mesangial area was decreased in the diabetic mice with PVT1-siRNA at young (22%), middle-aged (30%) and old (30%) group. A representative of microscopic images of kidney sections from siRNA-treated diabetic and control mice of different age groups was shown in Figure 4.25.

Figure 4.23: The glomerular area of siRNA-treated diabetic and control mice of different age groups.

Diabetic mice were treated with either scramble-siRNA (DM+siRNA(scramble)) or PVT1-siRNA (DM+siRNA(PVT1)), whereas control mice were normal mice without siRNA injection (Control). Results were expressed in mean ± SEM, n = 6. A p-value < 0.05 was considered statistically significant using one-way ANOVA with Tukey post-test (*p < 0.05, **p < 0.01, ***p < 0.001 vs control; ^p < 0.05, ^^p < 0.01, ^^^p < 0.001 vs DM+siRNA(scramble); $^{\#}$p < 0.05, $^{\#\#}$p < 0.01 vs specified groups).

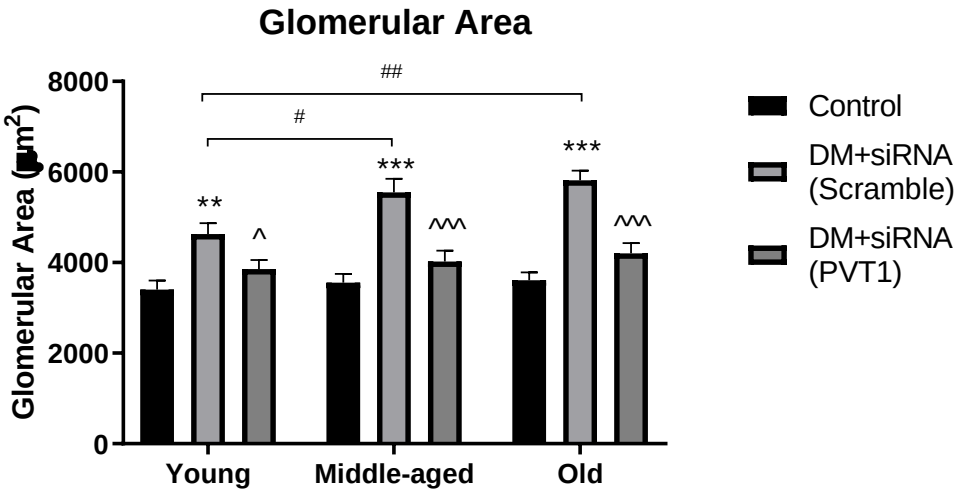

Figure 4.24: The mesangial area of siRNA-treated diabetic and control mice of different age groups.

Diabetic mice were treated with either scramble-siRNA (DM+siRNA(scramble)) or PVT1-siRNA (DM+siRNA(PVT1)), whereas control mice were normal mice without siRNA injection (Control). Results were expressed in mean ± SEM, n = 6. A p-value < 0.05 was considered statistically significant using one-way ANOVA with Tukey post-test (*p < 0.05, **p < 0.01, ***p < 0.001 vs control; ^p < 0.05, ^^p < 0.01, ^^^p < 0.001 vs DM+siRNA(scramble); #p < 0.05 vs specified groups).

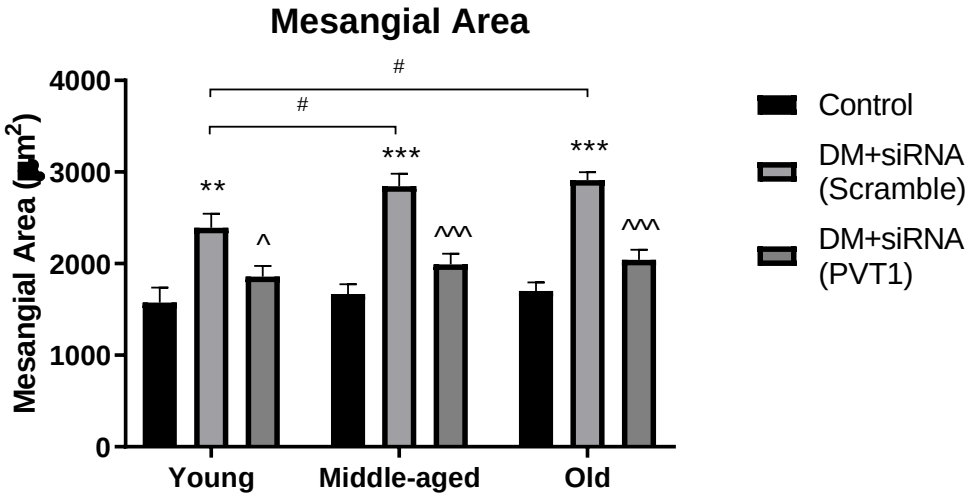

Figure 4.25: The microscopic images of kidney sections from siRNA-treated diabetic and control mice of different age groups, (A) young, (B) middle-aged and (C) old. Diabetic mice were treated with either scramble-siRNA (DM+siRNA(scramble)) or PVT1-siRNA (DM+siRNA(PVT1)), whereas control mice were normal mice without siRNA injection (Control). The kidney sections were stained with periodic acid Schiff (PAS) and counterstained with Mayer's hematoxylin, and viewed under 40X.

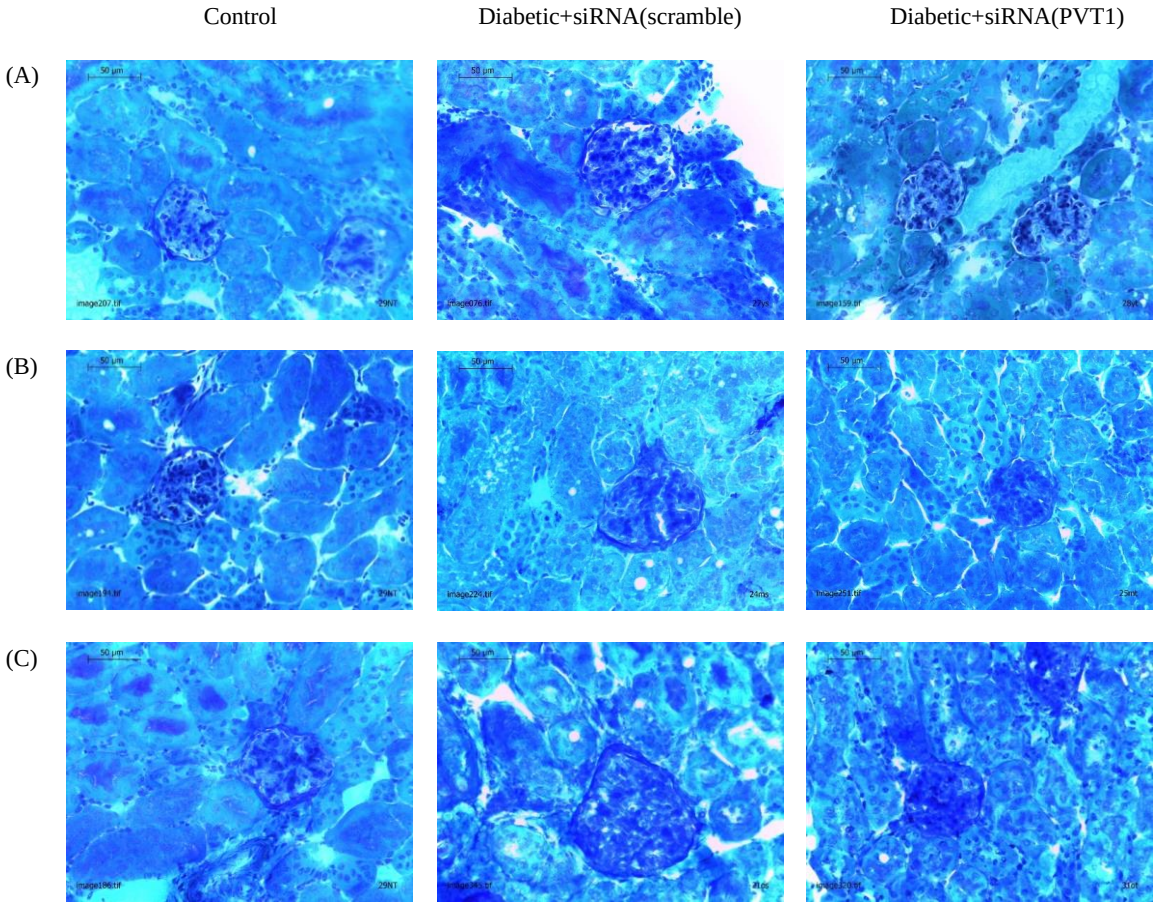

4.8.9 **Gene expression analysis**

The gene expressions of PVT1 (Figure 4.26), TGF-β1 (Figure 4.27), PAI-1 (Figure 4.28), FN1 (Figure 4.29), COL4A1 (Figure 4.30) and BMP7 (Figure 4.31) of siRNA-treated diabetic and control mice of different age groups were shown in the corresponding figures. The gene expressions of PVT1, TGF-β1, PAI-1, FN1 and COL4A1 were significantly increased in diabetic mice treated with scramble-siRNA when compared to the normal control, while that of BMP7 was markedly decreased. The changes of the expressions were more obvious over time. These results were comparable to that in the previous chapter where diabetic and control mice without siRNA injection were studied.

The PVT1 expression was increased significantly in diabetic mice treated with scramble-siRNA of young (by 271%, $p < 0.05$), middle-aged (by 310%, $p < 0.01$) and old (by 347%, $p < 0.001$) group when compared to the age-matched control mice. Diabetic mice with PVT1-siRNA treatment had decreased the PVT1 expression in young (by 48%, $p < 0.05$), middle-aged (by 43%, $p < 0.05$), and old (by 51%, $p < 0.001$) when compared to the diabetic mice treated with scramble-siRNA. The PVT1 expression was moderately higher in diabetic mice with PVT1-siRNA than in control mice.

The TGF-β1 mRNA expression was increased significantly in diabetic mice treated with scramble-siRNA of young (by 207%, $p < 0.05$), middle-aged (by 244%, $p < 0.001$) and old (by 374%, $p < 0.001$) group when compared to the age-matched control mice. Diabetic mice with PVT1-siRNA treatment had decreased the TGF-β1 expression in young (by 42%, $p < 0.05$), middle-aged (by 38%, $p < 0.001$), and old (by 43%, $p < 0.001$) when compared to the diabetic mice treated with scramble-siRNA. At old age, the TGF-β1 mRNA expression was significantly higher in diabetic mice with PVT1-siRNA than in control mice.

The PAI-1 mRNA expression was increased significantly in diabetic mice treated with scramble-siRNA of young (by 203%, $p < 0.05$), middle-aged (by 235%, $p < 0.01$) and old (by 306%, $p < 0.05$) group when compared to the age-matched control mice. Diabetic mice with PVT1-siRNA treatment had decreased the PAI-1 expression in young (by 26%, $p > 0.05$), middle-aged (by 39%, $p < 0.05$), and old (by 51%, $p < 0.05$) when compared to the diabetic mice treated with scramble-siRNA. The PAI-1 mRNA expression was moderately higher in diabetic mice with PVT1-siRNA than in control mice.

The FN1 mRNA expression was increased significantly in diabetic mice treated with scramble-siRNA of young (by 196%, $p < 0.05$), middle-aged (by 215%, $p < 0.01$) and old (by 212%, $p < 0.001$) group when compared to the age-matched control mice. Diabetic mice with PVT1-siRNA treatment had decreased the FN1 expression in young (by 40%, $p < 0.05$), middle-aged (by 34%, $p < 0.01$), and old (by 34%, $p < 0.001$) when compared to the diabetic mice treated with scramble-siRNA. The FN1 mRNA expression was moderately higher in diabetic mice with PVT1-siRNA than in control mice.

The COL4A1 mRNA expression was increased significantly in diabetic mice treated with scramble-siRNA of young (by 207%, $p < 0.05$), middle-aged (by 234%, $p < 0.001$) and old (by 365%, $p < 0.001$) group when compared to the age-matched control mice. Diabetic mice with PVT1-siRNA treatment had decreased the COL4A1 expression in young (by 37%, $p < 0.05$), middle-aged (by 33%, $p < 0.01$), and old (by 43%, $p < 0.001$) when compared to the diabetic mice treated with scramble-siRNA. At old age, the COL4A1 mRNA expression was significantly higher in diabetic mice with PVT1-siRNA than in control mice.

In contrast to the PVT1 and ECM components mentioned above, the BMP7 mRNA expression was significantly reduced in diabetic mice treated with scramble-siRNA of young (by 35%, $p < 0.01$), middle-aged (by 51%, $p < 0.001$) and old (by 63%, $p < 0.001$) group when compared to the age-matched control mice. The BMP7 mRNA expression

was higher in diabetic mice treated with PVT1-siRNA than that with scramble-siRNA in young (by 31%, $p < 0.05$), middle-aged (by 49%, $p < 0.05$), and old (by 89%, $p < 0.001$) age. At old age, the BMP7 mRNA expression was significantly higher in diabetic mice with PVT1-siRNA than in control mice.

In summary, the PVT1-siRNA treatment partially attenuated the upregulation of PVT1, TGF-β1, PAI-1, FN1 and COL4A1 while prevented the downregulation of BMP7 in diabetic mice in all age groups, which restored these mRNA expressions closer to the normal control. The moderate changes in PVT1, PAI-1 and FN1 mRNA expressions were statistically insignificant between PVT1-siRNA treated diabetic mice and control mice in all age groups. The marked increase in TGF-β1 and COL4A1 mRNA expressions as well as decrease in BMP7 mRNA expression observed in diabetic mice of old age were not adequately counteracted by the PVT-siRNA treatment, while these changes remained comparable to the normal control in young and middle-aged groups.

Figure 4.26: The PVT1 expression of siRNA-treated diabetic and control mice of different age groups.

Diabetic mice were treated with either scramble-siRNA (DM+siRNA(scramble)) or PVT1-siRNA (DM+siRNA(PVT1)), whereas control mice were normal mice without siRNA injection (Control). Results were expressed in mean ± SEM, n = 6. A p-value < 0.05 was considered statistically significant using one-way ANOVA with Tukey post-test (*p < 0.05, **p < 0.01, ***p < 0.001 vs control; ^p < 0.05, ^^p < 0.01, ^^^p < 0.001 vs DM+siRNA(scramble)).

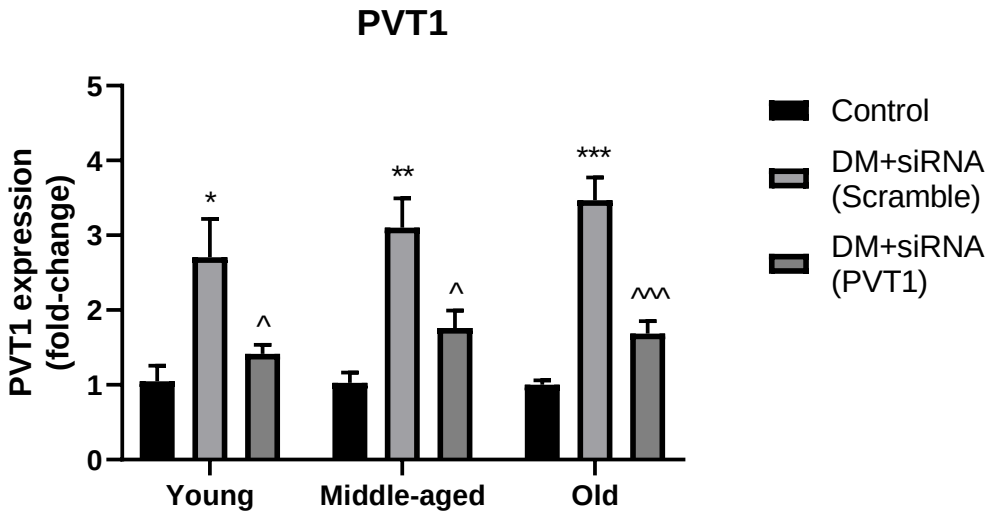

Figure 4.27: The TGF-β1 mRNA expression of siRNA-treated diabetic and control mice of different age groups.

Diabetic mice were treated with either scramble-siRNA (DM+siRNA(scramble)) or PVT1-siRNA (DM+siRNA(PVT1)), whereas control mice were normal mice without siRNA injection (Control). Results were expressed in mean ± SEM, n = 6. A p-value < 0.05 was considered statistically significant using one-way ANOVA with Tukey post-test (*p < 0.05, **p < 0.01, ***p < 0.001; ^p < 0.05, ^^p < 0.01, ^^^p < 0.001 vs DM+siRNA(scramble)).

.

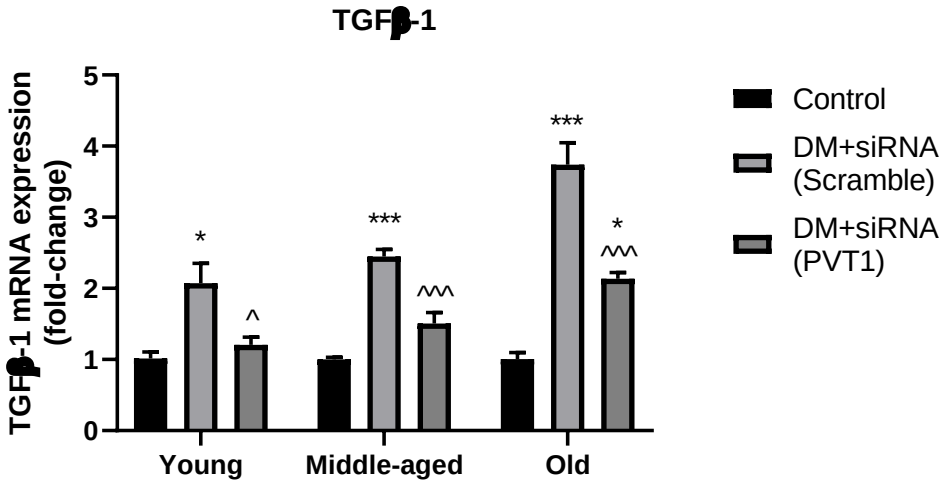

Figure 4.28: The PAI-1 mRNA expression of siRNA-treated diabetic and control mice of different age groups.

Diabetic mice were treated with either scramble-siRNA (DM+siRNA(scramble)) or PVT1-siRNA (DM+siRNA(PVT1)), whereas control mice were normal mice without siRNA injection (Control). Results were expressed in mean ± SEM, n = 6. A p-value < 0.05 was considered statistically significant using one-way ANOVA with Tukey post-test (*p < 0.05, **p < 0.01 vs control; ^p < 0.05 vs DM+siRNA(scramble)).

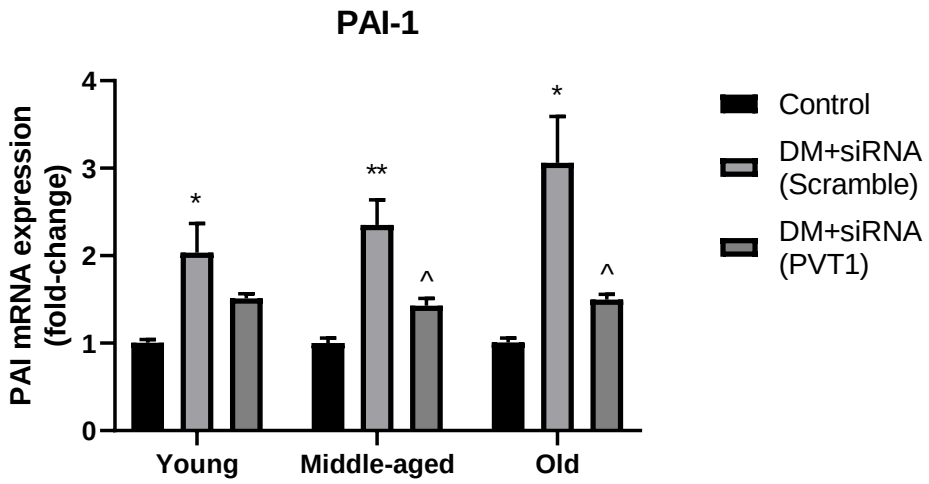

Figure 4.29: The FN1 mRNA expression of siRNA-treated diabetic and control mice of different age groups.

Diabetic mice were treated with either scramble-siRNA (DM+siRNA(scramble)) or PVT1-siRNA (DM+siRNA(PVT1)), whereas control mice were normal mice without siRNA injection (Control). Results were expressed in mean ± SEM, n = 6. A p-value < 0.05 was considered statistically significant using one-way ANOVA with Tukey post-test (*p < 0.05, **p < 0.01, ***p < 0.001 vs control; ^p < 0.05, ^^p < 0.01, ^^^p < 0.001 vs DM+siRNA(scramble)).

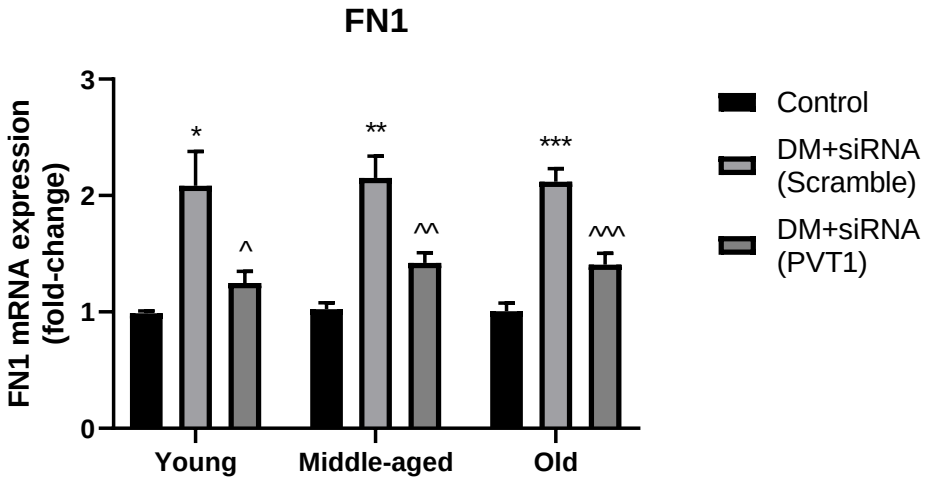

Figure 4.30: The COL4A1 mRNA expression of siRNA-treated diabetic and control mice of different age groups.

Diabetic mice were treated with either scramble-siRNA (DM+siRNA(scramble)) or PVT1-siRNA (DM+siRNA(PVT1)), whereas control mice were normal mice without siRNA injection (Control). Results were expressed in mean ± SEM, n = 6. A p-value < 0.05 was considered statistically significant using one-way ANOVA with Tukey post-test (*p < 0.05, **p < 0.01, ***p < 0.001 vs control; ^p < 0.05, ^^p < 0.01, ^^^p < 0.001 vs DM+siRNA(scramble)).

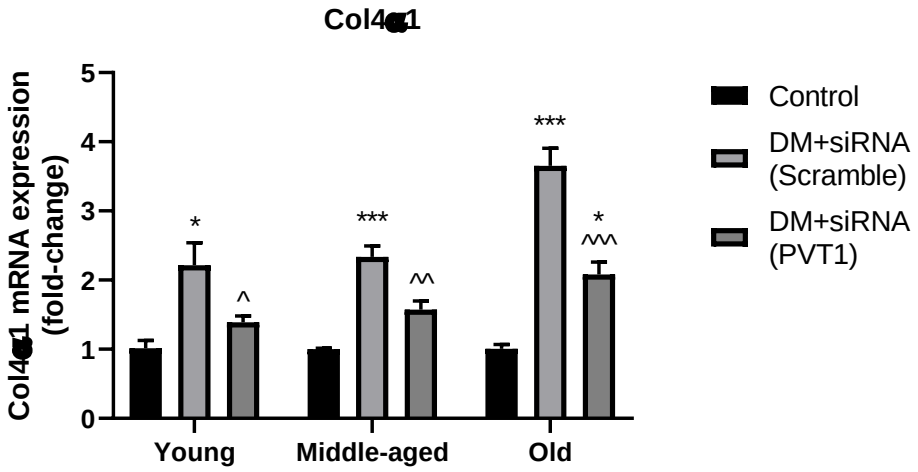

Figure 4.31: The BMP7 mRNA expression of siRNA-treated diabetic and control mice of different age groups.

Diabetic mice were treated with either scramble-siRNA (DM+siRNA(scramble)) or PVT1-siRNA (DM+siRNA(PVT1)), whereas control mice were normal mice without siRNA injection (Control). Results were expressed in mean ± SEM, n = 6. A p-value < 0.05 was considered statistically significant using one-way ANOVA with Tukey post-test (*p < 0.05, **p < 0.01, ***p < 0.001 vs control; ^p < 0.05, ^^p < 0.01, ^^^p < 0.001 vs DM+siRNA(scramble)).

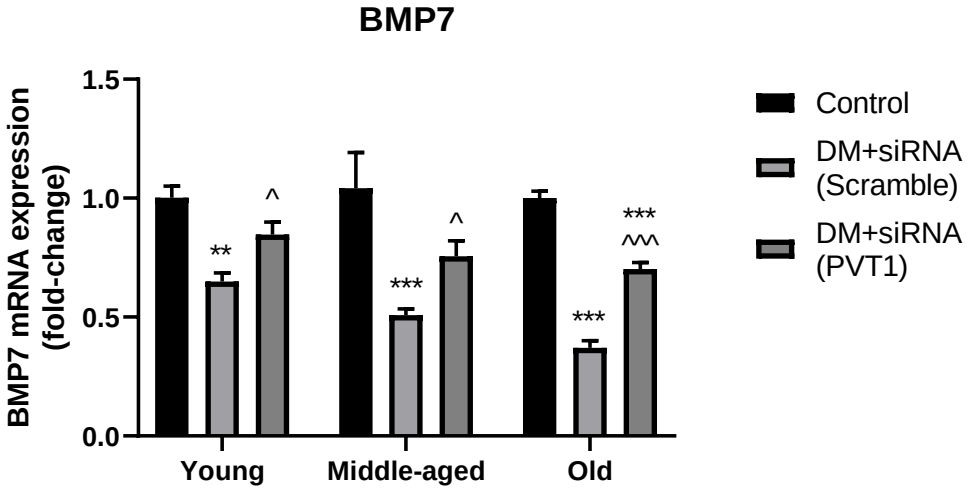

4.9 Discussions

Characteristics of DN, such as kidney hypertrophy, albuminuria, reduced creatinine clearance and increased glomerular and mesangial areas were observed in the diabetic mice treated with scramble-siRNA, which was similar to the diabetic mice in Chapter 3. Diabetic mice regardless of different siRNA treatments were heavier than the age-matched controls. At young and middle-aged, diabetic mice with PVT1-siRNA had obviously lower percentage of weight gain than diabetic mice with scramble-siRNA. However, the difference in percentage of body weight gain between the diabetic and control mice became smaller as the animals aged (i.e. no statistical difference at old age), which might be due to the heterogeneity of the response to high fat diet within the inbred C57BL/6 strain. It was reported that while all C57BL/6 mice fed with high fat diet were insulin resistant in a study, approximately 50% of them became obese and diabetic, 10% lean and diabetic, 10% lean and nondiabetic, and 30% displayed intermediate phenotype. The body weight gain of those mice was widely scattered at 6 and 9 months old, with values lower, similar, or higher than the body weights of the control mice (Burns et al., 2006). Taken together, the PVT1-siRNA treatment did not suppress the high fat diet-induced weight gain in diabetic mice.

Blood glucose concentration is the most common end-point measurement to evaluate the treatment effectiveness in diabetic subjects. Since different species tend to have different blood glucose concentrations than humans, extra attention should be paid when defining if the animal models are considered diabetic. It was reported that mice tend to have higher blood glucose concentrations than humans, the non-fasting blood glucose concentration over 13.8mmol/L (250mg/dL) or preferably a chronic elevation over 16.7mmol/L (300mg/dL) is appropriate to consider a mouse diabetic (King, 2012). In our study, the

mice received high fat diet and STZ became diabetic after 2 weeks post-injection. The blood glucose level gradually increased and remained steadily high from 10-week-old till the end of the experiment in middle-aged and old groups. The chronic hyperglycemia present in diabetic mice had suggested the diabetes was effectively induced and maintained through the high fat diet and STZ. The control mice with low fat diet and vehicle injection remained non-diabetic throughout their life. The significant difference (about 2.1 to 2.5-fold) in blood glucose concentration between the diabetic and control mice at all ages (young, middle-aged and old) had indicated that these murine models were useful for evaluating treatment of diabetes and associated DN. One study has shown a marked suppression on elevated blood glucose in uninephrectomized STZ-treated and HF/HG diet-fed diabetic mice treated with shRNA-PVT1 (D.-W. Liu et al., 2019). On the contrary, the PVT1-siRNA treatment slightly reduced the blood glucose (by 5-8%) in diabetic mice, but the level remained significantly high (about 1.9 to 2.4-fold) relative to the age-matched controls, which suggested PVT1-siRNA treatment might not have a role in glucose metabolism to combating chronic hyperglycemia.

Renal hypertrophy is a consistent finding in the early stage of type 1 diabetes mellitus in humans and in the STZ-diabetes model (Weston et al., 2003). Kidney weight is measured as an index of renal hypertrophy (Sharma & Ziyadeh, 1994). In our study, the diabetic mice with scramble-siRNA had the highest kidney weight and kidney to body weight ratio among all mice at all ages, which suggested the existence of renal hypertrophy. PVT1-siRNA treatment markedly reduced the kidney to body weight ratio in diabetic mice and brought such kidney index closer to the controls, which suggested a beneficial effect of PVT1-siRNA treatment to restoring normal kidney morphology.

The UAE (2.20-fold, 2.97-fold, 3.05-fold vs control at young, middle-aged, old, respectively) and UACR (2.02-fold, 2.01-fold, 2.48-fold vs control at young, middle-aged, old, respectively) were significantly higher in diabetic mice with scramble-siRNA than the age-matched controls. Albuminuria became more severe as the diabetic mice aged, which showed notable progression of DN occurred if the diabetic condition was not intervened, while the UAE and UACR remained unchanged in controls over time. This suggested these sets of diabetic and control models provided a good platform for studying the treatment of DN. The PVT1-siRNA treatment had significantly attenuated the diabetes-induced elevation of UAE and UACR in diabetic mice and restore them closer to that of the controls, which indicated a protective effect of PVT1-siRNA on kidney function restoration. Previous study had demonstrated that the urine total protein measurement is less robust at low levels of protein than is urine albumin measurement and it is insufficiently sensitive to detect all clinically important concentrations of urine albumin (Moon et al., 2017). This was agreed with our results on UPE and UPCR, which the significant difference in UPE was not observed in the young group, the fold-change increases were smaller than that in UAE and UPCR, and UPCR was not significantly different across time. Hence, UAE and UACR remained to be the important and reliable markers for assessing proteinuria. Despite so, the PVT1-siRNA treatment markedly decreased the elevation of UPE in middle-aged and old diabetic mice with relative to the scramble-siRNA treatment. Taken together, PVT1-siRNA was suggested to protect renal function in diabetic mice and delayed the progression of DN.

The creatinine clearance was markedly declined in diabetic mice treated with scramble-siRNA at middle-aged and old age when compared with age-matched controls, which had indicated that the glomerular filtration rate was significantly reduced. The greater the decline, the greater the loss of glomerular filtration and the more likely to have end-stage

renal disease. The significant difference in creatinine clearance between the diabetic mice of young and old age had suggested a progression of DN. It was worthy to note that the creatinine clearance in young diabetic mice was only slightly reduced when compared with its control. This could be explained by the compensatory changes in surviving nephrons after the nephron loss in kidney injury, which are commonly observed in the clinical practice. This leads to a lesser loss of total renal function than anticipated by the extent of anatomic damage. In fact, the earliest nephron losses are likely to be invisible due to functional compensation, which would bring GFR back into the normal range. For example, a loss of half the functioning nephrons leads to a decrease in GFR of only 20–30%, rather than the anticipated 50% (Yokoi et al., 2002). As the well-known reciprocal relationship between serum creatinine and GFR, serum creatinine was considered an index of kidney injury as well. The marked elevation of serum creatinine concentration in diabetic mice suggested a progressive kidney injury and renal function deterioration. PVT1-siRNA treatment markedly supressed the decline of creatinine clearance as well as the elevation of serum creatinine in diabetic mice. Taken together, PVT1-siRNA was suggested to restore the GFR in diabetic mice and delayed the progression of DN.

Albuminuria and decreased glomerular filtration rate, correlated strongly to mesangial expansion while related poorly or not at all to GBM thickening (Mauer et al., 1984). Mesangial matrix expansion appears to be the main cause of declining renal function in DN (Steffes et al., 1989). The GMB thickening and mesangial expansion do not completely explain the decline in renal function as some patients with persistent proteinuria did not have diabetic glomerulopathy (Dalla Vestra et al., 2003) or *vice versa* (Caramori et al., 2003; MacIsaac et al., 2004). Other structural changes, such as podocyte foot process effacement, decrease in podocyte number and density, are involved, in which podocyte injury leads directly to proteinuria (Dronavalli et al., 2008; Jefferson et al., 2008;

Wolf et al., 2005). Our study showed marked increase in glomerular and mesangial matrix areas in diabetic mice than their age-matched controls in all age groups, which paralleled with elevated albuminuria and reduced creatinine clearance. Both glomerular and mesangial areas were progressively and markedly increased over time, suggesting structural deterioration of glomeruli and progression of DN. PVT1-sRNA treatment markedly suppressed the increase in both glomerular and mesangial areas, which suggested a protective effect of PVT1 inhibition on maintaining normal glomerular morphology.

The gene expression of ECM components (FN1 and COL4A1) and regulators (TGF-β1 and PAI-1) were upregulated together with that of PVT1, while another regulator BMP7 expression was downregulated in diabetic mice with scramble-siRNA. To elucidate the role of PVT1 in relation to the ECM components and regulators, the effects of PVT1 inhibition using PVT1-siRNA was evaluated. Our preliminary pilot study had demonstrated a successful inhibition of PVT1 expression in both diabetic and control two days post PVT-siRNA injection. The magnitude of decrease was greater in the control than the diabetic mice, which might be due to the higher basal PVT1 levels in the diabetic models. Also, the expression of TGF-β1, PAI-1, FN1 and COL4A1 were significantly downregulated by the PVT1-siRNA treatment, which suggested they were associated with PVT1 in which their suppression was likely due to the reduced PVT1 level. Unlike the other two ECM regulators, the BMP7 expression remained unchanged two days after the PVT1-siRNA treatment. This might suggest that (i) BMP7 might not be directly regulated by PVT1 expression, or it might take longer time to see a change if other regulatory molecules were involved in relaying the responses, (ii) its level was relatively steadily maintained in normal condition, and (iii) the compensational effect between the lower basal level of BMP7 and increased BMP7 level in response to reduced TGF-β1 by

PVT1-siRNA treatment in diabetic mice. The expression of PVT1, FN1, COL4A1, TGF-β1, PAI-1, and BMP7 in diabetic mice treated with or without PVT1-siRNA at different ages were compared.

Our study showed that the gene expression of ECM major components FN1 and COL4A1, and regulators such as TGF-β1 and PAI-1, were significantly increased in diabetic mice with scramble-siRNA at all ages. The expression of PVT1, TGF-β1, PAI-1, FN1 and COL4A1 became higher in diabetic mice regardless of which siRNA treatment as they aged, which indicated a continual ECM accumulation in the glomeruli. TGF-β1 is a powerful regulator promoting fibrosis, which increases production of fibronectin and type IV collagen as well as decreases their degradation through increasing the activity of PAI-1. The autocrine action of TGF-β1 that stimulates its own production might partly account for the higher expression level of TGF-β1. The PVT1 expression was significantly increased (up to about 2.71-fold, 3.10-fold and 3.47-fold at young, middle-aged and old, respectively) in diabetic mice with scramble-siRNA, which suggested the diabetic or hyperglycemic condition promoting the upregulation of PVT1 expression. One study showed an approximate 3-fold increase in PVT1 expression in C57BL/6 mice which were uninephrectomised, fed with high fat high sugar diet, and injected with five consecutive low dose STZ (55mg/kg of body weight), and culled at ages over 37 week-old (D.-W. Liu et al., 2019). Another study showed PVT1 expression increased up to 5-fold in db/db mice, which was a well-established murine model of type 2 diabetes susceptible to DN (J. Li et al., 2020). Taking the more rigorous method to establish DN and the more susceptible genetic background into consideration, the magnitude of expression of PVT1 in our study might be comparable to that in the two studies. In contrast, BMP7 expression was decreased in diabetic mice with scramble-siRNA at all ages. The decrease might be resulted from the overexpression of TGF-β1 that exerted inhibitory effects on BMP7 as

well as due to the diabetic condition, as reported in other studies (S.-N. Wang et al., 2001; Shinong Wang & Hirschberg, 2003; Q. Yang et al., 2007; Yeh et al., 2009). The downregulation of BMP7 might fail to counteract the fibrotic actions of TGF-β1, to reduce the action of PAI-1 directly or indirectly through TGF-β1, which in turn promoted the ECM accumulation as well as to glomerular podocytes apoptosis in diabetic mice. A much milder decline of BMP7 expression was noted in diabetic mice with PVT1-siRNA than with scramble-siRNA, which suggested the protective effect of PVT1-siRNA treatment on maintaining BMP7 expression that prevent podocyte damage. Of note, the upregulation of PVT1 expression paralleled with the increase in TGF-β1, PAI-1, FN1 and COL4A1, and decrease in BMP7, which suggested an interrelationship among each other. Taken together, the continual ECM accumulation might partly account for the increased albuminuria and reduced creatinine clearance in diabetic mice with scramble-siRNA, which promoted the progression of DN. The PVT1 inhibition greatly suppressed the upregulation of TGF-β1, PAI-1, FN1 and COL4A1 and the downregulation of BMP7 in diabetic mice at all ages to levels closer to the age-matched controls, which suggested PVT1 inhibition reduced ECM accumulation. Despite the PVT1-siRNA treatment, the expression of TGF-β1, COL4A1 and BMP7 were significantly higher in old diabetic mice than old controls, which might imply that the PVT1-siRNA treatment was effective in slow down the rate of ECM accumulation but failed to completely suspend or reverse it at advanced stage of DN. PVT1-siRNA treatment attenuated the functional and structural deteriorations in the old diabetic mice, which suggested PVT1 inhibition might protect renal function through other pathways in addition to ECM accumulation or TGF-β signalling. These findings were in line with some studies that suggested PVT1 might promote excessive ECM accumulation, contributing to development of DN, and inhibition on PVT1 expression abolished the ECM accumulation (Alvarez & DiStefano, 2011; Dean, 2012). Targeting PVT1 might be a potential therapeutic for DN treatment.

4.10 Conclusions

Inhibition of PVT1 expression was successfully demonstrated by *in vivo* delivery of PVT1-siRNA into the C57BL/6 mice. Diabetic mice treated with scramble-siRNA exhibited marked hyperglycemia, kidney hypertrophy, albuminuria, reduced creatinine clearance, elevated serum creatinine level, and increased glomerular and mesangial areas, which were comparable to that observed in the age-matched diabetic mice in Chapter 3. These manifestations were intensified as the diabetic mice aged and were significantly different from the age-matched controls. PVT1-siRNA treatment supressed some hallmarks of DN, such as kidney hypertrophy, albuminuria, serum creatinine elevation, glomerular mesangial expansion and creatinine clearance decline, while hyperglycemia persisted, in diabetic mice. Furthermore, PVT1-siRNA treatment supressed the upregulation of TGF-β1, PAI-1, FN1, COL4A1, and downregulation of BMP7 in the diabetic mice. In conclusion, PVT1 inhibition had ameliorated DN in terms of kidney function and histology in diabetic mice without altering hyperglycemia. The improvement might be resulted from reducing ECM accumulation through suppression of TGF-β1 and PAI-1 expressions as well as preservation of BMP7 expression. It is therefore suggested that PVT1 might play an important role in ECM and its inhibition might be a potential approach for the prevention and treatment of DN.

CHAPTER 5: DISCUSSION AND CONCLUSIONS

5.1 Discussion

5.1.1 Role of PVT1 on DN

Most of the lncRNAs usually express at low levels, and thus their expression arise at a specific stage of disease progression (Bhat et al., 2016). Several studies have reported that PVT1 expression is significantly higher in serum of patients with DN (D.-W. Liu et al., 2019; Zhong, Zeng, Xue, Du, & Xu, 2020) and in diabetic animals (J. Li et al., 2020; D.-W. Liu et al., 2019). Likewise, our study has shown the PVT1 expression is significantly increased in mice with DN, and the expression increased with the progression of DN over time.

Based on the current study, the potential role of PVT1 in ECM accumulation was suggested in Figure 5.1. Diabetes induces persistent hyperglycemia in murine models. Hyperglycemia causes an excessive ECM accumulation in the glomerular mesangium which constitutes the major pathological feature of the glomerular fibrosis. Hyperglycemic or diabetic conditions induce an increase in PVT1 expression which contributes to the increase of the two main ECM components (FN1 and COL4A1) and the two main regulators of ECM accumulation (PAI-1 and TGF-β1), while to the decrease of BMP7. PAI-1 is the main inhibitor of glomerular ECM degradation and TGF-β1 promotes glomerular fibrosis by upregulating genes encoding ECM proteins and PAI-1. PAI-1 and TGF-β1 transcriptionally regulate each other creating a vicious cycle of reciprocal stimulation that perpetuates the fibrotic response. In addition, the autocrine action of TGF-β1 to stimulate its own production further promotes its effects on ECM accumulation. The anti-fibrotic actions of BMP7 (e.g. reduces FN1, COL4A1 and PAI-

1) are inhibited by TGF-β1 in diabetic conditions, which in turn contribute to enhanced ECM accumulation. In summary, diabetic condition results in an upregulation of PVT1, which increases ECM accumulation through increasing TGF-β1, PAI-1 and decreasing BMP7. Inhibition of PVT1 by RNA interference suppress the increase in ECM accumulation through reducing expression of TGF-β1, PAI-1, FN1 and COL4A1, while increasing that of BMP7. A recent study has suggested that PVT1 inhibition supressed renal fibrosis through inactivation of TGF-β signalling, in which expression of PVT1, TGF-βR1, p-Smad3 and fibronectin were associated, in UUO-induced murine model (L. Cao et al, 2020). Although the UUO-induced model that primarily featured with tubular injury as a result of obstructed urine flow mimicking human chronic obstructive nephropathy is different from the diabetic model, the resulting renal fibrosis is the common pathway for most forms of progressive renal disease including DN. Hence, our study showed that the positive association between PVT1 and TGF-β1 expression (i.e. parallelly upregulated in diabetic status while downregulated in PVT1-siRNA treatment) might suggest PVT1 inhibition suppresses TGF-β1-mediated renal fibrosis in DN.

Furthermore, inhibition of PVT1 suppresses kidney hypertrophy, proteinuria (elevation of UAE, UACR, UPE and UPCR), kidney function decline (reduced creatinine clearance and elevated serum creatinine) and histological changes (increased glomerular and mesangial areas) in diabetic mice without altering the blood glucose level. This suggests that PVT1 inhibition might provide renal protection against DN through reduced ECM accumulation and was independent of blood glucose regulation. PVT1 is reported to promote glycolysis in cancerous cells where it is overexpressed and the rate of glucose consumption has been significantly reduced in PVT1 knockdown cells (J. Song et al, 2017; J. Chen et al, 2019). Several lncRNAs (e.g. lncRNA PLUTO, Meg3, LOC283177, H19) have been shown to regulate glucose metabolism and be associated with the pathogenesis

of type 2 diabetes mellitus, which involves changes in the growth of pancreatic β-cell, insulin synthesis, insulin secretion, and insulin signalling in peripheral tissues (including liver, skeletal muscle, and adipocyte) (T. Zhang et al, 2020; I. Akerman et al, 2017; N. Wang et al, 2018; J. Fadista et al, 2014; N. Goyal et al, 2017). However, the effect of PVT1 on glucose metabolism in DN is not yet known. Further investigation on the changes in insulin secretion and hepatic gluconeogenesis (e.g. expression of gluconeogenic genes) in PVT1 knockdown diabetic models may be useful to provide more evidence on characterization of PVT1. Glycemic control is beneficial for preventing microvascular complications in newly diagnosed diabetic patients, as reported by the DCCT and UKPDS trials, but it is not beneficial in established diabetic patients for the prevention of significant outcomes of DN, as reported in recent trials (B. Hemmingsen et al, 2011; S. Coca et al., 2012; Y. Slinin et al., 2012). Late-stage diabetes, hypertension, and proteinuria may be the predominant causes of the progression of DN, which suggests antihypertensive/antiproteinuric measures are more useful to prevent further disease progression (K. Kanasaki, G. Taduri & D. Koya, 2013).

A growing amount of knowledge on lncRNAs, their potential modes of actions and RNAi technology have opened new research areas for researchers to explore the pathogenesis as well as treatment of different diseases. In the past decades, the majority of studies on PVT1 were related to cancers (such as breast cancer, ovarian cancer, prostate cancer, gastric cancer, lung cancer, pancreatic cancer and melanoma), in which PVT1 is highly expressed (D. Lu et al, 2017; T. Colombo et al, 2015). To date, the role of PVT1 on diabetes and its complications, fibrosis of different organs and aging are gaining increasing attention. Excessive or uncontrolled ECM accumulation is a characteristic feature of all chronic diabetic complications (Biswas & Chakrabarti, 2019). Emerging evidence have strongly suggested that PVT1 is a key regulator of DN, in which its

mechanistic actions is more than the widely recognized ECM accumulation. Recent studies have shown inhibition of PVT1 might offer protective effects against DN through other ways, such as (i) inhibiting podocyte damage and apoptosis by upregulation of FOXA1 (forkhead box A1) of the podocytes (D.-W. Liu et al., 2019); and (ii) acting as a molecular sponge for miR-23b-3p to modulate expression of Wilms tumor protein 1 (WT1, a podocyte specific marker, is upregulated in DN). PVT1 knockdown alleviates high glucose-induced proliferation and fibrosis in mesangial cells by the miR-23b-3p/WT axis (Zhong et al., 2020). The lncRNA functions as the molecular sponge or the competing endogenous RNAs (ceRNAs) are the classic example of mRNA translation regulation in cytoplasm, to which an increasing number of studies is related. Furthermore, PVT1 has been shown to trigger inflammatory responses involving TNF-α, IL-1β and IL-6 in LPS-induced septic acute kidney injury through regulation of JNK/NF-κB signalling pathway (W. Huang et al, 2017) and inhibition of PVT1 decreased IL-1β-mediated inflammatory responses in osteoarthritic chondrocytes (Y. Zhao et al, 2018). Inflammation greatly contributes to the development of DN, which involves increased chemokine production (e.g. monocyte chemoattractant protein (MCP-1)), pro-inflammatory cytokine production (e.g. TGF-β1, IL-1, IL-6, TNF-α and Smads), infiltration of inflammatory cells (e.g. monocytes, macrophages and T lymphocytes) to the kidney, and tissue damage (Duran-Salgado et al, 2014). IL-1 stimulates expression of cell adhesion molecules and profibrotic growth factors and increases endothelial permeability. IL-6 promotes mesangial proliferation, glomerular hypertrophy, fibronectin production and increases endothelial permeability. TNF-α promotes production of reactive oxygen species (ROS), induces cell injury, and increases endothelial permeability (A.K. Lim & G.H. Tesch, 2012). Sustained inflammation promotes fibroblast activation and renal fibrosis, which results in kidney structural and functional deterioration. Despite the role of PVT1 on inflammation in DN has not been reported, it

is reasonable to speculate that inhibition of PVT1 may attenuate the development of DN through reduced inflammatory responses as well as TGF-β1-mediated fibrosis.

Regarding renal diseases, many studies on PVT1 were *in vitro* studies that evaluated its functions in various renal cultured cells and primary cells of human and murine origins. While *in vivo* studies evaluating the role of PVT1 in different disease models, one recent study was performed in DN model but with a focus on podocyte apoptosis instead of the ECM accumulation. At present, our study appears to be the first to report the role of PVT1 on progression of DN in diabetic mice, which specifically assessed the glomerular ECM accumulation, kidney functional and structural aspects. Moreover, our data suggested that PVT1 may play a key role in ECM accumulation and progression of DN, which its inhibition markedly attenuated the renal functional and structural deteriorations in diabetic mice and maintained the respective physiological conditions closer to age-matched controls. Last but not least, our study has established a desirable model of DN using a combination of high fat diet and low dose STZ in male C57BL/6 mice. These non-genetically modified models of DN associated to type 2 diabetes mellitus have exhibited hallmarks (including steady hyperglycemia, kidney hypertrophy, progressive increase in proteinuria and serum creatinine and decline in creatinine clearance, and glomerular and mesangial area expansion), which offered a relatively cost-effective platform for testing potential treatment of DN.

5.1.2 **lncRNA-miRNA-based treatment on DN**

Many noncoding RNAs (miRNAs, lncRNAs, circRNAs) are known to play an important role in the development of DN, which may potentially be used as biomarkers and therapeutic targets. Currently, several miRNA-based treatments have proceeded to the

human clinical trials (including a phase II clinical trial on Miravirsen, a miR-122 inhibitor, for treatment of HCV infection in patients) (Labovsky et al., 2017). Although there is no miRNA-based treatment for DN, such option remains a new research interest. Alternatively, possible treatment using lncRNAs for DN may also be considered. Targeting lncRNA expression is favourable when compared to the miRNAs, due to its functional role in transcriptional regulation, tissue-specific expression, cell-specific and disease-specific dysregulation. Like miRNA-based treatments, the real challenge is the application of lncRNA-based treatment *in vivo* that efficient delivery and efficacy have to be guaranteed. Therefore, further investigations are needed to explore the potential as well as feasibility of the new miRNA- or lncRNA-based treatments in the management of DN.

Figure 5.1: Potential role of PVT1 in ECM accumulation. Diabetes induces persistent hyperglycemia in murine models.

Hyperglycemia causes an excessive ECM accumulation in the glomerular mesangium which constitutes the major pathological feature of the glomerulosclerosis or glomerular fibrosis. Hyperglycemic or diabetic conditions induce an increase in PVT1 expression which contributes to the increase of the two main ECM components (FN1 and COL4A1) and the two main regulators of ECM accumulation in the glomeruli (PAI-1 and TGF-β1), while to the decrease of BMP7. PAI-1 is the main inhibitor of glomerular ECM degradation and TGF-β1 promotes glomerular fibrosis by upregulating genes encoding ECM proteins and PAI-1. PAI-1 and TGF-β1 transcriptionally regulate each other creating a vicious cycle of reciprocal stimulation that perpetuates the fibrotic response. TGF-β1 also inhibits the anti-fibrotic actions of BMP7. In addition, the autocrine action of TGF-β1 to stimulate its own production further promotes its effects on ECM accumulation. FN1: fibronectin 1; COL4A1: alpha 1 type IV collagen; PAI-1: plasminogen activator inhibitor; TGF-β1: transforming growth factor-β1; BMP7: bone morphogenetic protein 7; Red upward arrow represents a stimulatory response; Blue downward arrow represents an inhibitory response.

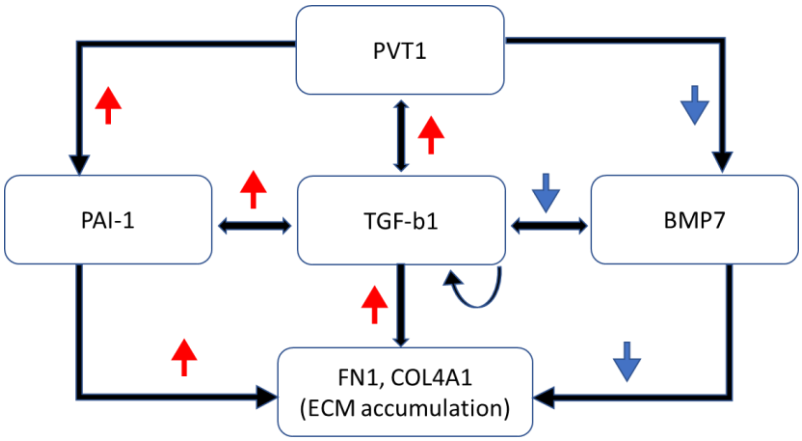

5.1.3 **Limitations of this study**

There were some limitations on the animal model, number of animals and materials used in this study. Firstly, according to the AMDCC, the ideal murine model of DN should fulfil three criteria: (1) more than 50% decline in glomerular filtration rate (GFR) over the lifetime of the animal; (2) greater than 10-fold increase in albuminuria compared with controls for that strain at the same age and gender; (3) histopathology findings which include mesangial sclerosis (a 50% increase in mesangial volume), any degree of arteriolar hyalinosis, glomerular basement membrane thickening (a >25% increase compared with baseline by electron microscopy morphometry), and tubulointerstitial fibrosis (Alpers & Hudkins, 2011; Brosius et al., 2009; Inada et al., 2005; Kong et al., 2013; Schlöndorff, 2010; Greg H Tesch & Allen, 2007). There are no murine models that meet all three criteria so far. The C57BL/6 murine model adopted in this study was not ideal as only one criterion might be achievable that the glomerular filtration rate evaluated as creatinine clearance was close to 50% decline after 16 weeks old. C57BL/6 mice were culled at designated time instead of natural death. The albuminuria evaluated as 24hr albumin creatinine excretion was about 2.0-3.3-fold increase compared with the age-matched controls, which agreed with some *in vivo* studies in the literature. The characteristics of advanced DN (such as arteriolar hyalinosis, nodular glomerulosclerosis or Kimmelstiel-Wilson lesion) were not observed, which is found in human but are generally absent in mice.

Secondly, the principles of the 3Rs (Replacement, Reduction and Refinement) on animal study was followed as far as possible regarding the ethical considerations. The number of mice used were minimized in this study. Therefore, the study was focused on the comparison between normal and diabetic mice in Chapter 3, while the comparison

between diabetic mice with and without PVT1-siRNA treatment in Chapter 4. A positive treatment group was not included as a reference for assessing how well the established murine model of DN would respond to the standard therapy for DN (such as drugs for controlling blood glucose, blood pressure and proteinuria) as well as for comparing the effectiveness of PVT1-siRNA treatment in comparison to it. Besides, it was well documented that male C57BL/6 mice were more susceptible to DN than the female, for which its use was justified for the purpose of this study. If the female mice were used, they might not respond to the induction of DN as well as the treatment of PVT1-siRNA to the same extent as the male mice did. The gender-related differences might be partly attributed to the actions of estrogens, which are the major female sex hormone that protect pancreatic β cells from apoptosis induced by oxidative stress and in the pervasiveness of obesity, insulin resistance and type 2 diabetes (Yokoi et al., 2004). It was widely accepted to use animal of same gender for various studies to reduce biological variations and enhance consistency. If the results were derived from both genders, the findings might be more comprehensive and indicative of a thorough evaluation since DN occurred in both genders.

Thirdly, the successful induction of DN relied on the administration of both high fat diet and STZ. Due to the high fat content, the high fat diet was softer, less dense and decompose more easily than the control low fat diet. Extra care was needed for dispensing the high fat diet to the mice. As the STZ disintegrated readily when it was converted into liquid form, it should be kept in moisture free environment. However, exposure to moisture would be inevitable when the bottle was opened and STZ was weighed on the digital balance. Reduced stability of STZ was observed after frequent use of the bottle. In order to safeguard its bioactivity for effective induction, new batch and freshly prepared STZ was used.

Fourthly, the systolic blood pressure measurement was not feasible due to the measurement limitation of the non-invasive blood pressure system. It is well-recognized that poor blood pressure control is one of the major risk factors contributing to progression of DN. The role of PVT1 on progression of DN could be further characterized in aspect of blood pressure control, if the blood pressure measurements were available to comparing among normal and diabetic models with and without PVT1-siRNA treatment.

Lastly, this study only focused on the effect of PVT1 on ECM accumulation which specifically covered on expression of TGF-β1, PAI-1, FN1, COL4A1 and BMP7. As mentioned above, PVT1 may exert its effects on progression of DN following other mechanisms besides ECM accumulation. Further studies are needed to delineate the comprehensive network of PVT1 and its interactions with other biological molecules.

5.1.4 **The way forward**

Characterization of PVT1 on progression of DN is an interesting research area evidenced by the increasing publication numbers on PVT1 to date. In addition to ECM accumulation, PVT1 has been shown to be involved in other biological responses important to DN. For instance, PVT1 regulates inflammation through the MAPK/NF-kB pathway and influences podocyte survival under diabetic condition, on which further studies may provide more evidence for the development and treatment of DN.

Despite the RNAi technology tool continues to improve, the effectiveness of *in vivo* siRNA delivery and gene silencing are still yet to be compared with that of *in vitro* setting.

It may be desirable to use dual-targeting siRNAs that are designed so that both strands target different sites within a single mRNA target or two separate target mRNAs. This may reduce the potential for off-target gene silencing, increase the opportunity to knock down the desired target genes, and potentially provide additive or even synergistic effects by both siRNAs (Burnett et al., 2011).

5.2 Conclusions

The murine model of DN was successfully established by using a combination treatment of high fat diet and low dose STZ in male C57BL/6 mice. Hyperglycemia, kidney hypertrophy, albuminuria, reduced creatinine clearance, and increased glomerular and mesangial areas were observed in the diabetic mice. These manifestations were intensified as the diabetic mice aged and were significantly different from the age-matched controls. This set of diabetic and control models was suitable for testing the treatment of DN.

The expression of PVT1 was upregulated along with that of TGF-β1, PAI-1, FN1, COL4A1 while BMP7 was downregulated in diabetic model. The findings were in agreement with most *in vitro* studies. Inhibition of PVT1 expression was successfully demonstrated by *in vivo* delivery of PVT1-siRNA into the C57BL/6 mice. Diabetic mice treated with scramble-siRNA exhibited marked hyperglycemia, kidney hypertrophy, albuminuria, reduced creatinine clearance, elevated serum creatinine level, and increased glomerular and mesangial areas, which were comparable to that observed in the age-matched diabetic mice in Chapter 3. These conditions were intensified as the diabetic mice aged and were significantly different from the age-matched normal controls. Diabetic mice treated with PVT1-siRNA had reduced kidney hypertrophy, albuminuria,

serum creatinine, glomerular mesangial expansion and increased creatinine clearance, while hyperglycemia persisted. The PVT1-siRNA treatment had supressed the upregulation of TGF-β1, PAI-1, FN1, COL4A1, and downregulation of BMP7 in the kidney of diabetic mice. In conclusion, PVT1 inhibition could ameliorated DN in terms of kidney function and histology in diabetic mice without altering hyperglycemia. The improvement might be resulted from reducing ECM accumulation through suppression of TGF-β1, PAI-1, FN1 and COL4AA1 expression as well as preservation of BMP7 expression. It is therefore suggested that PVT1 may play an important role in ECM accumulation and its inhibition may be a potential approach for the prevention or treatment of DN.

REFERENCES

Adler, S. (1994). Structure-function relationships associated with extracellular matrix alterations in diabetic glomerulopathy. *Journal of the American Society of Nephrology, 5*(5), 1165-1172.

Aigner, A. (2006). Gene silencing through RNA interference (RNAi) in vivo: strategies based on the direct application of siRNAs. *Journal of biotechnology, 124*(1), 12-25.

Akerman, I., Tu, Z., Beucher, A., Rolando, D. M., Sauty-Colace, C., Benazra, M., . . . Pasquali, L. (2017). Human pancreatic β cell lncRNAs control cell-specific regulatory networks. *Cell metabolism, 25*(2), 400-411.

Akhtar, S., & Benter, I. F. (2007). Nonviral delivery of synthetic siRNAs in vivo. *The Journal of clinical investigation, 117*(12), 3623.

Alpers, C. E., & Hudkins, K. L. (2011). Mouse models of diabetic nephropathy. *Current opinion in nephrology and hypertension, 20*(3), 278.

Alvarez, M. L., & DiStefano, J. K. (2011). Functional characterization of the plasmacytoma variant translocation 1 gene (PVT1) in diabetic nephropathy. *PLoS One, 6*(4), e18671.

Alvarez, M. L., & DiStefano, J. K. (2013). The role of non-coding RNAs in diabetic nephropathy: Potential applications as biomarkers for disease development and progression. *Diabetes Research and Clinical Practice, 99*, 1-11.

Alvarez, M. L., Khosroheidari, M., Eddy, E., & Kiefer, J. (2013). Role of microRNA 1207-5P and its host gene, the long non-coding RNA Pvt1, as mediators of extracellular matrix accumulation in the kidney: implications for diabetic nephropathy. *PLoS One, 8*(10), e77468. https://doi.org/10.1371/journal.pone.0077468

Baricos, W. H., CORTEZ, S. L., Deboisblanc, M., & XIN, S. (1999). Transforming growth factor-β is a potent inhibitor of extracellular matrix degradation by cultured human mesangial cells. *Journal of the American Society of Nephrology, 10*(4), 790-795.

Behlke, M. A. (2008). Chemical modification of siRNAs for in vivo use. *Oligonucleotides, 18*(4), 305-320.

Beulens, J. W., Grobbee, D. E., & Nealb, B. (2010). The global burden of diabetes and its complications: an emerging pandemic. *European Journal of Cardiovascular Prevention & Rehabilitation, 17*(1 suppl), s3-s8.

Bhat, S. A., Ahmad, S. M., Mumtaz, P. T., Malik, A. A., Dar, M. A., Urwat, U., . . . Ganai, N. A. (2016). Long non-coding RNAs: mechanism of action and functional utility. *Non-coding RNA research, 1*(1), 43-50.

Biswas, S., & Chakrabarti, S. (2019). Increased extracellular matrix protein production in chronic diabetic complications: implications of non-coding RNAs. *Non-coding RNA, 5*(1), 30.

Böger, C. A., & Heid, I. M. (2011). Chronic kidney disease: novel insights from genome-wide association studies. *Kidney and Blood Pressure Research, 34*(4), 225-234.

Border, W. A., Okuda, S., Languino, L. R., & Ruoslahti, E. (1990). Transforming growth factor-bold beta regulates production of proteoglycans by mesangial cells. *Kidney International, 37*, 689-695.

Border, W. A., & Ruoslahti, E. (1992). Transforming growth factor-beta in disease: the dark side of tissue repair. *Journal of Clinical Investigation, 90*(1), 1.

Border, W. A., Yamamoto, T., & Noble, N. A. (1996). Transforming growth factor β in diabetic nephropathy. *Diabetes/metabolism reviews, 12*(4), 309-339.

Breyer, M. D., Böttinger, E., Brosius, Frank C., Coffman, T. M., Harris, R. C., Heilig, C. W., Sharma, K. . (2005). Mouse models of diabetic nephropathy. *Journal of the American Society of Nephrology, 16*(1), 27-45.

Brosius, F. C., Alpers, C. E., Bottinger, E. P., Breyer, M. D., Coffman, T. M., Gurley, S. B., . . . Leiter, E. H. (2009). Mouse models of diabetic nephropathy. *Journal of the American Society of Nephrology, 20*(12), 2503-2512.

Brownlee, M. (2001). Biochemistry and molecular cell biology of diabetic complications. *Nature, 414*(6865), 813-820.

Bumcrot, D., Manoharan, M., Koteliansky, V., & Sah, D. W. (2006). RNAi therapeutics: a potential new class of pharmaceutical drugs. *Nature chemical biology, 2*(12), 711-719.

Burnett, J. C., Rossi, J. J., & Tiemann, K. (2011). Current progress of siRNA/shRNA therapeutics in clinical trials. *Biotechnology journal, 6*(9), 1130-1146.

Burns, W. C., Twigg, S. M., Forbes, J. M., Pete, J., Tikellis, C., Thallas-Bonke, V., . . . Kantharidis, P. (2006). Connective tissue growth factor plays an important role in advanced glycation end product–induced tubular epithelial-to-mesenchymal transition: implications for diabetic renal disease. *Journal of the American Society of Nephrology, 17*(9), 2484-2494.

Cao, F., Li, Z., Ding, W.-m., Yan, L., & Zhao, Q.-y. (2019). LncRNA PVT1 regulates atrial fibrosis via miR-128-3p-SP1-TGF-β1-Smad axis in atrial fibrillation. *Molecular Medicine, 25*(1), 1-11.

Caramori, M. L., Fioretto, P., & Mauer, M. (2003). Low glomerular filtration rate in normoalbuminuric type 1 diabetic patients an indicator of more advanced glomerular lesions. *Diabetes, 52*(4), 1036-1040.

Caramori, M. L., Kim, Y., Huang, C., Fish, A. J., Rich, S. S., Miller, M. E., . . . Mauer, M. (2002). Cellular basis of diabetic nephropathy 1. Study design and renal structural-functional relationships in patients with long-standing type 1 diabetes. *Diabetes, 51*(2), 506-513.

Chen, D., & Wang, M. W. (2005). Development and application of rodent models for type 2 diabetes. *Diabetes, Obesity and Metabolism, 7*(4), 307-317.

Chen, J., Yu, Y., Li, H., Hu, Q., Chen, X., He, Y., . . . Li, J. (2019). Long non-coding RNA PVT1 promotes tumor progression by regulating the miR-143/HK2 axis in gallbladder cancer. *Molecular cancer, 18*(1), 33.

Chen, S., Hong, S. W., Iglesias-dela Cruz, M. C., Isono, M., Casaretto, A., & Ziyadeh, F. N. (2001). The key role of the transforming growth factor-β system in the pathogenesis of diabetic nephropathy. *Renal failure, 23*(3-4), 471-481.

Chen, S., Iglesias-de la Cruz, M. C., Jim, B., Hong, S. W., Isono, M., & Ziyadeh, F. N. (2003). Reversibility of established diabetic glomerulopathy by anti-TGF-β antibodies in db/db mice. *Biochemical and Biophysical Research Communications, 300*(1), 16-22.

Chen, S., Jim, B., & Ziyadeh, F. N. (2003). Diabetic nephropathy and transforming growth factor-β: transforming our view of glomerulosclerosis and fibrosis build-up*Elsevier*. Symposium conducted at the meeting of the Seminars in nephrology

Coca, S. G., Ismail-Beigi, F., Haq, N., Krumholz, H. M., & Parikh, C. R. (2012). Role of intensive glucose control in development of renal end points in type 2 diabetes mellitus: systematic review and meta-analysis. *Archives of internal medicine, 172*(10), 761-769.

Collins, S. J., Alexander, S. L., Lopez-Guisa, J. M., Cai, X., Maruvada, R., Chua, S. C., . . . Eddy, A. A. (2006). Plasminogen activator inhibitor-1 deficiency has renal benefits but some adverse systemic consequences in diabetic mice. *Nephron Experimental Nephrology, 104*(1), e23-e34.

Colombo, T., Farina, L., Macino, G., & Paci, P. (2015). PVT1: A Rising Star among Oncogenic Long Noncoding RNAs. *BioMed research international, 2015*.

Cooper, M. E. (1998). Pathogenesis, prevention, and treatment of diabetic nephropathy. *The Lancet, 352*(9123), 213-219.

Couchman, J. R., Beavan, L. A., & McCarthy, K. J. (1994). Glomerular matrix: synthesis, turnover and role in mesangial expansion. *Kidney International, 45*(2), 328-335.

Craig, D., Millis, M., & DiStefano, J. (2009). Genome-wide SNP genotyping study using pooled DNA to identify candidate markers mediating susceptibility to end-stage renal disease attributed to Type 1 diabetes. *Diabetic Medicine, 26*(11), 1090-1098.

Cui, M., You, L., Ren, X., Zhao, W., Liao, Q., & Zhao, Y. (2016). Long non-coding RNA PVT1 and cancer. *Biochemical and Biophysical Research Communications, 471*(1), 10-14.

Dalla Vestra, M., Masiero, A., Roiter, A. M., Saller, A., Crepaldi, G., & Fioretto, P. (2003). Is podocyte injury relevant in diabetic nephropathy? Studies in patients with type 2 diabetes. *Diabetes, 52*(4), 1031-1035.

David, J. M., Duarte Vogel, S., Longo, K., Sanchez, D., & Lawson, G. (2014). The use of eutectic mixture of lidocaine and prilocaine in mice (Mus musculus) for tail vein injections. *Veterinary anaesthesia and analgesia, 41*(6), 654-659.

de Fougerolles, A., Vornlocher, H.-P., Maraganore, J., & Lieberman, J. (2007). Interfering with disease: a progress report on siRNA-based therapeutics. *Nature reviews Drug discovery, 6*(6), 443-453.

Dean, L. (2012). Pertuzumab Therapy and ERBB2 (HER2) Genotype. In V. Pratt, H. McLeod, L. Dean, A. Malheiro, & W. Rubinstein (Eds.), *Medical Genetics Summaries* (28520364). Bethesda (MD). Retrieved from http://www.ncbi.nlm.nih.gov/pubmed/28520364

Declèves, A.-E., & Sharma, K. (2010). New pharmacological treatments for improving renal outcomes in diabetes. *Nature Reviews Nephrology, 6*(6), 371-380.

Deji, N., Kume, S., Araki, S.-i., Soumura, M., Sugimoto, T., Isshiki, K., . . . Haneda, M. (2009). Structural and functional changes in the kidneys of high-fat diet-induced obese mice. *American Journal of Physiology-Renal Physiology, 296*(1), F118-F126.

Divers, J., & Freedman, B. I. (2010). Susceptibility genes in common complex kidney disease. *Current opinion in nephrology and hypertension, 19*(1), 79.

Dronavalli, S., Duka, I., & Bakris, G. L. (2008). The pathogenesis of diabetic nephropathy. *Nature clinical practice Endocrinology & metabolism, 4*(8), 444-452.

Dudley, A. T., Lyons, K. M., & Robertson, E. J. (1995). A requirement for bone morphogenetic protein-7 during development of the mammalian kidney and eye. *Genes & development, 9*(22), 2795-2807.

Duran-Salgado, M. B., & Rubio-Guerra, A. F. (2014). Diabetic nephropathy and inflammation. *World journal of diabetes, 5*(3), 393.

Dyer, A. R., Greenland, P., Elliott, P., Daviglus, M. L., Claeys, G., Kesteloot, H., . . . Group, I. R. (2004). Evaluation of measures of urinary albumin excretion in epidemiologic studies. *American journal of epidemiology, 160*(11), 1122-1131.

Eddy, A. A. (2002). Plasminogen activator inhibitor-1 and the kidney. *American Journal of Physiology-Renal Physiology, 283*(2), F209-F220.

Eddy, A. A., & Fogo, A. B. (2006). Plasminogen activator inhibitor-1 in chronic kidney disease: evidence and mechanisms of action. *Journal of the American Society of Nephrology, 17*(11), 2999-3012.

Edelstein, M. L., Abedi, M. R., & Wixon, J. (2007). Gene therapy clinical trials worldwide to 2007—an update. *The journal of gene medicine, 9*(10), 833-842.

Epstein, F. H., Blobe, G. C., Schiemann, W. P., & Lodish, H. F. (2000). Role of transforming growth factor β in human disease. *New England Journal of Medicine, 342*(18), 1350-1358.

Fadista, J., Vikman, P., Laakso, E. O., Mollet, I. G., Esguerra, J. L., Taneera, J., . . . Prasad, R. B. (2014). Global genomic and transcriptomic analysis of human pancreatic islets reveals novel genes influencing glucose metabolism. *Proceedings of the National Academy of Sciences, 111*(38), 13924-13929.

Feng, F., Qi, Y., Dong, C., & Yang, C. (2018). PVT1 regulates inflammation and cardiac function via the MAPK/NF-κB pathway in a sepsis model. *Experimental and therapeutic medicine, 16*(6), 4471-4478.

Floege, J., Johnson, R. J., Gordon, K., Iida, H., Pritzl, P., Yoshimura, A., . . . Couser, W. G. (1991). Increased synthesis of extracellular matrix in mesangial proliferative nephritis. *Kidney int, 40*(3), 477-488.

Forbes, J. M., & Cooper, M. E. (2013). Mechanisms of diabetic complications. *Physiological reviews, 93*(1), 137-188.

Freedman, B. I., Bostrom, M., Daeihagh, P., & Bowden, D. W. (2007). Genetic factors in diabetic nephropathy. *Clinical Journal of the American Society of Nephrology, 2*(6), 1306-1316.

Fried, L. F., Emanuele, N., Zhang, J. H., Brophy, M., Conner, T. A., Duckworth, W., . . . Palevsky, P. M. (2013). Combined angiotensin inhibition for the treatment of diabetic nephropathy. *New England Journal of Medicine, 369*(20), 1892-1903.

Gansevoort, R. T., Verhave, J. C., Hillege, H. L., Burgerhof, J. G., Bakker, S. J., de Zeeuw, D., & de Jong, P. E. (2005). The validity of screening based on spot morning urine samples to detect subjects with microalbuminuria in the general population. *Kidney International, 67*, S28-S35.

Garrett, M. R., Pezzolesi, M. G., & Korstanje, R. (2010). Integrating human and rodent data to identify the genetic factors involved in chronic kidney disease. *Journal of the American Society of Nephrology, 21*(3), 398-405.

Geurt Stokman, Y. Q., Zsuzsanna Rácz, Peter Hamar, Leo S. Price. (2010). Application of siRNA in targeting protein expression in kidney disease. *Advanced Drug Delivery Reviews, 62*, 1378-1389.

Gilbert, E. R., Fu, Z., & Liu, D. (2011). Development of a nongenetic mouse model of type 2 diabetes. *Experimental diabetes research, 2011*.

Godin, R. E., Takaesu, N. T., Robertson, E. J., & Dudley, A. T. (1998). Regulation of BMP7 expression during kidney development. *Development, 125*(17), 3473-3482.

Goyal, N., Sivadas, A., Shamsudheen, K., Jayarajan, R., Verma, A., Sivasubbu, S., . . . Datta, M. (2017). RNA sequencing of db/db mice liver identifies lncRNA H19 as a key regulator of gluconeogenesis and hepatic glucose output. *Scientific reports, 7*(1), 1-12.

Gross, J. L., De Azevedo, M. J., Silveiro, S. P., Canani, L. H., Caramori, M. L., & Zelmanovitz, T. (2005). Diabetic nephropathy: diagnosis, prevention, and treatment. *Diabetes care, 28*(1), 164-176.

Guan, Y., Kuo, W.-L., Stilwell, J. L., Takano, H., Lapuk, A. V., Fridlyand, J., . . . Santos, J. L. (2007). Amplification of PVT1 contributes to the pathophysiology of ovarian and breast cancer. *Clinical Cancer Research, 13*(19), 5745-5755.

Guha, M., Xu, Z.-G., Tung, D., Lanting, L., & Natarajan, R. (2007). Specific down-regulation of connective tissue growth factor attenuates progression of nephropathy in mouse models of type 1 and type 2 diabetes. *The FASEB Journal, 21*(12), 3355-3368.

Gurley, S. B., Clare, S. E., Snow, K. P., Hu, A., Meyer, T. W., & Coffman, T. M. (2006). Impact of genetic background on nephropathy in diabetic mice. *American Journal of Physiology-Renal Physiology, 290*(1), F214-F222.

Ha, H., & Lee, H. B. (2003). Reactive oxygen species and matrix remodeling in diabetic kidney. *Journal of the American Society of Nephrology, 14*(suppl 3), S246-S249.

Ha, H., Oh, E. Y., & Lee, H. B. (2009). The role of plasminogen activator inhibitor 1 in renal and cardiovascular diseases. *Nature Reviews Nephrology, 5*(4), 203-211.

Hannon, G. J. (2002). RNA interference. *Nature, 418*(6894), 244-251.

Hanson, R. L., Craig, D. W., Millis, M. P., Yeatts, K. A., Kobes, S., Pearson, J. V., . . . Wolford, J. K. (2007). Identification of PVT1 as a candidate gene for end-stage renal disease in type 2 diabetes using a pooling-based genome-wide single nucleotide polymorphism association study. *Diabetes, 56*(4), 975-983.

Hemmingsen, B., Lund, S. S., Gluud, C., Vaag, A., Almdal, T., Hemmingsen, C., & Wetterslev, J. (2011). Intensive glycaemic control for patients with type 2 diabetes: systematic review with meta-analysis and trial sequential analysis of randomised clinical trials. *Bmj, 343*.

Hill, C., Flyvbjerg, A., Grønbaek, H., Petrik, J., Hill, D., Thomas, C., . . . Logan, A. (2000). The Renal Expression of Transforming Growth Factor-β Isoforms and Their Receptors in Acute and Chronic Experimental Diabetes in Rats 1. *Endocrinology, 141*(3), 1196-1208.

Hilliard, T., Miklossy, G., Chock, C., Yue, P., Williams, P., & Turkson, J. (2017). 15∝-methoxypuupehenol induces antitumor effects in vitro and in vivo against human glioblastoma and breast cancer models. *Molecular Cancer Therapeutics*, molcanther. 0291.2016.

Hogan, B. L. (1996). Bone morphogenetic proteins in development. *Current opinion in genetics & development, 6*(4), 432-438.

Hong, S. W., Isono, M., Chen, S., Iglesias-de la Cruz, M. C., Han, D. C., & Ziyadeh, F. N. (2001). Increased glomerular and tubular expression of transforming growth factor-β1, its type II receptor, and activation of the Smad signaling pathway in the db/db mouse. *The American journal of pathology, 158*(5), 1653-1663.

Huang, W., Lan, X., Li, X., Wang, D., Sun, Y., Wang, Q., . . . Yu, K. (2017). Long non-coding RNA PVT1 promote LPS-induced septic acute kidney injury by regulating TNFα and JNK/NF-κB pathways in HK-2 cells. *International immunopharmacology, 47*, 134-140.

Huang, Y., Border, W. A., Yu, L., Zhang, J., Lawrence, D. A., & Noble, N. A. (2008). A PAI-1 mutant, PAI-1R, slows progression of diabetic nephropathy. *Journal of the American Society of Nephrology, 19*(2), 329-338.

Huppi, K., Pitt, J. J., Wahlberg, B. M., & Caplen, N. J. (2012). The 8q24 gene desert: an oasis of non-coding transcriptional activity. *Frontiers in genetics, 3*.

Huppi, K., Volfovsky, N., Runfola, T., Jones, T. L., Mackiewicz, M., Martin, S. E., . . . Caplen, N. J. (2008). The identification of microRNAs in a genomically unstable region of human chromosome 8q24. *Molecular Cancer Research, 6*(2), 212-221.

Iglesias-De la Cruz, M. C., Ziyadeh, F. N., Isono, M., Kouahou, M., Han, D. C., Kalluri, R., . . . Chen, S. (2002). Effects of high glucose and TGF-β1 on the expression of collagen IV and vascular endothelial growth factor in mouse podocytes. *Kidney International, 62*(3), 901-913.

Ignarski, M., Islam, R., & Müller, R.-U. (2019). Long non-coding RNAs in kidney disease. *International journal of molecular sciences, 20*(13), 3276.

Inada, A., Nagai, K., Arai, H., Miyazaki, J.-i., Nomura, K., Kanamori, H., . . . Weir, G. C. (2005). Establishment of a diabetic mouse model with progressive diabetic nephropathy. *The American journal of pathology, 167*(2), 327-336.

Isono, M., Mogyorósi, A., Han, D. C., Hoffman, B. B., & Ziyadeh, F. N. (2000). Stimulation of TGF-β type II receptor by high glucose in mouse mesangial cells and in diabetic kidney. *American Journal of Physiology-Renal Physiology, 278*(5), F830-F838.

Ivanac-Janković, R., Ćorić, M., Furić-Čunko, V., Lovčić, V., Bašić-Jukić, N., & Kes, P. (2015). BMP-7 protein expression is downregulated in human diabetic nephropathy. *Acta Clinica Croatica, 54*(2.), 164-168.

Jefferson, J., Shankland, S., & Pichler, R. (2008). Proteinuria in diabetic kidney disease: a mechanistic viewpoint. *Kidney International, 74*(1), 22-36.

Jiang, T., Wang, Z., Proctor, G., Moskowitz, S., Liebman, S. E., Rogers, T., . . . Levi, M. (2005). Diet-induced obesity in C57BL/6J mice causes increased renal lipid accumulation and glomerulosclerosis via a sterol regulatory element-binding protein-1c-dependent pathway. *Journal of Biological Chemistry, 280*(37), 32317-32325.

Johnson, C. A., Levey, A. S., Coresh, J., Levin, A., & Eknoyan, J. G. L. (2004). Clinical practice guidelines for chronic kidney disease in adults: Part II. Glomerular filtration rate, proteinuria, and other markers. *American family physician, 70*(6), 1091-1097.

Kaiser, P. K., Symons, R. A., Shah, S. M., Quinlan, E. J., Tabandeh, H., Do, D. V., . . . Guerciolini, R. (2010). RNAi-based treatment for neovascular age-related macular degeneration by Sirna-027. *American journal of ophthalmology, 150*(1), 33-39. e32.

Kanasaki, K., Taduri, G., & Koya, D. (2013). Diabetic nephropathy: the role of inflammation in fibroblast activation and kidney fibrosis. *Frontiers in endocrinology, 4*, 7.

Kang, M. J., Ingram, A., Ly, H., Thai, K., & Scholey, J. W. (2000). Effects of diabetes and hypertension on glomerular transforming growth factor-&bgr; receptor expression. *Kidney International, 58*(4), 1677-1685.

Katagiri, T., & Watabe, T. (2016). Bone morphogenetic proteins. *Cold Spring Harbor Perspectives in Biology, 8*(6), a021899.

Kawakami, S., & Hashida, M. (2007). Targeted delivery systems of small interfering RNA by systemic administration. *Drug metabolism and pharmacokinetics, 22*(3), 142-151.

Kim, D. H., & Rossi, J. J. (2007). Strategies for silencing human disease using RNA interference. *Nature reviews genetics, 8*(3), 173-184.

Kim, H. W., Kim, B. C., Song, C. Y., Kim, J. H., Hong, H. K., & Lee, H. S. (2004). Heterozygous mice for TGF-βIIR gene are resistant to the progression of streptozotocin-induced diabetic nephropathy. *Kidney International, 66*(5), 1859-1865.

Kim, J., Kim, K. M., Noh, J. H., Yoon, J.-H., Abdelmohsen, K., & Gorospe, M. (2016). Long noncoding RNAs in diseases of aging. *Biochimica et Biophysica Acta (BBA)-Gene Regulatory Mechanisms, 1859*(1), 209-221.

King, A. J. (2012). The use of animal models in diabetes research. *British journal of pharmacology, 166*(3), 877-894.

Kolb-Bachofen, V., Epstein, S., Kiesel, U., & Kolb, H. (1988). Low-dose streptozocin-induced diabetes in mice: electron microscopy reveals single-cell insulitis before diabetes onset. *Diabetes, 37*(1), 21-27.

Kong, L.-l., Wu, H., Cui, W.-p., Zhou, W.-h., Luo, P., Sun, J., . . . Miao, L.-n. (2013). Advances in murine models of diabetic nephropathy. *Journal of Diabetes Research, 2013*.

Kopp, J. B. (2000). BMP receptors in kidney. *Kidney International, 58*(5), 2237-2238.

Kraynak, A., Storer, R., Jensen, R., Kloss, M., Soper, K., Clair, J., . . . Eydelloth, R. (1995). Extent and persistence of streptozotocin-induced DNA damage and cell proliferation in rat kidney as determined by in vivo alkaline elution and BrdUrd labeling assays. *Toxicology and applied pharmacology, 135*(2), 279-286.

Kunjathoor, V., Wilson, D., & LeBoeuf, R. (1996). Increased atherosclerosis in streptozotocin-induced diabetic mice. *Journal of Clinical Investigation, 97*(7), 1767.

Kuwabara, T., Mori, K., Mukoyama, M., Kasahara, M., Yokoi, H., Saito, Y., . . . Ishii, A. (2012). Exacerbation of diabetic nephropathy by hyperlipidaemia is mediated by Toll-like receptor 4 in mice. *Diabetologia, 55*(8), 2256-2266.

Labovsky, V., Martinez, L. M., Davies, K. M., Calcagno, M. L., García-Rivello, H., Wernicke, A., . . . Borzone, F. R. (2017). Prognostic significance of TRAIL-R3 and CCR-2 expression in tumor epithelial cells of patients with early breast cancer. *BMC cancer, 17*(1), 280.

Larson, S. D., Jackson, L. N., Chen, L. A., Rychahou, P. G., & Evers, B. M. (2007). Effectiveness of siRNA uptake in target tissues by various delivery methods. *Surgery, 142*(2), 262-269.

Lee, E. A., Seo, J. Y., Jiang, Z., Yu, M. R., Kwon, M. K., Ha, H., & Lee, H. B. (2005). Reactive oxygen species mediate high glucose–induced plasminogen activator inhibitor-1 up-regulation in mesangial cells and in diabetic kidney. *Kidney International, 67*(5), 1762-1771.

Lee, H. B., & Ha, H. (2005). Plasminogen activator inhibitor-1 and diabetic nephropathy. *Nephrology, 10*(s2), S11-S13.

Lehmann, R., & Schleicher, E. D. (2000). Molecular mechanism of diabetic nephropathy. *Clinica Chimica Acta, 297*(1), 135-144.

Leiter, E. H. (1982). Multiple low-dose streptozotocin-induced hyperglycemia and insulitis in C57BL mice: influence of inbred background, sex, and thymus. *Proceedings of the National Academy of Sciences, 79*(2), 630-634.

Lenzen, S. (2008). The mechanisms of alloxan-and streptozotocin-induced diabetes. *Diabetologia, 51*(2), 216-226.

Leung, A., & Natarajan, R. (2014). Noncoding RNAs in vascular disease. *Current opinion in cardiology, 29*(3), 199-206.

Lewis, D. L., Hagstrom, J. E., Loomis, A. G., Wolff, J. A., & Herweijer, H. (2002). Efficient delivery of siRNA for inhibition of gene expression in postnatal mice. *Nature genetics, 32*(1), 107-108.

Lewis, D. L., & Wolff, J. A. (2007). Systemic siRNA delivery via hydrodynamic intravascular injection. *Advanced Drug Delivery Reviews, 59*(2), 115-123.

Li, F., WANG, C. H., WANG, J. G., Thai, T., Boysen, G., Xu, L., . . . Maeda, N. (2010). Elevated tissue factor expression contributes to exacerbated diabetic nephropathy in mice lacking eNOS fed a high fat diet. *Journal of Thrombosis and Haemostasis, 8*(10), 2122-2132.

Li, J., Zhao, Q., Jin, X., Li, Y., & Song, J. (2020). Silencing of LncRNA PVT1 inhibits the proliferation, migration and fibrosis of high glucose-induced mouse mesangial cells via targeting microRNA-93-5p. *Bioscience Reports, 40*(5).

Li, T., Surendran, K., Zawaideh, M. A., Mathew, S., & Hruska, K. A. (2004). Bone morphogenetic protein 7: a novel treatment for chronic renal and bone disease. *Current opinion in nephrology and hypertension, 13*(4), 417-422.

Li, Y., Xu, K., Xu, K., Chen, S., Cao, Y., & Zhan, H. (2019). Roles of identified long noncoding RNA in diabetic nephropathy. *Journal of Diabetes Research, 2019*.

Like, A., Appel, M., Williams, R., & Rossini, A. (1978). Streptozotocin-induced pancreatic insulitis in mice. Morphologic and physiologic studies. *Laboratory investigation; a journal of technical methods and pathology, 38*(4), 470-486.

Like, A. A., & Rossini, A. A. (1976). Streptozotocin-induced pancreatic insulitis: new model of diabetes mellitus. *Science, 193*(4251), 415-417.

Lim, A. K., & Tesch, G. H. (2012). Inflammation in diabetic nephropathy. *Mediators of inflammation, 2012*.

Liu, D.-W., Zhang, J.-H., Liu, F.-X., Wang, X.-T., Pan, S.-K., Jiang, D.-K., . . . Liu, Z.-S. (2019). Silencing of long noncoding RNA PVT1 inhibits podocyte damage and apoptosis in diabetic nephropathy by upregulating FOXA1. *Experimental & molecular medicine, 51*(8), 1-15.

Liu, F., Song, Y., & Liu, D. (1999). Hydrodynamics-based transfection in animals by systemic administration of plasmid DNA. *Gene therapy, 6*(7), 1258-1266.

Locatelli, F., Pozzoni, P., & Del Vecchio, L. (2004). Renal replacement therapy in patients with diabetes and end-stage renal disease. *Journal of the American Society of Nephrology, 15*(1 suppl), S25-S29.

López-Hernández, F. J., & López-Novoa, J. M. (2012). Role of TGF-β in chronic kidney disease: an integration of tubular, glomerular and vascular effects. *Cell and tissue research, 347*(1), 141-154.

Lu, D., Luo, P., Wang, Q., Ye, Y., & Wang, B. (2017). lncRNA PVT1 in cancer: a review and meta-analysis. *Clinica Chimica Acta, 474*, 1-7.

Luo, G., Hofmann, C., Bronckers, A., Sohocki, M., Bradley, A., & Karsenty, G. (1995). BMP-7 is an inducer of nephrogenesis, and is also required for eye development and skeletal patterning. *Genes & development, 9*(22), 2808-2820.

Ma, D., Lim, T., Xu, J., Tang, H., Wan, Y., Zhao, H., . . . Maze, M. (2009). Xenon preconditioning protects against renal ischemic-reperfusion injury via HIF-1α activation. *Journal of the American Society of Nephrology, 20*(4), 713-720.

Ma, L. J., Mao, S. L., Taylor, K. L., Kanjanabuch, T., Guan, Y. F., Zhang, Y. H., . . . Wasserman, D. H. (2004). Prevention of obesity and insulin resistance in mice lacking plasminogen activator inhibitor 1. *Diabetes, 53*(2), 336-346.

MacIsaac, R. J., Tsalamandris, C., Panagiotopoulos, S., Smith, T. J., McNeil, K. J., & Jerums, G. (2004). Nonalbuminuric renal insufficiency in type 2 diabetes. *Diabetes care, 27*(1), 195-200.

Maeda, S. (2008). Review: Genetics of diabetic nephropathy. *Therapeutic advances in cardiovascular disease, 2*(5), 363-371.

Makino, H., Shikata, K., Hironaka, K., Kushiro, M., Yamasaki, Y., Sugimoto, H., . . . Horiuchi, S. (1995). Ultrastructure of nonenzymatically glycated mesangial matrix in diabetic nephropathy. *Kidney International, 48*(2), 517-526.

Manjunath, G., Sarnak, M. J., & Levey, A. S. (2001). Estimating the glomerular filtration rate: dos and don'ts for assessing kidney function. *Postgraduate medicine, 110*(6), 55-62.

Mason, R. M., & Wahab, N. A. (2003). Extracellular matrix metabolism in diabetic nephropathy. *Journal of the American Society of Nephrology, 14*(5), 1358-1373.

Mauer, S. M. (1994). Structural-functional correlations of diabetic nephropathy. *Kidney International, 45*, 612-612.

Mauer, S. M., Steffes, M. W., & Brown, D. M. (1981). The kidney in diabetes. *The American journal of medicine, 70*(3), 603-612.

Mauer, S. M., Steffes, M. W., Ellis, E. N., Sutherland, D., Brown, D. M., & Goetz, F. C. (1984). Structural-functional relationships in diabetic nephropathy. *Journal of Clinical Investigation, 74*(4), 1143.

McDonough, C. W., Palmer, N. D., Hicks, P. J., Roh, B. H., An, S. S., Cooke, J. N., . . . Rudock, M. E. (2011). A genome-wide association study for diabetic nephropathy genes in African Americans. *Kidney International, 79*(5), 563-572.

McKnight, A. J., Currie, D., & Maxwell, A. P. (2010). Unravelling the genetic basis of renal diseases; from single gene to multifactorial disorders. *The Journal of pathology, 220*(2), 198-216.

McLennan, S., Wang, X., Moreno, V., Yue, D., & Twigg, S. (2004). Connective tissue growth factor mediates high glucose effects on matrix degradation through tissue inhibitor of matrix metalloproteinase type 1: implications for diabetic nephropathy. *Endocrinology, 145*(12), 5646-5655.

Mclennan, S. V., Fisher, E., Martell, S. Y., Death, A. K., Williams, P. F., Lyons, J. G., & Yue, D. K. (2000). Effects of glucose on matrix metalloproteinase and plasmin activities in

mesangial cells: possible role in diabetic nephropathy. *Kidney International, 58*, S81-S87.

McManus, M. T., & Sharp, P. A. (2002). Gene silencing in mammals by small interfering RNAs. *Nature reviews genetics, 3*(10), 737-747.

Miller, C. G., Pozzi, A., Zent, R., & Schwarzbauer, J. E. (2014). Effects of high glucose on integrin activity and fibronectin matrix assembly by mesangial cells. *Molecular biology of the cell, 25*(16), 2342-2350.

Millis, M. P., Bowen, D., Kingsley, C., Watanabe, R. M., & Wolford, J. K. (2007). Variants in the plasmacytoma variant translocation gene (PVT1) are associated with end-stage renal disease attributed to type 1 diabetes. *Diabetes, 56*(12), 3027-3032.

Miner, J. H. (2012). The glomerular basement membrane. *Experimental cell research, 318*(9), 973-978.

Mitu, G., & Hirschberg, R. (2008). Bone morphogenetic protein-7 (BMP7) in chronic kidney disease. *Front Biosci, 13*, 4726-4739.

Mitu, G. M., Wang, S., & Hirschberg, R. (2007). BMP7 is a podocyte survival factor and rescues podocytes from diabetic injury. *American Journal of Physiology-Renal Physiology, 293*(5), F1641-F1648.

Mogensen, C. (1987). Microalbuminuria as a predictor of clinical diabetic nephropathy. *Kidney int, 31*(2), 673-689.

Mohanram, A., Zhang, Z., Shahinfar, S., Keane, W. F., Brenner, B. M., & D TOTO, R. (2004). Anemia and end-stage renal disease in patients with type 2 diabetes and nephropathy. *Kidney International, 66*(3), 1131-1138.

Moon, Z., Moss-Morris, R., Hunter, M. S., & Hughes, L. D. (2017). Measuring illness representations in breast cancer survivors (BCS) prescribed tamoxifen: Modification and validation of the Revised Illness Perceptions Questionnaire (IPQ-BCS). *Psychology & Health*, 1-20.

Mori, T., Kawara, S., Shinozaki, M., Hayashi, N., Kakinuma, T., Igarashi, A., . . . Takehara, K. (1999). Role and interaction of connective tissue growth factor with transforming growth factor-β in persistent fibrosis: a mouse fibrosis model. *Journal of cellular physiology, 181*(1), 153-159.

Nakamura, T., Fukui, M., Ebihara, I., Osada, S., Nagaoka, I., Tomino, Y., & Koide, H. (1993). mRNA expression of growth factors in glomeruli from diabetic rats. *Diabetes, 42*(3), 450-456.

Nakamura, T., Miller, D., Ruoslahti, E., & Border, W. A. (1992). Production of extracellular matrix by glomerular epithelial cells is regulated by transforming growth factor-bold beta. *Kidney International, 41*, 1213-1221.

Nerlich, A., & Schleicher, E. (1991). Immunohistochemical localization of extracellular matrix components in human diabetic glomerular lesions. *The American journal of pathology, 139*(4), 889.

Nguyen, T., Menocal, E. M., Harborth, J., & Fruehauf, J. H. (2008). RNAi therapeutics: an update on delivery. *Current opinion in molecular therapeutics, 10*(2), 158-167.

Nicholas, S. B., Aguiniga, E., Ren, Y., Kim, J., Wong, J., Govindarajan, N., . . . Collins, A. (2005). Plasminogen activator inhibitor-1 deficiency retards diabetic nephropathy. *Kidney International, 67*(4), 1297-1307.

O'Seaghdha, C. M., & Fox, C. S. (2012). Genome-wide association studies of chronic kidney disease: what have we learned? *Nature Reviews Nephrology, 8*(2), 89-99.

Østerby, R., Parving, H.-H., Hommel, E., Jørgensen, H. E., & Løkkegaard, H. (1990). Glomerular structure and function in diabetic nephropathy: early to advanced stages. *Diabetes, 39*(9), 1057-1063.

Østerby, R., Tapia, J., Nyberg, G., Tencer, J., Willner, J., Rippe, B., & Torffvit, O. (2001). Renal structures in type 2 diabetic patients with elevated albumin excretion rate. *APmIs, 109*(11), 751-761.

Ozkaynak, E., Rueger, D. C., Drier, E. A., Corbett, C., Ridge, R. J., Sampath, T. K., & Oppermann, H. (1990). OP-1 cDNA encodes an osteogenic protein in the TGF-beta family. *The EMBO Journal, 9*(7), 2085-2093.

Palmer, N. D., & Freedman, B. I. (2012). Insights into the genetic architecture of diabetic nephropathy. *Current diabetes reports, 12*(4), 423-431.

Pankewycz, G., Guan, J.-X., Bolton, W. K., Gomez, A., & Benedict, J. F. (1994). Renal TGF-bold beta regulation in spontaneously diabetic NOD mice with correlations in mesangial cells. *Kidney International, 46*, 748-758.

Patel, S. R., & Dressler, G. R. (2005). BMP7 signaling in renal development and disease. *Trends in molecular medicine, 11*(11), 512-518.

Paueksakon, P., Revelo, M. P., Ma, L.-J., Marcantoni, C., & Fogo, A. B. (2002). Microangiopathic injury and augmented PAI-1 in human diabetic nephropathy. *Kidney International, 61*(6), 2142-2148.

Phanish, M. K., Winn, S., & Dockrell, M. (2009). Connective tissue growth factor-(CTGF, CCN2)–a marker, mediator and therapeutic target for renal fibrosis. *Nephron Experimental Nephrology, 114*(3), e83-e92.

Qi, W., Mu, J., Luo, Z.-F., Zeng, W., Guo, Y.-H., Pang, Q., . . . Feng, B. (2011). Attenuation of diabetic nephropathy in diabetes rats induced by streptozotocin by regulating the endoplasmic reticulum stress inflammatory response. *Metabolism, 60*(5), 594-603.

Qi, Z., Fujita, H., Jin, J., Davis, L. S., Wang, Y., Fogo, A. B., & Breyer, M. D. (2005). Characterization of susceptibility of inbred mouse strains to diabetic nephropathy. *Diabetes, 54*(9), 2628-2637.

Raut, S. K., & Khullar, M. (2018). The big entity of new RNA world: long non-coding RNAs in microvascular complications of diabetes. *Frontiers in endocrinology, 9*, 300.

Raval, N., Jogi, H., Gondaliya, P., Kalia, K., & Tekade, R. K. (2019). Method and its Composition for encapsulation, stabilization, and delivery of siRNA in Anionic polymeric nanoplex: An In vitro-In vivo Assessment. *Scientific reports, 9*(1), 1-18.

Reed, M., Meszaros, K., Entes, L., Claypool, M., Pinkett, J., Gadbois, T., & Reaven, G. (2000). A new rat model of type 2 diabetes: the fat-fed, streptozotocin-treated rat. *Metabolism, 49*(11), 1390-1394.

Reeves, W. B., & Andreoli, T. E. (2000). Transforming growth factor β contributes to progressive diabetic nephropathy. *Proceedings of the National Academy of Sciences, 97*(14), 7667-7669.

Rerolle, J.-P., Hertig, A., Nguyen, G., Sraer, J.-D., & Rondeau, E. P. (2000). Plasminogen activator inhibitor type 1 is a potential target in renal fibrogenesis. *Kidney International, 58*(5), 1841-1850.

Reynolds, A., Leake, D., Boese, Q., Scaringe, S., Marshall, W. S., & Khvorova, A. (2004). Rational siRNA design for RNA interference. *Nature biotechnology, 22*(3), 326-330.

Russo, L. M., del Re, E., Brown, D., & Lin, H. Y. (2007). Evidence for a role of transforming growth factor (TGF)-β1 in the induction of postglomerular albuminuria in diabetic nephropathy amelioration by soluble TGF-β type II receptor. *Diabetes, 56*(2), 380-388.

Satirapoj, B., & Adler, S. G. (2014). Comprehensive approach to diabetic nephropathy. *Kidney Research and Clinical Practice, 33*(3), 121-131.

Schiffer, M., Bitzer, M., Roberts, I. S., Kopp, J. B., ten Dijke, P., Mundel, P., & Böttinger, E. P. (2001). Apoptosis in podocytes induced by TGF-β and Smad7. *The Journal of clinical investigation, 108*(6), 807-816.

Schlöndorff, D. (2010). Choosing the right mouse model for diabetic nephropathy. *Kidney International, 77*(9), 749-750.

Shankland, S. J., Scholey, J. W., Ly, H., & Thai, K. (1994). Expression of transforming growth factor-beta 1 during diabetic renal hypertrophy. *Kidney International, 46*(2), 430-442.

Sharma, K., Ix, J. H., Mathew, A. V., Cho, M., Pflueger, A., Dunn, S. R., . . . McGowan, T. A. (2011). Pirfenidone for diabetic nephropathy. *Journal of the American Society of Nephrology, 22*(6), 1144-1151.

Sharma, K., Jin, Y., Guo, J., & Ziyadeh, F. N. (1996). Neutralization of TGF-β by anti-TGF-β antibody attenuates kidney hypertrophy and the enhanced extracellular matrix gene expression in STZ-induced diabetic mice. *Diabetes, 45*(4), 522-530.

Sharma, K., & Ziyadeh, F. N. (1994). Renal hypertrophy is associated with upregulation of TGF-beta 1 gene expression in diabetic BB rat and NOD mouse. *American Journal of Physiology-Renal Physiology, 267*(6), F1094-F1001.

Sharma, K., Ziyadeh, F. N., Alzahabi, B., McGowan, T. A., Kapoor, S., Kurnik, B. R., . . . Weisberg, L. S. (1997). Increased renal production of transforming growth factor-β1 in patients with type II diabetes. *Diabetes, 46*(5), 854-859.

Sheetz, M. J., & King, G. L. (2002). Molecular understanding of hyperglycemia's adverse effects for diabetic complications. *Jama, 288*(20), 2579-2588.

Shim, M. S., & Kwon, Y. J. (2010). Efficient and targeted delivery of siRNA in vivo. *FEBS journal, 277*(23), 4814-4827.

Singh, P., Carraher, C., & Schwarzbauer, J. E. (2010). Assembly of fibronectin extracellular matrix. *Annual review of cell and developmental biology, 26*, 397.

Siu, B., Saha, J., Smoyer, W. E., Sullivan, K. A., & Brosius, F. C. (2006). Reduction in podocyte density as a pathologic feature in early diabetic nephropathy in rodents: prevention by lipoic acid treatment. *BMC nephrology, 7*(1), 6.

Skovsø, S. (2014). Modeling type 2 diabetes in rats using high fat diet and streptozotocin. *Journal of diabetes investigation, 5*(4), 349-358.

Slinin, Y., Ishani, A., Rector, T., Fitzgerald, P., MacDonald, R., Tacklind, J., . . . Wilt, T. J. (2012). Management of hyperglycemia, dyslipidemia, and albuminuria in patients with diabetes and CKD: a systematic review for a KDOQI clinical practice guideline. *American Journal of Kidney Diseases, 60*(5), 747-769.

Soler, M. J., Riera, M., & Batlle, D. (2012). New experimental models of diabetic nephropathy in mice models of type 2 diabetes: efforts to replicate human nephropathy. *Experimental diabetes research, 2012*.

Song, J., Wu, X., Liu, F., Li, M., Sun, Y., Wang, Y., . . . Wang, B. (2017). Long non-coding RNA PVT1 promotes glycolysis and tumor progression by regulating miR-497/HK2 axis in osteosarcoma. *Biochemical and Biophysical Research Communications, 490*(2), 217-224.

Sonoki, T. (2014). PVT1: A Cancer-associated Non-coding Gene Revisited. *Cloning & Transgenesis*.

Sørensen, D. R., Leirdal, M., & Sioud, M. (2003). Gene silencing by systemic delivery of synthetic siRNAs in adult mice. *Journal of molecular biology, 327*(4), 761-766.

Srinivasan, K., & Ramarao, P. (2007). Animal model in type 2 diabetes research: An overview. *Indian Journal of Medical Research, 125*(3), 451.

Srinivasan, K., Viswanad, B., Asrat, L., Kaul, C., & Ramarao, P. (2005). Combination of high-fat diet-fed and low-dose streptozotocin-treated rat: a model for type 2 diabetes and pharmacological screening. *Pharmacological Research, 52*(4), 313-320.

Steffes, M. W., Østerby, R., Chavers, B., & Mauer, S. M. (1989). Mesangial expansion as a central mechanism for loss of kidney function in diabetic patients. *Diabetes, 38*(9), 1077-1081.

Stumvoll, M., Goldstein, B. J., & van Haeften, T. W. (2005). Type 2 diabetes: principles of pathogenesis and therapy. *The Lancet, 365*(9467), 1333-1346.

Sugano, M., Yamato, H., Hayashi, T., Ochiai, H., Kakuchi, J., Goto, S., . . . Takeuchi, T. (2006). High-fat diet in low-dose-streptozotocin-treated heminephrectomized rats induces all features of human type 2 diabetic nephropathy: a new rat model of diabetic nephropathy. *Nutrition, metabolism and cardiovascular diseases, 16*(7), 477-484.

Surwit, R., Feinglos, M., Rodin, J., Sutherland, A., Petro, A., Opara, E., . . . Rebuffe-Scrive, M. (1995). Differential effects of fat and sucrose on the development of obesity and diabetes in C57BL/6J and AJ mice. *Metabolism, 44*(5), 645-651.

Surwit, R. S., Kuhn, C. M., Cochrane, C., McCubbin, J. A., & Feinglos, M. N. (1988). Diet-induced type II diabetes in C57BL/6J mice. *Diabetes, 37*(9), 1163-1167.

Susztak, K., Böttinger, E., Novetsky, A., Liang, D., Zhu, Y., Ciccone, E., . . . Sharma, K. (2004). Molecular profiling of diabetic mouse kidney reveals novel genes linked to glomerular disease. *Diabetes, 53*(3), 784-794.

Szkudelski, T. (2001). The mechanism of alloxan and streptozotocin action in B cells of the rat pancreas. *Physiological research, 50*(6), 537-546.

Tamsma, J., Van den Born, J., Bruijn, J., Assmann, K., Weening, J., Berden, J., . . . Veerkamp, J. (1994). Expression of glomerular extracellular matrix components in human diabetic nephropathy: decrease of heparan sulphate in the glomerular basement membrane. *Diabetologia, 37*(3), 313-320.

Tay, Y.-C., Wang, Y., Kairaitis, L., Rangan, G. K., Zhang, C., & Harris, D. C. (2005). Can murine diabetic nephropathy be separated from superimposed acute renal failure&quest. *Kidney International, 68*(1), 391-398.

Tervaert, T. W. C., Mooyaart, A. L., Amann, K., Cohen, A. H., Cook, H. T., Drachenberg, C. B., . . . de Heer, E. (2010). Pathologic classification of diabetic nephropathy. *Journal of the American Society of Nephrology, 21*(4), 556-563.

Tesch, G. H., & Allen, T. J. (2007). Rodent models of streptozotocin-induced diabetic nephropathy (Methods in Renal Research). *Nephrology, 12*(3), 261-266.

Tesch, G. H., & Nikolic-Paterson, D. J. (2006). Recent insights into experimental mouse models of diabetic nephropathy. *Nephron Experimental Nephrology, 104*(2), e57-e62.

Van de Water, F. M., Boerman, O. C., Wouterse, A. C., Peters, J. G., Russel, F. G., & Masereeuw, R. (2006). Intravenously administered short interfering RNA accumulates in the kidney and selectively suppresses gene function in renal proximal tubules. *DRUG METABOLISM AND DISPOSITION, 34*(8), 1393-1397.

Van Den Born, J., Van den Heuvel, L., Bakker, M. A. H., Veerkamp, J. H., Assmann, K., Weening, J. J., & Berden, J. H. M. (1993). Distribution of GBM heparan sulfate proteoglycan core protein and side chains in human glomerular diseases. *Kidney International, 43*, 454-454.

Van Den Hoven, M., Wijnhoven, T., Li, J.-P., Zcharia, E., Dijkman, H., Wismans, R., . . . van Kuppevelt, T. (2008). Reduction of anionic sites in the glomerular basement membrane by heparanase does not lead to proteinuria. *Kidney International, 73*(3), 278-287.

van Dijk, C., & Berl, T. (2004). Pathogenesis of diabetic nephropathy. *Reviews in Endocrine and Metabolic Disorders, 5*(3), 237-248.

Vernier, R. L., Steffes, M. W., Sisson-Ross, S., & Mauer, S. M. (1992). Heparan sulfate proteoglycan in the glomerular basement membrane in type 1 diabetes mellitus. *Kidney int, 41*(4), 1070-1080.

Wada, J., Zhang, H., Tsuchiyama, Y., Hiragushi, K., Hida, K., Shikata, K., . . . Makino, H. (2001). Gene expression profile in streptozotocin-induced diabetic mice kidneys undergoing glomerulosclerosis. *Kidney International, 59*(4), 1363-1373.

Wahab, N. A., YEVDOKIMOVA, N., WESTON, B. S., ROBERTS, T., LI, X. J., BRINKMAN, H., & MASON, R. M. (2001). Role of connective tissue growth factor in the pathogenesis of diabetic nephropathy. *Biochemical Journal, 359*(1), 77-87.

Wang, N., Zhu, Y., Xie, M., Wang, L., Jin, F., Li, Y., . . . De, W. (2018). Long noncoding RNA Meg3 regulates mafa expression in mouse beta cells by inactivating Rad21, Smc3 or Sin3α. *Cellular Physiology and Biochemistry, 45*(5), 2031-2043.

Wang, S.-N., Lapage, J., & Hirschberg, R. (2000). Role of glomerular ultrafiltration of growth factors in progressive interstitial fibrosis in diabetic nephropathy. *Kidney International, 57*(3), 1002-1014.

Wang, S.-N., Lapage, J., & Hirschberg, R. (2001). Loss of tubular bone morphogenetic protein—7 in diabetic nephropathy. *Journal of the American Society of Nephrology, 12*(11), 2392-2399.

Wang, S., Chen, Q., Simon, T. C., Strebeck, F., Chaudhary, L., Morrissey, J., . . . Hruska, K. A. (2003). Bone morphogenic protein-7 (BMP-7), a novel therapy for diabetic nephropathy. *Kidney International, 63*(6), 2037-2049.

Wang, S., de Caestecker, M., Kopp, J., Mitu, G., LaPage, J., & Hirschberg, R. (2006). Renal bone morphogenetic protein-7 protects against diabetic nephropathy. *Journal of the American Society of Nephrology, 17*(9), 2504-2512.

Wang, S., & Hirschberg, R. (2003). BMP7 antagonizes TGF-β-dependent fibrogenesis in mesangial cells. *American Journal of Physiology-Renal Physiology, 284*(5), F1006-F1013.

Watts, J. K., & Corey, D. R. (2010). Clinical status of duplex RNA. *Bioorganic & medicinal chemistry letters, 20*(11), 3203-3207.

Wei, P., Lane, P. H., Lane, J. T., Padanilam, B., & Sansom, S. (2004). Glomerular structural and functional changes in a high-fat diet mouse model of early-stage Type 2 diabetes. *Diabetologia, 47*(9), 1541-1549.

Wesche-Soldato, D. E., Chung, C.-S., Lomas-Neira, J., Doughty, L. A., Gregory, S. H., & Ayala, A. (2005). In vivo delivery of caspase-8 or Fas siRNA improves the survival of septic mice. *Blood, 106*(7), 2295-2301.

Weston, B. S., Wahab, N. A., & Mason, R. M. (2003). CTGF Mediates TGF-β–Induced Fibronectin Matrix Deposition by Upregulating Active α5β1 Integrin in Human Mesangial Cells. *Journal of the American Society of Nephrology, 14*(3), 601-610.

Whelan, J. (2005). First clinical data on RNAi. *Drug discovery today, 10*(15), 1014-1015.

White, K. E., & Bilous, R. W. (2000). Type 2 diabetic patients with nephropathy show structural—functional relationships that are similar to type 1 disease. *Journal of the American Society of Nephrology, 11*(9), 1667-1673.

Wijnhoven, T. J., Lensen, J. F., Wismans, R. G., Lefeber, D. J., Rops, A. L., van der Vlag, J., . . . van Kuppevelt, T. H. (2007). Removal of heparan sulfate from the glomerular basement membrane blocks protein passage. *Journal of the American Society of Nephrology, 18*(12), 3119-3127.

Winzell, M. S., & Ahrén, B. (2004). The high-fat diet–fed mouse a model for studying mechanisms and treatment of impaired glucose tolerance and type 2 diabetes. *Diabetes, 53*(suppl 3), S215-S219.

Witte, E. C., Heerspink, H. J. L., de Zeeuw, D., Bakker, S. J., de Jong, P. E., & Gansevoort, R. (2009). First morning voids are more reliable than spot urine samples to assess microalbuminuria. *Journal of the American Society of Nephrology, 20*(2), 436-443.

Wolf, G., Chen, S., & Ziyadeh, F. N. (2005). From the periphery of the glomerular capillary wall toward the center of disease podocyte injury comes of age in diabetic nephropathy. *Diabetes, 54*(6), 1626-1634.

Wolf, G., & Ziyadeh, F. N. (2007). Cellular and molecular mechanisms of proteinuria in diabetic nephropathy. *Nephron Physiology, 106*(2), p26-p31.

Wu, G.-C., Pan, H.-F., Leng, R.-X., Wang, D.-G., Li, X.-P., Li, X.-M., & Ye, D.-Q. (2015). Emerging role of long non-coding RNAs in autoimmune diseases. *Autoimmunity reviews*.

Yamamoto, T., Nakamura, T., Noble, N. A., Ruoslahti, E., & Border, W. A. (1993). Expression of transforming growth factor beta is elevated in human and experimental diabetic nephropathy. *Proceedings of the National Academy of Sciences, 90*(5), 1814-1818.

Yamamoto, T., Noble, N. A., Cohen, A. H., Nast, C. C., Hishida, A., Gold, L. I., & Border, W. A. (1996). Expression of transforming growth factor-bold beta isoforms in human glomerular diseases. *Kidney International, 49*, 461-469.

Yang, Q., Han, B., Xie, R.-J., & Cheng, M.-L. (2007). Changes of bone morphogenetic protein-7 and inhibitory Smad expression in streptozotocin-induced diabetic nephropathy rat kidney. *Sheng li xue bao:[Acta physiologica Sinica], 59*(2), 190-196.

Yang, Z., Jiang, S., Shang, J., Jiang, Y., Dai, Y., Xu, B., . . . Yang, Y. (2019). LncRNA: Shedding light on mechanisms and opportunities in fibrosis and aging. *Ageing research reviews, 52*, 17-31.

Yeh, C.-H., Chang, C.-K., Cheng, M.-F., Lin, H.-J., & Cheng, J.-T. (2009). Decrease of bone morphogenetic protein-7 (BMP-7) and its type II receptor (BMP-RII) in kidney of type 1-like diabetic rats. *Hormone and Metabolic Research, 41*(08), 605-611.

Yokoi, H., Mukoyama, M., Nagae, T., Mori, K., Suganami, T., Sawai, K., . . . Takigawa, M. (2004). Reduction in connective tissue growth factor by antisense treatment ameliorates renal tubulointerstitial fibrosis. *Journal of the American Society of Nephrology, 15*(6), 1430-1440.

Yokoi, H., Mukoyama, M., Sugawara, A., Mori, K., Nagae, T., Makino, H., . . . Tanaka, I. (2002). Role of connective tissue growth factor in fibronectin expression and tubulointerstitial fibrosis. *American Journal of Physiology-Renal Physiology, 282*(5), F933-F942.

Yokozawa, T., Nakagawa, T., Wakaki, K., & Koizumi, F. (2001). Animal model of diabetic nephropathy. *Experimental and Toxicologic Pathology, 53*(5), 359-363.

Zeisberg, M. (2006). Bone morphogenic protein-7 and the kidney: current concepts and open questions. *Nephrology Dialysis Transplantation, 21*(3), 568-573.

Zeisberg, M., & Kalluri, R. (2008). Reversal of experimental renal fibrosis by BMP7 provides insights into novel therapeutic strategies for chronic kidney disease. *Pediatric nephrology, 23*(9), 1395-1398.

Zeisberg, M., Müller, G. A., & Kalluri, R. (2004). Are there endogenous molecules that protect kidneys from injury? The case for bone morphogenic protein-7 (BMP-7). *Nephrology Dialysis Transplantation, 19*(4), 759-761.

Zhang, M., Lv, X.-Y., Li, J., Xu, Z.-G., & Chen, L. (2009). The characterization of high-fat diet and multiple low-dose streptozotocin induced type 2 diabetes rat model. *Experimental diabetes research, 2008*.

Zhang, Q., Shi, Y., Wada, J., Malakauskas, S. M., Liu, M., Ren, Y., . . . Li, Y. (2010). In vivo delivery of Gremlin siRNA plasmid reveals therapeutic potential against diabetic nephropathy by recovering bone morphogenetic protein-7. *PLoS One, 5*(7), e11709.

Zhang, T.-N., Wang, W., Yang, N., Huang, X.-M., & Liu, C.-F. (2020). Regulation of Glucose and Lipid Metabolism by Long Non-coding RNAs: Facts and Research Progress. *Frontiers in endocrinology, 11*.

Zhao, Y., Zhao, J., Guo, X., She, J., & Liu, Y. (2018). Long non-coding RNA PVT1, a molecular sponge for miR-149, contributes aberrant metabolic dysfunction and inflammation in IL-1β-simulated osteoarthritic chondrocytes. *Bioscience Reports, 38*(5).

Zheng, J., Yu, F., Dong, P., Wu, L., Zhang, Y., Hu, Y., & Zheng, L. (2016). Long non-coding RNA PVT1 activates hepatic stellate cells through competitively binding microRNA-152. *Oncotarget, 7*(39), 62886.

Zhong, W., Zeng, J., Xue, J., Du, A., & Xu, Y. (2020). Knockdown of lncRNA PVT1 alleviates high glucose-induced proliferation and fibrosis in human mesangial cells by miR-23b-3p/WT1 axis. *Diabetology & Metabolic Syndrome, 12*, 1-11.

Zhu, X., Shi, J., & Chen, F. (2018). PVT1 knockdown alleviates vancomycin-induced acute kidney injury by targeting miR-124 via inactivation of NF-κB signaling. *RSC advances, 8*(55), 31725-31734.

Ziyadeh, F. N. (2004). Mediators of diabetic renal disease: the case for TGF-β as the major mediator. *Journal of the American Society of Nephrology, 15*(1 suppl), S55-S57.

Ziyadeh, F. N., Hoffman, B. B., Han, D. C., Iglesias-De la Cruz, M. C., Hong, S. W., Isono, M., . . . Sharma, K. (2000). Long-term prevention of renal insufficiency, excess matrix gene expression, and glomerular mesangial matrix expansion by treatment with monoclonal antitransforming growth factor-β antibody in db/db diabetic mice. *Proceedings of the National Academy of Sciences, 97*(14), 8015-8020.

Ziyadeh, F. N., Sharma, K., Ericksen, M., & Wolf, G. (1994). Stimulation of collagen gene expression and protein synthesis in murine mesangial cells by high glucose is mediated by autocrine activation of transforming growth factor-beta. *Journal of Clinical Investigation, 93*(2), 536.

GLOSSARY & ABBREVIATIONS

ACE	Angiotensin-converting enzyme
AEC	Animal Ethics Committee
AGEs	Advanced glycosylation products
ALT	Alanine aminotransferase
AMD	Age-related macular degeneration
AMDCC	Animal Models of Diabetic Complications Consortium
Ang II	Angiotensin II
ARBs	Angiotensin receptor blockers
BB	Biobreeding
BMP7	Bone morphogenetic protein 7
BMP-RII	BMP type II receptor
BSA	Bovine serum albumin
C57BL/6	C57BL/6 mice
cDNA	Complementary DNA
COL4A1	Collagen type IV alpha 1
CO2	Carbon dioxide
CTGF	Connective tissue growth factor
DCCT	Diabetes Control and Complications Trial

DM	Diabetes mellitus
DN	Diabetic nephropathy
DNA	Deoxyribonucleic acid
dNTP	Deoxyribonucleotide triphosphate
dsRBD	Double-stranded RNA binding domain
ECM	Extracellular matrix
ELISA	Enzyme-linked immunosorbent assay
ESRD	End stage renal disease
FN1	Fibronectin 1
GAPDH	Glyceraldehyde 3-phosphate dehydrogenase
GBM	Glomerular basement membrane
GWAS	Genome-wide association study
H&E	Haematoxylin and eosin
HBSS	Hank’s Balanced Salt Solution
HFD	High fat diet
HFD-STZ	High fat diet- Streptozotocin treatment
HRP	Horseradish peroxidase
HSPG	Heparan sulfate proteoglycan
HS	Heparan sulfate
IL-1	Interleukin-1

IL-6	Interleukin-6
i.p.	Intraperitoneal injection
i.v.	Intravenous injection
LFD	Low fat diet
LFD-vehicle	Low fat diet-vehicle treatment
lncRNAs	Long non-coding RNAs
MALD	Mapping by admixture linkage disequilibrium
MAPK	Mitogen-activated protein kinase
miRNAs	Small noncoding RNAs
MMPs	Matrix metalloproteinases
NIBP	Non-invasive blood pressure
NOD	Nonobese diabetic
nt	Nucleotide
OCT	Optimal cutting temperature
OP 1	Osteogenic protein 1
OTEs	Off-target effects
PA	Plasminogen activators
PAI-1	Plasminogen activator inhibitor-1
PAS	Periodic acid–Schiff
PAZ	Piwi/Argonaute/Zwille

PBS	Phosphate-buffered saline
PCR	Polymerase Chain Reaction
PEG	Polyethyleneimine
PTGS	Post-transcriptional gene silencing
PVT1	Plasmacytoma variant translocation 1
RRT	Renal replacement therapy
RISC	RNA-induced silencing complex
RNA	Ribonucleic acid
RNAi	RNA interference
ROS	Reactive oxygen species
RSV	Respiratory syncytial virus
SBP	Systolic blood pressure
SERPIN	Serine protease inhibitor
siRNAs	small interfering RNAs
SNP	Single nucleotide polymorphism
STZ	Streptozotocin
TGF-β1	Transforming growth factor beta 1
TIMPs	Tissue inhibitors of metalloproteinases
TMB	3,3’,5,5’-tetramethylbenzidine
tPA	Tissue-type plasminogen activators

UACR	Urinary albumin to creatinine Ratio
UAE	Urinary albumin excretion
TNFα	Tumor necrosis factor-α
TSP	Thrombospondin
UDG	Uracil-DNA glycosylase
UKPDS	United Kingdom Prospective Diabetes Study
UPCR	Urinary protein to creatinine Ratio
UPE	Urinary protein excretion
uPA	Urokinase-type plasminogen activators
uPAR	Urokinase-type plasminogen activator receptor
VJU	Vernon Jansen Unit

APPENDIX

Ethics approval letter

Office of the Vice-Chancellor
Research Office
Post-Award Support Services

THE UNIVERSITY OF AUCKLAND
NEW ZEALAND

The University of Auckland
Private Bag 92019
Auckland, New Zealand

Research Office
Level 10, 49 Symonds Street
Auckland, New Zealand
Telephone 86356
Facsimile 64 9 373 7432

UNIVERSITY OF AUCKLAND ANIMAL ETHICS COMMITTEE (AEC)

20-Oct-2015

MEMORANDUM TO:

Dr Jun Lu
Faculty of Health and Environmental Sciences
Auckland University of Technology
Jun.lu@aut.ac.nz

Application for ethics approval (Our Ref. 001644): Research application approved

The Committee considered your application for animal ethics approval for your project entitled **AUT - Plasmacytoma Variant Translocation 1 Gene (PVT1) as a potential novel target for the treatment of diabetic nephropathy.** The Committee is pleased to advise you that this application has now been approved for a period of three years.

The approval date is 20-Oct-2015.

The expiry date is 20-Oct-2018.

Conditions of approval
All deaths which occur prior to the planned end of experiment must be notified to the AEC so that a post mortem may be performed by the Animal Welfare Officer if considered necessary. This includes all animals that are found dead or moribund, or are killed due to abnormalities which make them not fit for purpose.

Please note the requirement of reporting animal use under the Animal Welfare Act 1999. As Responsible Investigator it is your statutory responsibility to provide:

- An annual Animal Usage Return to the Ministry of Primary Industries (MPI) for incorporation into the nationwide animal usage figures.
- An End of Approval Report at completion of the project is to be submitted to this office. Please request the report template from animalethics@auckland.ac.nz.

If you have any queries regarding your ethics application or wish to discuss general matters relating to ethics approvals, please contact the Animal Ethics Administrator at animalethics@auckland.ac.nz or +64 9 373 7599 ext 86356.

Please quote reference 001644 for all communication with the AEC regarding this application.

(This is a computer generated letter. No signature required.)

Animal Ethics Administrator
University of Auckland Animal Ethics Committee

c.c. Sao Keng (Helen) Mok
Miguel Jo Avila